

INTRAVENOUS IMMUNOGLOBULIN EFFECTS IN  
EXPERIMENTAL MODELS OF IMMUNE  
THROMBOCYTOPENIA

by

Ryan John Hansen

May, 2002

A dissertation submitted to the Faculty of the Graduate School of  
State University of New York at Buffalo  
in partial fulfillment of the requirements for the degree of  
Doctor of Philosophy

# Table of Contents

ABSTRACT	i
PREFACE	iii
CHAPTER ONE	1
Current Hypotheses Regarding the Mechanism of Action of Intravenous Immunoglobulin in Immune Thrombocytopenic Purpura.	
CHAPTER TWO	26
An ELISA for Quantification of Murine IgG in Rat Plasma: Application to the Pharmacokinetic Characterization of AP-3, a Murine Anti-Glycoprotein IIIa Monoclonal Antibody, in the Rat.	
CHAPTER THREE	46
Pharmacokinetics, Pharmacodynamics, and Platelet Binding of an Anti-Glycoprotein IIb/IIIa Monoclonal Antibody (7E3) in the Rat: A Quantitative Model of Immune Thrombocytopenic Purpura.	
CHAPTER FOUR	86
Effects of Intravenous Immunoglobulin on Platelet Count and Anti-Platelet Antibody Disposition in a Rat Model of Immune Thrombocytopenia.	
CHAPTER FIVE	123
Intravenous Immunoglobulin Mediates an Increase in Anti-Platelet Antibody Clearance via the FcRn Receptor.	
CHAPTER SIX	137
Intravenous Immunoglobulin Effects on Anti-Platelet Antibody Secretion and Hybridoma Proliferation, In Vitro.	
CHAPTER SEVEN	166
Pharmacokinetic and Pharmacodynamic Modeling of the Effects of Intravenous Immunoglobulin on Anti-Platelet Antibody Disposition in a Rat Model of Immune Thrombocytopenia	
CHAPTER EIGHT	205
Conclusions	

## ABSTRACT

During the past 20 years, intravenous immunoglobulin (IVIG) therapy has become a standard treatment for patients with immune thrombocytopenic purpura (ITP). However, the mechanism(s) by which IVIG achieves beneficial effects in ITP are uncertain. The purpose of this research was to investigate mechanisms of IVIG action in quantitative models of ITP.

IVIG effects were studied *in vitro* and *in vivo*. Investigations in a cell-culture system demonstrated that IVIG decreases the production rate of anti-platelet antibodies, in a concentration-dependent manner. To facilitate the investigation of IVIG action *in vivo*, a quantitative, passive immune model of ITP was developed by administering a monoclonal anti-platelet antibody (7E3) to rats. This animal model of ITP is quite unique, as it is quantitative with respect to anti-platelet antibody concentrations and anti-platelet antibody effects. 7E3 administration led to rapid, severe thrombocytopenia, and to increases in bleeding tendency. Administration of IVIG protected the rats from 7E3-mediated thrombocytopenia, and also led to an unexpected increase in the clearance of the anti-platelet antibody, an effect that had not been previously demonstrated for IVIG. Studies in mice lacking expression of the FcRn receptor showed that this effect of IVIG was mediated by competition with 7E3 for occupancy of the FcRn receptor.

Because it is likely that multiple pathways are involved in IVIG effects in ITP, pharmacokinetic/pharmacodynamic modeling was used to estimate the importance of this new mechanism of action. IVIG effects on 7E3 pharmacokinetics were characterized

with a mechanism-based model of IgG pharmacokinetics, and an indirect response model was developed to relate 7E3 concentrations to the time-course of thrombocytopenia. These mathematical models predicted that ~50% of the total effect of IVIG on 7E3-induced thrombocytopenia could be accounted for by IVIG effects on anti-platelet antibody clearance, suggesting that this may be an important mechanism of IVIG action.

This dissertation introduces the approach of using quantitative experimental models of ITP, together with pharmacokinetic/pharmacodynamic modeling, to delineate the complex actions of IVIG. This approach has led to a better understanding of IVIG effects in ITP, and may lead to the development of new therapies of ITP and other autoimmune conditions.

## PREFACE

This dissertation presents a new approach to the study of intravenous immunoglobulin (IVIG) mechanism of action in immune thrombocytopenic purpura (ITP). Because IVIG may increase platelet counts via more than one mechanism, it has been difficult to determine which effects contribute most to the therapeutic benefit of IVIG. Our approach combines the use of animal models of disease, and pharmacokinetic/pharmacodynamic modeling analyses, in an attempt to determine the relative importance of specific mechanisms of IVIG action.

Each chapter of this dissertation will be submitted for publication in a scientific journal, and therefore, each chapter is written in the format required by that journal. As such, each chapter is its own body of work, and includes its own introduction and conclusion. The first chapter of the dissertation presents a review of proposed hypotheses concerning mechanisms of IVIG effects in the treatment of ITP, and is intended to serve as an introduction to the problem under consideration in this dissertation. This review addresses both the ‘traditional’ thinking regarding IVIG mechanism of action, as well as the newer mechanisms that have been proposed, including those described herein.

In Chapter 2, we present the development of an enzyme-linked immunosorbent assay for the quantification of anti-platelet antibody concentrations in rat plasma. This assay was developed to facilitate the creation of a quantitative animal model of ITP. The assay has a working range of 15-100 ng/ml, and intra-assay variability was < 9% for quality control

samples within the standard curve range. A demonstration of the utility of the assay for determination of anti-platelet antibody pharmacokinetics, in the rat, is presented.

Chapter 3 presents a quantitative rat model of ITP. This model is a passive immune model, where a monoclonal anti-platelet antibody (7E3) is administered intravenously to rats. This chapter presents the production, purification, and characterization of 7E3, and demonstrates the binding of 7E3 to rat platelets. 7E3 administration to rats causes severe thrombocytopenia, with platelet counts reaching  $18\pm 4\%$  of initial following the highest dose of 7E3. This model of ITP is unique, being the first model of ITP that is quantitative with respect to platelet counts and anti-platelet antibody concentrations.

IVIG effects on 7E3-mediated thrombocytopenia are characterized, and experimental support for a new mechanism of IVIG action in ITP is presented in Chapter 4. IVIG administration protects rats from 7E3-mediated thrombocytopenia, with nadir percent platelet counts 121-279% greater in IVIG treated animals (0.4-2 g/kg) than in animals receiving 7E3 alone. Additionally, this chapter reports that IVIG administration (2 g/kg) results in a dramatic (i.e., ~2.4-fold) increase anti-platelet antibody clearance ( $P < 0.001$ ). This chapter demonstrates that IVIG has efficacy in this rat model of ITP, and proposes that IVIG may achieve beneficial effects in ITP is by increasing the clearance of anti-platelet antibodies.

Chapter 5 explores the new mechanism of IVIG action that was introduced in Chapter 4. IVIG effects on 7E3 pharmacokinetics are characterized in mice lacking expression of the

FcRn protective receptor, and in control mice. IVIG administration increased 7E3 clearance from  $5.2 \pm 0.3$  ml/d/kg in control mice to  $14.4 \pm 1.4$  ml/d/kg in IVIG treated mice ( $p < 0.001$ ), but did not increase the clearance of 7E3 in FcRn-deficient mice. This chapter demonstrates that IVIG effects on 7E3 elimination are mediated by the FcRn receptor.

Chapter 6 presents the use of an in vitro system to study the possible effects of IVIG on anti-platelet antibody production. Studies using anti-platelet antibody-producing hybridoma cells show that IVIG may decrease anti-platelet antibody secretion, in a non-specific manner. The significance of this finding has yet to be demonstrated in vivo.

In Chapter 7, mathematical models are introduced to determine the significance of IVIG effects on anti-platelet antibody elimination, relative to overall effect of IVIG in the rat model of ITP. A mechanism-based model of IgG pharmacokinetics, and an indirect response model for 7E3-mediated thrombocytopenia are presented. These models predict that increased anti-platelet antibody clearance can account for  $50 \pm 11\%$  of the total protective effect of IVIG, in this model of ITP. We also suggest that this mechanism of action may be an important component of the total effect of IVIG, in humans.

Chapter 8 presents the conclusions drawn from the research presented in this dissertation, and attempts to put the research into the proper context. It is hoped that the findings of this dissertation will one day lead to the development of new therapies of immune thrombocytopenia.

# CHAPTER ONE

---

CURRENT HYPOTHESES REGARDING THE MECHANISM OF  
ACTION OF INTRAVENOUS IMMUNOGLOBULIN IN IMMUNE  
THROMBOCYTOPENIC PURPURA

---

## **Abstract**

Although intravenous immunoglobulin (IVIG) treatment has been an important therapy of immune thrombocytopenia (ITP) for more than 20 years, the mechanism of action is still unclear. In recent years, new mechanisms of IVIG action in ITP have been proposed. The purpose of this review is to present an update of the possible mechanisms of IVIG action in ITP, and to stimulate even greater interest in this important problem. This review discusses the traditional thinking regarding IVIG mechanism of action (e.g., blockade of Fc-receptor mediated platelet phagocytosis, suppression of anti-platelet antibody production, and anti-idiotypic inhibition of anti-platelet antibodies), as well as the more recent research in this area (e.g., stimulation of Fc $\gamma$ RIIb expression on phagocytic cells, and increasing anti-platelet antibody clearance). It is anticipated that promising new therapies of ITP, and other autoimmune conditions, will be developed based on a better understanding of IVIG mechanism of action.

Immune thrombocytopenic purpura (ITP) is a common autoimmune condition, diagnosed on the basis of decreased platelet counts, an otherwise normal complete blood cell count, and no other known cause of the thrombocytopenia.<sup>1</sup> Although the etiology of ITP is still unclear, over the past 50 years, researchers have gained much insight into the pathogenesis of ITP, and have established the autoimmune nature of the disease. In 1951, Harrington et al.<sup>2</sup> showed that healthy subjects developed thrombocytopenia following the infusion of plasma obtained from ITP patients. These classic experiments were the first to demonstrate that ITP was caused by a factor in plasma. Later work demonstrated similarities between the ITP-causing factor and immunoglobulins, and established that thrombocytopenia in ITP is likely caused by autoantibodies.<sup>3</sup> More recently, several platelet membrane targets for autoantibodies have been identified, including GPIIb/IIIa and GPIb/IX.<sup>4-7</sup> It is currently accepted that thrombocytopenia in ITP results from rapid destruction of platelets by cells of the reticuloendothelial system (RES), which is mediated by platelet opsonization with autoantibodies.

Current therapies of ITP include corticosteroids, splenectomy, anti-D immunoglobulin, or high dose intravenous immunoglobulin (IVIg) therapy.<sup>1,8</sup> The first use of IVIg to treat ITP was by Imbach et al.<sup>9</sup> in 1981. Subsequently, other studies have confirmed the efficacy of IVIg in ITP,<sup>10</sup> and IVIg has become a valuable therapy for ITP patients. Unfortunately, like all other therapies available for ITP patients, IVIg is not an ideal treatment. IVIg is not curative,<sup>9</sup> is very expensive,<sup>11</sup> and the mechanism of action is not fully understood.<sup>12</sup> Additionally, approximately 15% of ITP patients may not respond to

IVIG treatment.<sup>13</sup> A better understanding of the mechanism of action of IVIG in ITP could lead to the development of better therapies of ITP. The purpose of this review is to discuss the current thinking regarding IVIG mechanism of action in ITP.

### **Fc $\gamma$ R blockade**

One of the earliest, and perhaps most widely accepted explanations for IVIG effects in ITP, is that IVIG blocks Fc $\gamma$ R-mediated phagocytosis of antibody-opsonized platelets. Several general observations support the role of Fc $\gamma$ R blockade in IVIG effects. First, a number of studies have shown that that IVIG treatment does indeed lead to decreased platelet clearance.<sup>14-17</sup> Furthermore, several studies have reported decreased clearance of anti-D coated red blood cells (RBC) following IVIG therapy.<sup>18-20</sup> Because anti-D coated RBC are believed to be cleared solely via Fc $\gamma$ R pathways,<sup>18</sup> the Fc $\gamma$ R blockade hypothesis has gained widespread support. Additional support for the importance of Fc $\gamma$ R-mediated pathways of platelet destruction in ITP was obtained when Clynes and Ravetch demonstrated that mice lacking gamma-chain expression do not develop antibody-mediated thrombocytopenia.<sup>21</sup> Finally, studies involving administration of Fc $\gamma$  fragments,<sup>22</sup> anti-Fc $\gamma$  receptor antibodies,<sup>23</sup> and anti-D antibodies<sup>24,25</sup> all have shown clinical efficacy in ITP, further demonstrating the importance of Fc-receptor mediated clearance of platelets. Whether or not IVIG acts by blocking Fc $\gamma$ R-mediated platelet phagocytosis, development of therapies that target this pathway may be one effective way of raising platelet counts in ITP patients.

Many researchers have suggested possible mechanisms by which IVIG could block Fc-mediated platelet phagocytosis. Imbach et al.<sup>9</sup> initially proposed that IVIG could act by “overloading and blocking of the reticuloendothelial system by IgG catabolism.” Fehr et al.<sup>18</sup> offered several possible explanations to describe the decreased antibody-coated RBC clearance they observed following IVIG treatment. These explanations included the possibility of a physicochemical alteration of the IgG molecules during IVIG preparation that increases the affinity of monomeric IgG for the Fc receptors, the presence of dimers in the IVIG preparation that could compete with antibody-coated platelets for phagocytosis, and the possibility that a specific subclass of IgG may have high affinity for Fc receptors, blocking phagocytosis. Salama et al.<sup>24</sup> proposed that anti-RBC antibodies in IVIG opsonize RBC, and that the antibody coated RBC compete with antibody coated platelets for Fc-mediated phagocytosis. Anti-D therapy of ITP was later introduced, based on this hypothesis. Kimberly et al.<sup>20</sup> showed that IVIG treatment led to decreased affinity of IgG for Fc receptors, *in vitro*. Newland et al.<sup>26</sup> proposed that IVIG blocks Fc receptors on neutrophils, leading to an inhibition of neutrophils phagocytosis of opsonized platelets. Additionally, in the same report, Newland et al. also proposed that IVIG may opsonize neutrophils, and that the opsonized neutrophils may competitively inhibit platelet phagocytosis by monocytes (i.e., by competition for monocyte Fc receptor binding). Recently, Teeling et al.<sup>27</sup> have reported that IgG dimers are responsible for blockade of Fc-mediated phagocytosis of opsonized platelets.

Although inhibition of Fc $\gamma$ R-mediated phagocytosis of platelets has been the most discussed and studied of the potential mechanisms of IVIG action in ITP, it cannot

explain all experimental results. For example, Fc $\gamma$ R blockade cannot account for the response of some ITP patients to Fc-depleted IVIG treatment,<sup>28</sup> or for the long-term benefit derived by some ITP patients from IVIG therapy.<sup>29</sup> Fc $\gamma$ R blockade may be an important aspect of IVIG effects, but there are likely other important effects playing a role in the success of IVIG therapy in ITP.

### **Inhibition of anti-platelet antibody production/modulation of lymphocyte activity**

In some ITP patients, IVIG effects last longer than can be expected based on Fc $\gamma$ R-blockade effects alone.<sup>29</sup> Researchers have generally attributed the longer-term effects of IVIG to decreased anti-platelet antibody levels in the blood. This decrease in antibody concentrations could result from increased antibody elimination (see below) or inhibition of anti-platelet antibody production. Historically, most researchers have focused on IVIG effects on reduction of antibody production, rather than increased antibody elimination. Many studies have looked at IVIG effects on antibody synthesis, or surrogate measures of antibody synthesis, and the results have not always been in agreement. To date, no consensus has been reached on the complex effects of IVIG on lymphocyte proliferation and antibody production. Several of the findings are listed below.

The earliest report of IVIG effects on immunoglobulin synthesis in ITP patients showed that IVIG therapy led to decreased immunoglobulin synthesis, *in vitro*, by peripheral mononuclear cells stimulated with pokeweed mitogen. This study also reported decreases in the CD4<sup>+</sup>/CD8<sup>+</sup> T-cell ratios following IVIG therapy.<sup>30</sup> Dammacco et al.<sup>31</sup> confirmed these initial results with peripheral blood mononuclear cells, and Bordet

et al.<sup>32</sup> found that pokeweed mitogen-induced immunoglobulin synthesis from spleen mononuclear cells was also decreased following IVIG therapy. However, other studies have reported increased in vitro antibody secretion by ITP patients who responded to therapy, and/or increases in the CD4+/CD8+ T-cell ratios in ITP patients following IVIG therapy.<sup>29,33</sup> Still other studies have reported no change in the CD4+/CD8+ T-cell ratios,<sup>33,34</sup> but enhanced suppressor cell function in ITP patients following IVIG therapy.<sup>34</sup> It has been suggested that IVIG therapy leads to a normalization of immune function, with a decrease in anti-platelet antibody production resulting from this normalization.<sup>29</sup>

Various other effects of IVIG on cells of the immune system have been reported. Engelhard et al.<sup>35</sup> showed decreased natural killer cell activity in ITP patients following IVIG treatment. Using several experimental systems, others have shown decreased cytokine production resultant from IVIG,<sup>36-38</sup> binding of IVIG to various cytokines,<sup>39,40</sup> and induction of lymphocyte apoptosis by IVIG.<sup>41</sup> Overall, most researchers have supported the idea that IVIG treatment may lead to decreased anti-platelet antibody production. However, research specifically conducted on anti-platelet antibody producing cells has been lacking. Recently, our laboratory attempted to address this issue,<sup>42</sup> and showed that IVIG treatment decreases anti-platelet antibody production in an experimental system, by decreasing the apparent rate of cell growth. However, these effects were not specific to anti-platelet antibody producing cells, as control antibody producing cells showed similar effects.

In summary, many immunoregulatory effects of intravenous immunoglobulin have been reported. These effects appear to be very complex. However, no studies have clearly shown that IVIG can decrease anti-platelet antibody production in ITP patients. Furthermore, the clinical relevance of the effects of IVIG discussed above is far from being determined.

### **Anti-idiotypic inhibition of anti-platelet antibody-mediated platelet destruction**

Another commonly discussed hypothesis regarding IVIG effects in ITP is the possibility that anti-idiotypic antibodies exist in IVIG that prevent anti-platelet antibody binding to platelets. The first discussion of anti-idiotypic antibodies being relevant to IVIG treatment of ITP occurred after Tovo et al.<sup>28</sup> showed that an Fc-depleted IVIG preparation had efficacy in ITP. Others had previously shown that IVIG contains anti-idiotypic antibodies that could neutralize anti-Factor VIII autoantibodies,<sup>43</sup> so it was suggested that anti-idiotypic antibodies to anti-platelet antibodies might be present in IVIG as well.

Several studies have been performed to determine the importance of anti-idiotypic antibodies in ITP, with mixed conclusions. Berchtold et al.<sup>44</sup> reported that IVIG inhibited the in vitro binding of anti-GPIIb/IIIa autoantibody to GPIIb/IIIa, but that binding of alloantibody to the same target was not inhibited by IVIG. Mehta and Badakere<sup>45</sup> reported that IVIG and anti-D (as well as their Fab fragments) inhibited binding of anti-platelet autoantibodies to platelets, also in vitro. Other researchers have found no evidence for anti-idiotypic effects in various experimental systems;<sup>27,46</sup>

however, it is noted that in these cases, the anti-platelet antibodies were monoclonal antibodies exogenously administered, rather than human anti-platelet autoantibodies. No evidence exists to show the in vivo importance of anti-idiotypic interactions in ITP patients, but the importance of this effect cannot yet be ruled out.

### **Inhibition of complement-mediated platelet destruction**

The role of complement in the pathogenesis of ITP is still unclear.<sup>47</sup> Most studies regarding IVIG effects in ITP have focused on Fc-mediated phagocytosis of platelets, and ignored the possible role of the complement system in platelet destruction. However, several studies have suggested that complement may play a role in the destruction of platelets in patients with ITP,<sup>48-50</sup> suggesting that this pathway should not be overlooked when investigating IVIG effects in ITP. Additionally, studies have shown that platelet associated C3 and C4 levels may decrease following IVIG treatment,<sup>51</sup> suggesting possible effects of IVIG on complement mediated platelet destruction. However, no studies have directly investigated the role of IVIG in preventing complement mediated platelet destruction, in humans or in animal models of ITP.

Although there is little research regarding IVIG effects on complement in ITP, some studies have been performed in other experimental systems. Early in vitro studies of IVIG effects on the complement system showed that C3 deposition onto antibody-sensitized erythrocytes could be inhibited by IVIG.<sup>52</sup> Basta et al.<sup>53</sup> confirmed these initial results, and showed that C4 deposition onto antibody –sensitized erythrocytes was likewise inhibited by IVIG.<sup>54</sup> IVIG has also shown effects on complement in certain in

vivo situations, such as a guinea pig model of Forssman shock,<sup>55</sup> and in a mouse model of autoimmune myositis.<sup>56</sup> In light of the demonstrated effects of IVIG on complement-mediated damage in other conditions, and the likely role of complement in the pathogenesis of ITP, it is possible that IVIG may produce beneficial increases in platelet count by blocking complement-mediated destruction of platelets; however, more research is needed to assess the possible significance of this mechanism of IVIG effect in ITP.

### **Increased platelet production**

IVIG may increase platelet counts by increasing the rate of platelet production. Few studies have directly investigated IVIG effects on platelet production; however, Grossi et al.<sup>17</sup> performed <sup>51</sup>Cr-labeled platelet studies in ITP patients receiving IVIG, and concluded some of the patients may have benefited from an increase in platelet production. Additionally, Schmidt et al.<sup>16</sup> studied <sup>111</sup>In-labeled platelet kinetics in a child receiving IVIG and saw not only a decreased rate of platelet elimination following IVIG, but an increase in radio-labeled platelet counts. This increase was attributed to a release of platelets from extravascular pools, and could be classified as an apparent increase in the rate of platelet production into the vascular space.

Studies have shown that anti-platelet antibodies can affect megakaryocytopoiesis and pro-platelet formation, *in vitro*.<sup>57</sup> This finding is not surprising, given that megakaryocytes have many of the same membrane-bound proteins as platelets, including the most commonly reported target of anti-platelet antibodies, glycoprotein IIb/IIIa (GPIIb/IIIa).<sup>57</sup> In the same study, Takahashi et al. further showed that monoclonal

antibodies to different megakaryocyte antigens were able to inhibit megakaryocyte colony formation, pro-platelet formation, or both, in vitro. Thus, IVIG may lead to an increase in platelet production as a secondary effect related to IVIG inhibition of anti-platelet antibody production, acceleration of anti-platelet antibody elimination, or anti-idiotypic inhibition of the binding of anti-platelet antibodies to megakaryocyte antigens. Additionally, competition for Fc receptors on phagocytes may lead to re-distribution of platelets from extravascular pools, leading to an increase in the apparent rate of platelet production. IVIG effects on platelet production in ITP patients need further study.

### **Stimulation of Fc $\gamma$ RIIb receptor expression**

Samuelson et al.<sup>58</sup> recently proposed a new Fc $\gamma$ R receptor pathway for IVIG effects on antibody-mediated platelet phagocytosis. Studies performed in their murine model of ITP demonstrated that both intact IgG and the Fc portion of IgG prevented thrombocytopenia upon exogenous administration of an anti-platelet antibody. They further demonstrated that the Fc $\gamma$ RIIb receptor was necessary for prevention of thrombocytopenia by studying IVIG effects following administration of an Fc $\gamma$ RIIb receptor-blocking antibody and in mice lacking expression of the receptor. In each case, IVIG did not prevent the mice from developing thrombocytopenia. Additionally, they found increased Fc $\gamma$ RIIb receptor expression on spleen cells following IVIG treatment. They concluded that the Fc $\gamma$ RIIb receptor is necessary for IVIG effects in ITP, and that IVIG mediates its protective effect by inducing expression of this receptor on cells responsible for clearance of antibody coated platelets.

### **Stimulation of anti-platelet antibody clearance**

Some of the response of ITP patients to IVIG treatment has been attributed to decreased antibody concentrations following IVIG therapy. Decreased antibody levels have usually been attributed to decreased anti-platelet antibody production; however, recent experiments have shown that IVIG treatment increased the clearance of an anti-platelet antibody in a rat model of ITP.<sup>46</sup> This possibility of increased autoantibody clearance was expected, based on the known inverse relationship between IgG half-life and plasma concentration,<sup>59</sup> but until recently had not been demonstrated.

Further studies revealed that IVIG mediates this increase in anti-platelet antibody clearance via competition for the FcRn salvage receptor for IgG.<sup>60</sup> The FcRn, or neonatal Fc receptor, was identified in 1996 as the receptor responsible for protecting IgG from catabolism.<sup>61,62</sup> The presence of a protective receptor for IgG catabolism had been postulated as early as 1964, to explain the increased half-life of IgG relative to other proteins,<sup>63</sup> but until recently was unidentified. Studies in mice lacking expression of this FcRn receptor have demonstrated the importance of this receptor in protecting IgG from catabolism,<sup>61,62</sup> as well as in the effect of IVIG on increasing anti-platelet antibody clearance.<sup>46</sup>

Increased anti-platelet antibody clearance may account for reduced autoantibody titers following IVIG therapy, and may account for some of the beneficial effects of IVIG treatment in ITP and other autoimmune conditions. Further studies, using improved quantitative methodologies, will be required to determine the extent of the decrease in

anti-platelet antibody levels following IVIG treatment, in humans. This data will help to delineate the effects of decreased anti-platelet antibody production from the increase in anti-platelet antibody clearance seen following IVIG treatment. New therapies that target the FcRn receptor might prove valuable treatments for ITP and other autoimmune conditions.

### **A general approach to understanding IVIG mechanism of action**

Recent work conducted in this laboratory has led to the development of a new animal model of ITP,<sup>64</sup> and to the development of mathematical models that characterize IVIG effects in the animal model. This has allowed systematic investigation of mechanisms of IVIG action in ITP, where the relative importance of individual mechanisms of action may be determined through the use of the mathematical model. In these studies, a pharmacokinetic/pharmacodynamic model was used to relate anti-platelet antibody concentrations to the effects produced on platelet counts. Additionally, a mechanism-based model of IgG pharmacokinetics was developed to characterize our finding that IVIG increased anti-platelet antibody clearance. The mathematical models were used to estimate that increased anti-platelet antibody clearance could account for ~50% of the total effect of IVIG in an acute model of ITP. Application of this general approach to the understanding of the important mechanisms of IVIG action in ITP may identify key pathways to target for future therapies of ITP, and other autoimmune conditions.

## **Summary**

Intravenous immunoglobulin administration is an important therapy of immune thrombocytopenia. Many studies have attempted to determine the mechanism(s) by which IVIG effects are achieved. These studies have revealed many different ways IVIG may be acting to increase platelet counts. ITP is a likely a complex family of conditions, rather than a single condition, and IVIG may achieve effects by different pathways in different individuals. Recent research has revealed possible new pathways for IVIG effects, including an increased expression of inhibitory receptors on phagocytic cells, and increased anti-platelet antibody clearance following IVIG administration. Although IVIG effects are likely many and complex, quantitative models of disease and therapy may give great insight into which effects are likely to be the most important effects, and which pathways will be the most useful to target for the development of new therapies of ITP.

## References

1. George JN, Woolf SH, Raskob GE, et al. Idiopathic thrombocytopenic purpura: a practice guideline developed by explicit methods for the American Society of Hematology. *Blood*. 1996;88:3-40.
2. Harrington W, Minnich V, Hollingsworth J, Moore C. Demonstration of a thrombocytopenic factor in the blood of patients with thrombocytopenic purpura. *J Lab Clin Med*. 1951;38:1-10.
3. Shulman N, Marder V, Weinrach R. Similarities between known antiplatelet antibodies and the factor responsible for thrombocytopenia in idiopathic purpura. *Ann NY Acad Sci*. 1965;124:499-542.
4. van Leeuwen EF, van der Ven JT, Engelfriet CP, von dem Borne AE. Specificity of autoantibodies in autoimmune thrombocytopenia. *Blood*. 1982;59:23-26.
5. Woods VL, Jr., Kurata Y, Montgomery RR, et al. Autoantibodies against platelet glycoprotein Ib in patients with chronic immune thrombocytopenic purpura. *Blood*. 1984;64:156-160.
6. Fujisawa K, Tani P, McMillan R. Platelet-associated antibody to glycoprotein IIb/IIIa from chronic immune thrombocytopenic purpura patients often binds to

divalent cation-dependent antigens. *Blood*. 1993;81:1284-1289.

7. Hou M, Stockelberg D, Kutti J, Wadenvik H. Immunoglobulins targeting both GPIIb/IIIa and GPIb/IX in chronic idiopathic thrombocytopenic purpura (ITP): evidence for at least two different IgG antibodies. *Br J Haematol*. 1997;98:64-67.
8. Blanchette V, Freedman J, Garvey B. Management of chronic immune thrombocytopenic purpura in children and adults. *Semin Hematol*. 1998;35:36-51.
9. Imbach P, Barandun S, d'Apuzzo V, et al. High-dose intravenous gammaglobulin for idiopathic thrombocytopenic purpura in childhood. *Lancet*. 1981;1:1228-1231.
10. Bussel JB, Hilgartner MW. Intravenous immunoglobulin therapy of idiopathic thrombocytopenic purpura in childhood and adolescence. *Hematol Oncol Clin North Am*. 1987;1:465-482.
11. Simpson KN, Coughlin CM, Eron J, Bussel JB. Idiopathic thrombocytopenia purpura: Treatment patterns and an analysis of cost associated with intravenous immunoglobulin and anti-D therapy. *Semin Hematol*. 1998;35:58-64.
12. Freedman J, Blanchette M. Idiopathic thrombocytopenic purpura (ITP): a historical odyssey. *Acta Paediatr Suppl*. 1998;424:3-6.

13. Blanchette VS, Kirby MA, Turner C. Role of intravenous immunoglobulin G in autoimmune hematologic disorders. *Semin Hematol.* 1992;29:72-82.
14. Uchida T, Yui T, Umezu H, Kariyone S. Prolongation of platelet survival in idiopathic thrombocytopenic purpura by high-dose intravenous gamma globulin. *Thromb Haemost.* 1984;51:65-66.
15. Schmidt RE, Budde U, Broschen-Zywietz C, Schafer G, Mueller-Eckhardt C. High dose gammaglobulin therapy in adults with idiopathic thrombocytopenic purpura (ITP). Clinical effects. *Blut.* 1984;48:19-25.
16. Schmidt KG, Rasmussen JW, Diederichsen H, Ulrich M. Release of platelets into the circulation induced by gamma globulin treatment in a case of idiopathic thrombocytopenic purpura. *Blut.* 1984;48:27-31.
17. Grossi A, Vannucchi AM, Casprini P, Morfini M, Ferrini PR. Effects of high-dose intravenous gammaglobulin on kinetic parameters of <sup>51</sup>Cr-labelled platelets in chronic ITP. *Haematologica.* 1986;71:123-127.

18. Fehr J, Hofmann V, Kappeler U. Transient reversal of thrombocytopenia in idiopathic thrombocytopenic purpura by high-dose intravenous gamma globulin. *N Engl J Med.* 1982;306:1254-1258.
19. Bussel JB, Kimberly RP, Inman RD, et al. Intravenous gammaglobulin treatment of chronic idiopathic thrombocytopenic purpura. *Blood.* 1983;62:480-486.
20. Kimberly RP, Salmon JE, Bussel JB, Crow MK, Hilgartner MW. Modulation of mononuclear phagocyte function by intravenous gamma-globulin. *J Immunol.* 1984;132:745-750.
21. Clynes R, Ravetch JV. Cytotoxic antibodies trigger inflammation through Fc receptors. *Immunity.* 1995;3:21-26.
22. Debre M, Bonnet MC, Fridman WH, et al. Infusion of Fc gamma fragments for treatment of children with acute immune thrombocytopenic purpura. *Lancet.* 1993;342:945-949.
23. Clarkson SB, Bussel JB, Kimberly RP, Valinsky JE, Nachman RL, Unkeless JC. Treatment of refractory immune thrombocytopenic purpura with an anti-Fc gamma-receptor antibody. *N Engl J Med.* 1986;314:1236-1239.

24. Salama A, Mueller-Eckhardt C, Kiefel V. Effect of intravenous immunoglobulin in immune thrombocytopenia. *Lancet*. 1983;2:193-195.
25. Salama A, Kiefel V, Amberg R, Mueller-Eckhardt C. Treatment of autoimmune thrombocytopenic purpura with rhesus antibodies (anti-Rh0(D)). *Blut*. 1984;49:29-35.
26. Newland AC, Macey MG, Veys PA. Cellular changes during the infusion of high dose intravenous immunoglobulin. *Blut*. 1989;59:82-87.
27. Teeling JL, Jansen-Hendriks T, Kuijpers TW, et al. Therapeutic efficacy of intravenous immunoglobulin preparations depends on the immunoglobulin G dimers: studies in experimental immune thrombocytopenia. *Blood*. 2001;98:1095-1099.
28. Tovo PA, Miniero R, Fiandino G, Saracco P, Messina M. Fc-depleted vs intact intravenous immunoglobulin in chronic ITP. *J Pediatr*. 1984;105:676-677.
29. Bussel J, Pahwa S, Porges A, et al. Correlation of in vitro antibody synthesis with the outcome of intravenous gamma-globulin treatment of chronic idiopathic thrombocytopenic purpura. *J Clin Immunol*. 1986;6:50-56.

30. Tsubakio T, Kurata Y, Katagiri S, et al. Alteration of T cell subsets and immunoglobulin synthesis in vitro during high dose gamma-globulin therapy in patients with idiopathic thrombocytopenic purpura. *Clin Exp Immunol.* 1983;53:697-702.
31. Dammacco F, Iodice G, Campobasso N. Treatment of adult patients with idiopathic thrombocytopenic purpura with intravenous immunoglobulin: effects on circulating T cell subsets and PWM-induced antibody synthesis in vitro. *Br J Haematol.* 1986;62:125-135.
32. Bordet JC, Follea G, Carosella E, Dechavanne M. Intravenous high-dose IgG therapy induced alterations of spleen lymphocyte IgM secretion and T cell subsets in patients with idiopathic thrombocytopenic purpura. *Thromb Res.* 1987;47:165-174.
33. Winiarski J, Elinder G. Immunological effects of intravenous gammaglobulin treatment in childhood idiopathic thrombocytopenic purpura. *Scand J Haematol.* 1986;37:175-179.

34. Delfraissy JF, Tchernia G, Laurian Y, Wallon C, Galanaud P, Dormont J. Suppressor cell function after intravenous gammaglobulin treatment in adult chronic idiopathic thrombocytopenic purpura. *Br J Haematol.* 1985;60:315-322.
35. Engelhard D, Waner JL, Kapoor N, Good RA. Effect of intravenous immune globulin on natural killer cell activity: possible association with autoimmune neutropenia and idiopathic thrombocytopenia. *J Pediatr.* 1986;108:77-81.
36. Andersson JP, Andersson UG. Human intravenous immunoglobulin modulates monokine production in vitro. *Immunology.* 1990;71:372-376.
37. Andersson UG, Bjork L, Skansen-Saphir U, Andersson JP. Down-regulation of cytokine production and interleukin-2 receptor expression by pooled human IgG. *Immunology.* 1993;79:211-216.
38. Andersson U, Bjork L, Skansen-Saphir U, Andersson J. Pooled human IgG modulates cytokine production in lymphocytes and monocytes. *Immunol Rev.* 1994;139:21-42.
39. Svenson M, Hansen MB, Bendtzen K. Binding of cytokines to pharmaceutically prepared human immunoglobulin. *J Clin Invest.* 1993;92:2533-2539.

40. Svenson M, Hansen MB, Ross C, et al. Antibody to granulocyte-macrophage colony-stimulating factor is a dominant anti-cytokine activity in human IgG preparations. *Blood*. 1998;91:2054-2061.
41. Prasad NK, Papoff G, Zeuner A, et al. Therapeutic preparations of normal polyspecific IgG (IVIg) induce apoptosis in human lymphocytes and monocytes: a novel mechanism of action of IVIg involving the Fas apoptotic pathway. *J Immunol*. 1998;161:3781-3790.
42. Hansen R, Balthasar J. Intravenous immunoglobulin decreases the apparent rates of cell growth and anti-platelet antibody production from hybridoma cells. In preparation for submission to: *AAPS Pharmsci*. 2002. (see Ch. 6).
43. Sultan Y, Kazatchkine MD, Maisonneuve P, Nydegger UE. Anti-idiotypic suppression of autoantibodies to factor VIII (antihemophilic factor) by high-dose intravenous gammaglobulin. *Lancet*. 1984;2:765-768.
44. Berchtold P, Dale GL, Tani P, McMillan R. Inhibition of autoantibody binding to platelet glycoprotein IIb/IIIa by anti-idiotypic antibodies in intravenous gammaglobulin. *Blood*. 1989;74:2414-2417.

45. Mehta YS, Badakere SS. In-vitro inhibition of antiplatelet autoantibodies by intravenous immunoglobulins and Rh immunoglobulins. *J Postgrad Med.* 1996;42:46-49.
46. Hansen RJ, Balthasar JP. Intravenous immunoglobulin effects on platelet count and anti-platelet antibody disposition in a rat model of immune thrombocytopenia. *Blood.* 2001; Submitted.
47. Hed J. Role of complement in immune or idiopathic thrombocytopenic purpura. *Acta Paediatr Suppl.* 1998;424:37-40.
48. Hauch TW, Rosse WF. Platelet-bound complement (C3) in immune thrombocytopenia. *Blood.* 1977;50:1129-1136.
49. McMillan R, Martin M. Fixation of C3 to platelets in vitro by antiplatelet antibody from patients with immune thrombocytopenic purpura. *Br J Haematol.* 1981;47:251-256.
50. Tsubakio T, Tani P, Curd JG, McMillan R. Complement activation in vitro by antiplatelet antibodies in chronic immune thrombocytopenic purpura. *Br J Haematol.* 1986;63:293-300.

51. Winiarski J, Kreuger A, Ejderhamn J, Holm G. High dose intravenous IgG reduces platelet associated immunoglobulins and complement in idiopathic thrombocytopenic purpura. *Scand J Haematol.* 1983;31:342-348.
52. Berger M, Rosenkranz P, Brown CY. Intravenous and standard immune serum globulin preparations interfere with uptake of <sup>125</sup>I-C3 onto sensitized erythrocytes and inhibit hemolytic complement activity. *Clin Immunol Immunopathol.* 1985;34:227-236.
53. Basta M, Langlois PF, Marques M, Frank MM, Fries LF. High-dose intravenous immunoglobulin modifies complement-mediated in vivo clearance. *Blood.* 1989;74:326-333.
54. Basta M, Fries LF, Frank MM. High doses of intravenous Ig inhibit in vitro uptake of C4 fragments onto sensitized erythrocytes. *Blood.* 1991;77:376-380.
55. Basta M, Kirshbom P, Frank MM, Fries LF. Mechanism of therapeutic effect of high-dose intravenous immunoglobulin. Attenuation of acute, complement-dependent immune damage in a guinea pig model. *J Clin Invest.* 1989;84:1974-1981.

56. Wada J, Shintani N, Kikutani K, Nakae T, Yamauchi T, Takechi K. Intravenous immunoglobulin prevents experimental autoimmune myositis in SJL mice by reducing anti-myosin antibody and by blocking complement deposition. *Clin Exp Immunol.* 2001;124:282-289.
57. Takahashi R, Sekine N, Nakatake T. Influence of monoclonal antiplatelet glycoprotein antibodies on in vitro human megakaryocyte colony formation and proplatelet formation. *Blood.* 1999;93:1951-1958.
58. Samuelsson A, Towers TL, Ravetch JV. Anti-inflammatory activity of IVIG mediated through the inhibitory Fc receptor. *Science.* 2001;291:484-486.
59. Masson PL. Elimination of infectious antigens and increase of IgG catabolism as possible modes of action of IVIg. *J Autoimmun.* 1993;6:683-689.
60. Hansen RJ, Balthasar JP. Intravenous immunoglobulin mediates effects on anti-platelet antibody clearance via the FcRn receptor. *Blood.* 2002; Submitted (see Ch. 5).
61. Ghetie V, Hubbard JG, Kim JK, Tsen MF, Lee Y, Ward ES. Abnormally short serum half-lives of IgG in beta 2-microglobulin-deficient mice. *Eur J Immunol.* 1996;26:690-696.

62. Junghans RP, Anderson CL. The protection receptor for IgG catabolism is the beta2-microglobulin-containing neonatal intestinal transport receptor. Proc Natl Acad Sci U S A. 1996;93:5512-5516.
  
63. Brambell F, Hemmings W, Morris I. A theoretical model of gamma-globulin catabolism. Nature. 1964;203:1352-1355.
  
64. Hansen R, Balthasar J. PK/PD modeling of the effects of intravenous immunoglobulin on anti-platelet antibody clearance in a rat model of immune thrombocytopenia. In preparation for submission to: J Pharm Exp Ther. 2002. (see Ch. 7).

# CHAPTER TWO

---

AN ELISA FOR QUANTIFICATION OF MURINE IgG IN RAT  
PLASMA: APPLICATION TO THE PHARMACOKINETIC  
CHARACTERIZATION OF AP-3, A MURINE ANTI-GLYCOPROTEIN  
IIIa MONOCLONAL ANTIBODY, IN THE RAT

---

*This chapter has been published in J. Pharm. Biomed. Anal. 21 (1999) 1011-1016.*

## **Abstract**

An enzyme-linked immunosorbent assay (ELISA) has been developed to determine concentrations of murine IgG in rat plasma. Specifically, the assay was developed to measure a murine anti-glycoprotein IIIa antibody (AP-3) in rat plasma to facilitate future investigations of AP-3 pharmacokinetics and pharmacodynamics in the rat. The working range of the assay is 15-100 ng/ml, corresponding to a limit of quantification of 1.5 µg/ml in rat plasma. The assay was validated with respect to accuracy, precision, and cross-reactivity with both pooled rat and mouse IgG. Intra-assay recoveries of AP-3 in rat plasma ranged from 93 to 103% with CV% values ranging from 5.2 to 8.5%. Inter-assay recoveries of the plasma AP-3 samples ranged from 107 to 119% with CV% values ranging from 17.7-25.1%. The assay has no appreciable cross reactivity with pooled rat IgG and full cross reactivity with pooled mouse IgG, making this an ideal assay to determine plasma pharmacokinetics of mouse antibodies in the rat. The assay was used to determine the pharmacokinetics of AP-3 in a Sprague-Dawley rat.

Keywords: murine; IgG; ELISA; validation; pharmacokinetics; rat plasma; GPIIIa; AP-3

## **1. Introduction**

Immune thrombocytopenic purpura (ITP) is an autoimmune condition characterized by an increase in platelet destruction by the mononuclear phagocyte system due to the interaction of anti-platelet autoantibodies with platelet membrane proteins [1, 2]. In addition to the use of immunosuppressants or splenectomy, administration of intravenous high-dose pooled human immune gamma globulin (HD-IgG) has been used to treat patients with ITP [3]. Although several mechanisms have been proposed to explain the therapeutic activity of HD-IgG in ITP, a complete understanding of the mechanism(s) of this treatment has not yet been achieved [4-6].

The platelet membrane glycoprotein IIb/IIIa complex is a common target of autoantibodies in patients afflicted with ITP [2, 7]. AP-3, a mouse monoclonal IgG<sub>1</sub> antibody directed against human glycoprotein IIIa (GPIIIa), was first produced and characterized in 1984. This antibody was shown to bind human platelet GPIIIa with an affinity of  $1.4 \times 10^9 \text{ M}^{-1}$ , without inhibiting induced platelet aggregation by such agents as adenosine diphosphate, thrombin, collagen, or arachidonic acid [8].

A rat model of ITP is being developed in this laboratory to better understand the interaction of anti-platelet antibodies with platelet antigens, to investigate relationships between anti-platelet antibody concentrations and the kinetics of platelet destruction, and to test proposed hypotheses about the mechanism of HD-IgG in ITP treatment. This model attempts to induce immune thrombocytopenia through the administration of AP-3 to Sprague-Dawley rats. Preliminary results have demonstrated that AP-3 administration

leads to thrombocytopenia with a corresponding increase in tail-vein bleeding time (unpublished results). Quantitative pharmacokinetic and pharmacodynamic models will be created to facilitate testing of proposed hypotheses.

Quantitative modeling of the time course and effects of AP-3 requires the ability to accurately and precisely measure AP-3 levels in rat plasma. Radio-labeled IgG has been commonly used to determine mouse IgG concentrations in rat plasma for pharmacokinetic analyses [9, 10]. However, use of an ELISA to measure plasma concentrations of IgG in the rat circumvents the problems encountered using radio-labeled mouse IgG to study pharmacokinetics, such as difficulty separating metabolized antibody from intact antibody, and the safety issues involved with using radioactive substances.

Several researchers have reported using ELISA's to measure mouse IgG concentrations hybridoma supernatants, ascites [11], mouse serum [12], and human serum [13]; some groups have even reported use of an ELISA to determine mouse monoclonal antibody concentrations in rat plasma [14, 15]. However, to the authors' knowledge, this work represents the first report of an appropriately validated ELISA used to quantify a murine monoclonal antibody in rat plasma. The assay presented in this paper was validated with respect to intra-assay and inter-assay precision and accuracy, and was tested for cross-reactivity with pooled mouse and rat IgG.

## **2. Experimental**

### *2.1 Production and purification of AP-3*

Hybridoma cells producing the desired mouse anti-human GPIIIa antibody (AP-3) were obtained from the American Type Culture Collection (ATCC # HB-242, Manassas, VA). Balb/C mice (Harlan Sprague Dawley, Inc., Indianapolis, IN) were prepared for ascites production by an intraperitoneal injection of pristane (Sigma Chemical, St. Louis, MO), 0.5 ml/mouse, approximately one week prior to injection of antibody producing cells. Hybridoma cells,  $5 \times 10^5$  cells/mouse, were then injected intraperitoneally into the mice. Mice were sacrificed 10-20 days after injection of the cells, and ascitic fluid was obtained.

The ascitic fluid obtained from the mice was centrifuged and the straw-colored supernatant was isolated. Anti-GPIIIa IgG was purified from the supernatant by Protein G chromatography (Pharmacia Biotech Hi-Trap protein G column, Uppsala, Sweden) on a Bio-Rad medium pressure chromatography system. The loading buffer for the protein G chromatography was a 20 mM  $\text{Na}_2\text{HPO}_4$  (Sigma Chemical) buffer, pH 7.0; the elution buffer was a 0.1 M citric acid (Sigma Chemical) buffer, pH 2.7. Sodium dodecyl sulfate poly-acrylamide gel electrophoresis (SDS-PAGE) was utilized to ascertain the purity of the IgG pool, and a Micro-Bicinchoninic Acid (BCA) assay kit was used to determine protein concentration (Pierce Kit, #23235, Rockford, IL).

## 2.2 ELISA Procedure

Assays were performed in Nunc Maxisorp 96 well microplates (Nunc model # 4-42404, Roskilde, Denmark). Fc specific goat anti-mouse antibody (Pierce M-3534, 1:500 in 0.02 M  $\text{Na}_2\text{HPO}_4$ , no pH adjustment ), 0.2 ml, was placed in each of the wells to be tested and incubated at 4 °C overnight. The plate was then washed three times with a tween containing phosphate buffer (PB-Tween) consisting of 0.05% Tween 20 (Sigma Chemical) and 0.02 M  $\text{Na}_2\text{HPO}_4$  (Sigma Chemical, no pH adjustment). After the wash, the plate was incubated with samples and standards (0.1 ml) for 2 hours at room temperature. The plate was washed three times with PB-Tween, and then incubated with 0.2 ml Fab specific goat anti-mouse-antibody-Alkaline Phosphatase conjugate (Pierce A-1682, 1:500 in 0.02 M  $\text{Na}_2\text{HPO}_4$ , no pH adjustment ) for 1 hour at room temperature. Finally, after washing again with PB-Tween three times, 0.2 ml of p-nitro phenyl phosphate (Pierce, 5 mg/ml in distilled water) was added to each of the wells and the change in absorbance with time was monitored via a microplate reader at 405 nm (Spectra Max 250, Molecular Devices, Sunnyvale, CA). A standard curve was generated by plotting concentration of AP-3 verses the change in absorbance with time (dA/dt). Standards were made by diluting a stock AP-3 solution to the appropriate concentration (0, 15, 25, 50, 75, and 100 ng/ml) with phosphate buffered saline (PBS, pH 7.4), with addition of rat plasma (Hilltop Laboratories, Scottsdale, PA) to a final concentration of 1% (v/v). Standard curves included a blank standard; consequently no additional correction for non-specific binding was required to evaluate sample concentrations from the standard curve. The assay was validated for precision and accuracy by evaluating the recovery of AP-3 from rat plasma samples. The concentrations of AP-3 in rat plasma

samples were initially 1.5, 2.5, 5.0 and 10.0 µg/ml; samples were diluted by a factor of 100 in PBS immediately before analysis.

### *2.3 Cross-reactivity of the ELISA with mouse and rat IgG*

Mouse and rat IgG were purified from pooled mouse and rat plasma (Hilltop Laboratories). Purification was performed using protein G chromatography as described for AP-3. SDS-PAGE and BCA analysis were performed as described previously. Serial dilutions were made of the mouse or rat IgG, and assay response was determined using the procedures described above. Assay response to pooled mouse IgG was tested over a concentration range of 16.2 – 108 ng/ml. Assay response to pooled rat IgG was tested over a concentration range of 15 – 400 µg/ml.

### *2.4 Specific activity of AP-3 preparation*

AP-3, 5 µg/ml, was incubated with  $3 \times 10^9$ /ml outdated human platelets (American Red Cross, Salt Lake City, UT) in PBS, overnight while shaking. Samples were then centrifuged at 13,000 x g for 6 min to pellet out the platelets and the platelet-bound AP-3. After appropriate dilution in PBS, samples were analyzed for free AP-3 concentration using the ELISA. Samples of pooled mouse IgG were incubated with the platelets as a negative control, and samples of AP-3 and pooled mouse IgG incubated without platelets were used as a reference concentration for 100% recovery. The specific activity was defined as the percent of the IgG bound to the platelets.

### 2.5 Pharmacokinetic Studies

A female Sprague Dawley rat (Harlan Sprague-Dawley), 0.2 kg, was instrumented with an abdominal aorta cannula. AP-3, 1 ml of 0.5 mg/ml, was administered to the rat through the cannula. Blood samples (300  $\mu$ l) were taken at 1, 3, 6, 12, 26.5, 49.5, 80.5, 104.5, and 169 h, and placed into 50  $\mu$ l of an acid-citrate-dextrose anticoagulant (25 g l<sup>-1</sup> trisodium citrate dihydrate, 20 g l<sup>-1</sup> dextrose, 13.7 g l<sup>-1</sup> anhydrous citric acid). Plasma was isolated, and stored at 4 °C until analyzed. AP-3 concentrations were determined with the ELISA. The concentration vs. time profile was fit to a standard two compartment mammillary pharmacokinetic model using *The Scientist* software (MicroMath, Salt Lake City, UT), with the data weighted by a factor of  $y^{-1}$ .

### **3. Results and Discussion**

#### *3.1 Assay validation*

A typical standard curve for AP-3 is shown in figure 1. The best fit line shown in this figure was obtained by fitting the data to a cubic polynomial ( $r^2 = 0.9999$ ). Intra-assay and inter-assay recovery of AP-3 from rat plasma samples is shown in table 1. The intra-assay recovery ranged from 93-103%, and the coefficient of variation (CV) ranged from 5.2-8.5%. The inter-assay recovery ranged from 107-119% and the CV% ranged from 17.7-25.1%. The working range of the assay was 15-100 ng/ml, resulting in a limit of quantification for AP-3 in rat plasma of 1.5  $\mu\text{g/ml}$ .

Few studies have reported using an ELISA to measure murine IgG<sub>1</sub> concentrations in rat plasma. To the authors' knowledge, this is the first report of intra-assay and inter-assay variability for an ELISA measuring mouse IgG in rat plasma. Due to a lack of appropriate data, it is difficult to directly compare the precision and accuracy of this assay to other assays previously developed. Fleming et al. report CV% values of less than 7.6% for intra-assay and less than 15.6% for inter-assay variabilities for their ELISA determining mouse IgG levels in hybridoma supernatants and ascites [11]. The intra-assay variability of this ELISA is similar the Fleming assay, and the inter-assay variability is slightly larger. The larger inter-assay variability may be due to the more complex plasma matrix compared to the supernatant and ascites matrices in the Fleming study. The limit of quantification and the working range of the assay is comparable with other assays for mouse IgG reported in the literature [11, 13, 16].

### *3.2 Cross reactivity with mouse and rat IgG*

The response of the assay to pooled mouse and rat IgG is shown in figure 2, with plots of actual versus assayed concentration. The slope of the pooled mouse IgG plot is 1.04 and is not significantly different from 1 ( $p = 0.65$ ). The assay demonstrated complete cross reactivity with pooled mouse IgG, suggesting that this assay can be used to measure pooled mouse IgG concentrations in rat plasma.

A concentration of 0.4 mg/ml pooled rat IgG was needed for the assay to give a response of 3.5 ng/ml, a concentration well below the working range of the standard curve. The cross reactivity of the assay with rat IgG was therefore estimated to be less than  $1:10^5$ . Given this level of cross-reactivity and considering the normal range of IgG concentrations in undiluted Sprague-Dawley plasma ( $15.5 \pm 3.6$ mg/ml [17]), the presence of rat IgG in the assay matrix is expected to yield an assay response approximately 1-order of magnitude below that corresponding to the lowest standard in the standard curve, 15ng/ml. In the present assay, standards were prepared in 1% rat plasma and samples were diluted minimally by a factor of 100 (i.e., to a final concentration of 1% rat plasma); however, the assay could easily be adapted to achieve a lower limit of quantification of AP-3 by reducing the extent of plasma dilution, if greater sensitivity is deemed necessary for applications other than our proposed pharmacokinetic and pharmacodynamic studies.

### *3.3 Specific activity of AP-3*

Table 2 shows the results of the specific activity experiment. As shown in the table, 96% of the AP-3 preparation bound to the human platelets, and none of the pooled mouse IgG

bound to the platelets. By SDS-PAGE, the AP-3 preparation was shown to be exclusively IgG (data not shown). These results, taken together, have shown that only ~4% of the preparation was non-AP-3 mouse IgG.

### *3.4 Pharmacokinetics of AP-3 in the rat*

The concentration versus time profile for AP-3 in the rat is shown in figure 3, with a best fit line corresponding to a two-compartment mammillary model. Parameters generated using this model are shown in table 3. The pharmacokinetic parameters for AP-3 are on the same order of magnitude as those reported by other researchers who have studied monoclonal mouse IgG<sub>1</sub> pharmacokinetics in the rat [9, 14]. Figure 3 demonstrates that the assay presented in this paper is well suited to determine the pharmacokinetics of AP-3 in the rat.

## References

1. A.C. Newland, M.G. Macey, *Ann. Hematol.* 69 (2) (1994) 61-67.
2. K. Fujisawa, O.T. TE, P. Tani, J.C. Loftus, E.F. Plow, M.H. Ginsberg, R. McMillan, *Blood* 77 (10) (1991) 2207-2213.
3. M.D. Tarantino, G. Goldsmith, *Semin. Hematol.* 35 (1 Suppl 1) (1998) 28-35.
4. P. Imbach, V. d'Apuzzo, A. Hirt, E. Rossi, M. Vest, S. Barandun, C. Baumgartner, A. Morell, M. Schoni, H.P. Wagner, *Lancet* i (1981) 228-231.
5. A.C. Newland, *Br. J. Haematol.* 72 (3) (1989) 301-305.
6. P.A. Imbach, *Clin. Exp. Immunol.* 97 (Suppl 1) (1994) 25-30.
7. M. Hou, D. Stockelberg, J. Kutti, H. Wadenvik, *Br. J. Haematol.* 98 (1) (1997) 64-67.
8. P.J. Newman, R.W. Allen, R.A. Kahn, T.J. Kunicki, *Blood* 65 (1) (1985) 227-232.
9. M.I. Bazin Redureau, C.B. Renard, J.M. Scherrmann, *J. Pharm. Pharmacol.* 49 (3) (1997) 277-281.
10. J.S. Barrett, J.G. Wagner, S.J. Fisher, R.L. Wahl, *Cancer Res.* 51 (13) (1991) 3434-3444.
11. J.O. Fleming, L.B. Pen, *J. Immunol. Methods* 110 (1) (1988) 11-18.
12. A.S. Klein Schneegans, L. Kuntz, P. Fonteneau, F. Loor, *J. Immunol. Methods* 25 (1-2) (1989) 207-213.
13. K.E. Hellstrom, D.E. Yelton, H.P. Fell, D. Beaton, M. Gayle, M. MacLean, M. Kahn, I. Hellstrom, *Cancer Res.* 50 (8) (1990) 2449-2454.

14. F. Caballero, C. Pelegri, M. Castell, A. Franch, C. Castellote, *Immunopharmacology* 39 (2) (1998) 83-91.
15. C. Pelegri, M. Paz Morante, C. Castellote, M. Castell, A. Franch, *Cell. Immunol.* 65 (2) 177-182.
16. A.S. Klein Schneegans, C. Gaveriaux, P. Fonteneau, F. Loor, *J. Immunol. Methods* 119 (1) (1989) 117-125.
17. H.A. al Bander, V.I. Martin, G.A. Kaysen, *Am. J. Physiol.* 262 (3 Pt 2) (1992) F333-337.



Table 1. Variability of ELISA with respect to recovery of AP-3 from plasma samples.

Intra-Assay Variability (n=5)			
Actual Conc.(ng/ml)	Recovered Conc. (ng/ml)	%R	CV%
15	13.9	93	8.5
25	23.6	95	5.2
50	51.0	102	5.2
100	103.1	103	6.4
Inter-Assay Variability (n=4)			
Actual Conc. (ng/ml)	Recovered Conc. (ng/ml)	%R	CV%
15	17.9	119	17.8
25	27.1	108	25.1
50	54.5	109	18.5
100	107.4	107	17.7

Table 2. Specific activity of AP-3.

Sample	% Recovery <sup>a</sup>	SD	CV%	n	%Specific Activity <sup>b</sup>
AP3	4	1	20	2	96
Mouse	102	5	5	2	0

<sup>a</sup> Free AP-3/Mouse IgG recovered, compared to a control sample without platelets.

<sup>b</sup> Percent of AP-3/IgG bound to the platelets, representing the purity of the AP-3 samples.

Table 3. Pharmacokinetic Parameters for AP-3 in a 0.2 kg rat after administration of 0.5 mg AP-3 by IV bolus.

Parameter <sup>a</sup>	Value
V1	8.2 ± 0.4 mL
V2	5.5 ± 1.6 mL
CL	0.15 ± 0.01 mL hr <sup>-1</sup>
CLD	0.18 ± 0.06 mL hr <sup>-1</sup>
terminal t <sub>1/2</sub>	71 ± 4 hr

<sup>a</sup> V1 and V2 refer to central and peripheral compartment volumes, respectively. CL and CLD refer to systemic and distributional clearances.

### Figure Captions

Figure 1. Representative standard curve for AP-3 over the range 0-100 ng/ml. Curve is fitted with a cubic equation,  $r^2 = 0.9999$ . Error bars represent the standard deviation about the mean of three replicates.

Figure 2. Cross reactivity of ELISA with pooled mouse (●) and rat IgG (○). Concentrations of pooled mouse IgG ranged from 16.2 – 108 ng/ml, and concentrations of pooled rat IgG ranged from 15 - 400 µg/ml.

Figure 3. Pharmacokinetics of AP-3 in a 0.2 kg Sprague-Dawley rat following a 0.5 mg dose of AP-3. Error bars represent standard error of means, using two dilutions of AP-3 per time point, and 3 replicates per dilution.

Figure 1.

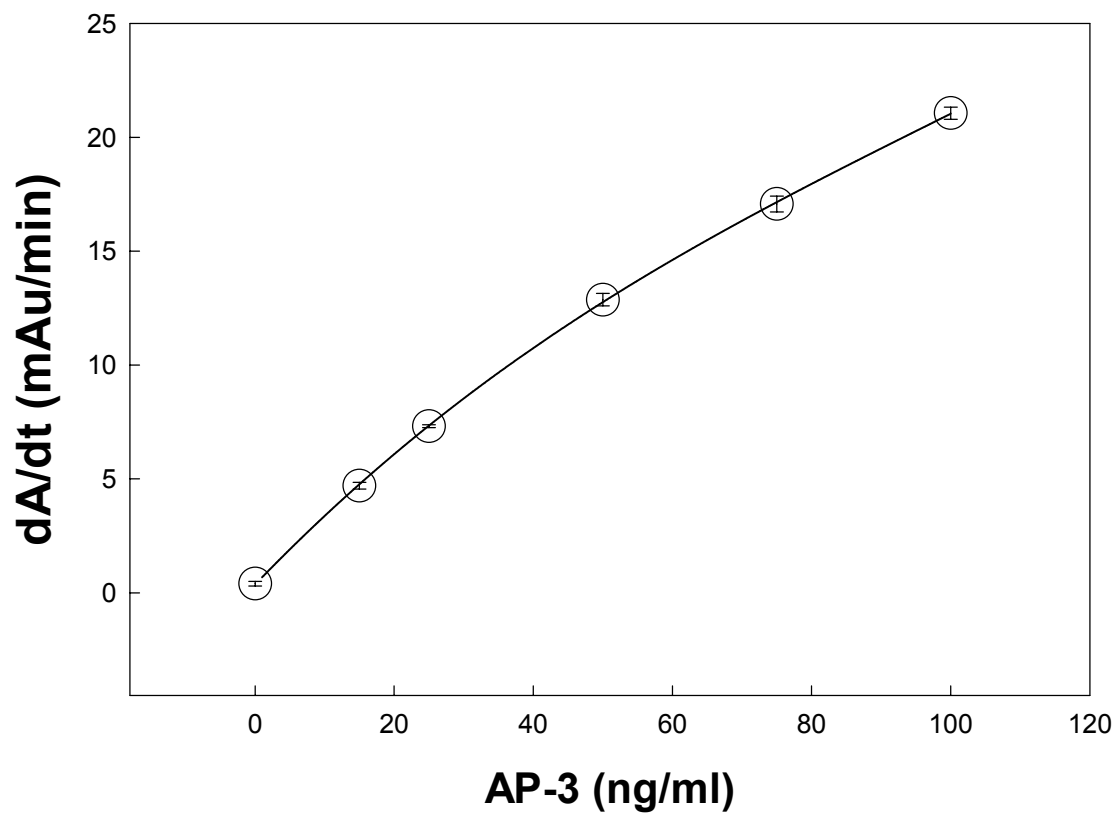


Figure 2.

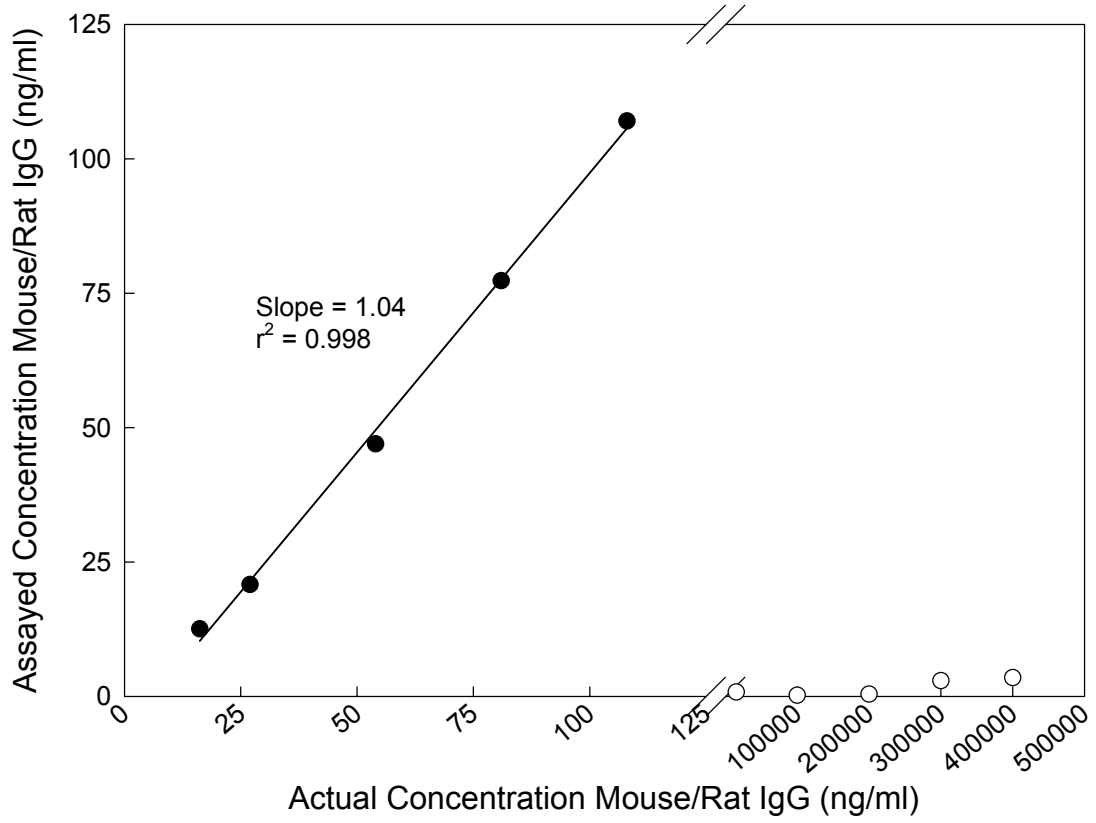
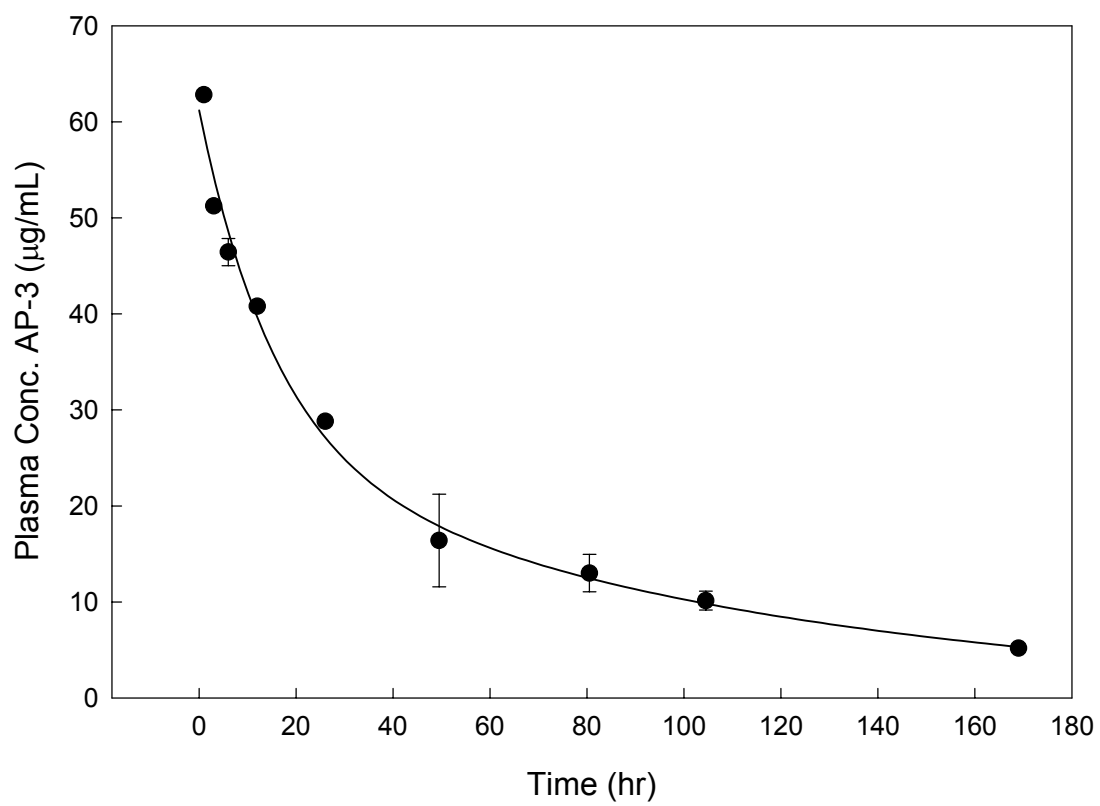


Figure 3.



# CHAPTER THREE

---

PHARMACOKINETICS, PHARMACODYNAMICS, AND PLATELET  
BINDING OF AN ANTI-GLYCOPROTEIN IIb/IIIa MONOCLONAL  
ANTIBODY (7E3) IN THE RAT: A QUANTITATIVE MODEL OF  
IMMUNE THROMBOCYTOPENIC PURPURA

---

*This chapter has been published in J. Pharmacol Exp. Ther. 298(1),165-171,2001.*

## Abstract

The pharmacokinetics, pharmacodynamics, and platelet binding of 7E3, an anti-glycoprotein IIb/IIIa (GPIIb/IIIa) monoclonal antibody, were studied in the rat in an attempt to develop a quantitative animal model of immune thrombocytopenia (ITP). 7E3, a murine IgG<sub>1</sub> antibody developed against human GPIIb/IIIa, demonstrated cross-reactivity with rat platelets by flow cytometry and via ELISA. The apparent affinity ( $K_A$ ) of 7E3–rat platelet binding was  $1.2 \pm 0.2 \times 10^7 \text{ M}^{-1}$ , with  $3.3 \pm 0.3 \times 10^4$  binding sites per platelet. Following intravenous 7E3 administration (0.8, 4, and 8 mg/kg), plasma concentrations declined in a bi-exponential manner, with a terminal half-life of  $61 \pm 5$  hr, and a steady-state volume of distribution of  $62 \pm 15$  ml/kg. Clearance was dose-dependent, with values ranging from  $0.64 \pm 0.08$  ml/hr/kg (8 mg/kg) to  $1.01 \pm 0.08$  ml/hr/kg (0.8 mg/kg). 7E3 induced a reproducible, severe thrombocytopenia in rats, and extended bleeding in a manner consistent with human ITP. Nadir platelet counts were  $79 \pm 33$ ,  $25 \pm 6$ , and  $17 \pm 2 \times 10^6$ /ml, for 7E3 doses of 0.8, 4, and 8 mg/kg, respectively. Bleeding times after a 10 mm tail-incision ranged from  $5 \pm 3$  min in control animals to  $15 \pm 0$  min (the maximum allowed time in this study) in animals receiving 8 mg/kg. Blood volumes lost during bleeding experiments ranged from  $30 \pm 24$   $\mu$ l (control) to  $349 \pm 358$   $\mu$ l (8 mg/kg). A reproducible, quantitative rat model of ITP has been created; this model is expected to facilitate the evaluation of new treatments for this disease.

Immune thrombocytopenic purpura (ITP) is a common autoimmune disease, with approximately 33,000 new cases diagnosed each year in the United States (George et al., 1996). Thrombocytopenia in ITP develops as a result of enhanced platelet destruction, precipitated by the interaction of auto-antibodies and platelet antigens. The resulting thrombocytopenia is often dramatic, and is associated with a variety of hemorrhagic sequelae, including epistaxis, petechiae, gastro-intestinal bleeding, and intracranial hemorrhage. The current 'standard' therapies for the disease, corticosteroid immunosuppressive therapy and splenectomy, are associated with significant morbidity and are not effective for 25-30% of patients with chronic ITP (McMillan, 1997). Intravenous administration of pooled human immunoglobulin (IVIG) provides a transient increase in platelet counts for a large fraction of ITP patients; however, the high cost of this therapy prevents routine administration to individuals with chronic ITP. At present, no feasible alternative therapy is available to treat chronic ITP that is refractory to standard therapy, and fatal hemorrhage occurs in approximately 16% of affected patients (McMillan, 1997).

In spite of significant need for the development of new therapies of ITP, little progress has been realized since the discovery of IVIG activity in 1981. The mechanism(s) of IVIG action are poorly understood, and consequently, more specific (and perhaps less costly) therapies derived from non-human sources have not been developed. Clinical investigations of new ITP therapies are complicated by a number of factors. First, a high fraction of ITP patients (e.g., ~30-40% of acute cases) experience spontaneous resolution of ITP symptoms, without therapeutic intervention (George et al, 1996). Second, like

other autoimmune diseases, the severity of ITP appears to wax and wane with time, as evidenced by a spontaneous oscillation of patient platelet count. This natural fluctuation in apparent disease severity confounds the quantitative evaluation of new treatments. Third, although it is accepted that patients with very low platelet counts are more likely to experience hemorrhage, no suitable surrogate marker has been definitively associated with patient risk for severe hemorrhage. Finally, no adequate assays exist for quantification of anti-platelet antibodies (Raife et al., 1997). Thus, it is impossible to evaluate treatment effects on auto-antibody production or elimination.

Considering the difficulties associated with evaluating ITP treatments in man, it may be advantageous to assess new therapies in animal models of the disease, which may allow systematic, quantitative investigation. Suitable animal models would provide a reproducible condition of severe thrombocytopenia, mediated by anti-platelet antibodies. Ideally, the model should allow accurate and precise quantification of the anti-platelet antibodies, as such a model may facilitate a mechanistic evaluation of therapy. Some animal models of thrombocytopenia have previously been developed, including models that produce thrombocytopenia by non-immune mediated mechanisms (Kuter and Rosenberg, 1995; Meade et al., 1991) and by immune mediated mechanisms (Agam and Livne, 1992; Alves-Rosa et al., 2000; Ashida and Abiko, 1975; Coetzee et al., 2000; Hosono et al., 1995; Nieswandt et al., 2000; Oyaizu et al., 1988). However, to the authors' knowledge, no previous model of ITP is quantitative with respect to both anti-platelet antibody kinetics and the time course of thrombocytopenia.

Our goal was to develop an animal model of thrombocytopenia that is mediated by anti-platelet antibodies, and that is quantitative in nature. Such a model may allow for mechanistic evaluation of existing therapies (e.g., IVIG), as well as provide a foundation for the development of new therapies of ITP. In an attempt to develop a quantitative, anti-platelet antibody-mediated animal model of ITP, we have investigated the pharmacokinetics, pharmacodynamics, and platelet binding of a monoclonal anti-platelet antibody in the Sprague-Dawley rat.

## **Methods**

### *Production and Purification of 7E3*

7E3 producing hybridoma cells were obtained from the American Type Culture Collection (ATCC # HB-242, Manassas, VA). Balb/C mice (Harlan Sprague Dawley, Inc., Indianapolis, IN) were prepared for ascites production by an intraperitoneal injection of Freund's Incomplete Adjuvant (Sigma Chemical, St. Louis, MO), 0.4 ml/mouse, one week prior to injection of antibody producing cells. Hybridoma cells,  $1 \times 10^6$  cells/mouse in sterile 0.9% NaCl, were then injected intraperitoneally into the mice. Ascitic fluid was collected 10-15 days after injection of the hybridoma cells.

Anti-GPIIb/IIIa IgG was purified from ascitic fluid using Protein G chromatography (Pharmacia Biotech Hi-Trap protein G column, Uppsala, Sweden) and a Bio-Rad medium pressure chromatography system. The loading buffer was 20 mM  $\text{Na}_2\text{HPO}_4$  (Sigma Chemical), pH 7.0; the elution buffer was 0.1 M glycine (BioRad), pH 2.8. Purity of the IgG pool was assessed via electrophoresis (SDS-PAGE), using a 12% gel and standard techniques (Harlow and Lane, 1988). Antibody concentration was determined from sample absorbance at 280 nm, with the assumption that 1.35 AU = 1 mg/ml 7E3 (Harlow and Lane, 1988).

### *ELISA Procedure*

Rat plasma 7E3 concentrations were determined using a previously reported ELISA for mouse IgG in rat plasma, with slight modification (Hansen and Balthasar, 1999). Briefly, Nunc Maxisorp 96 well microplates (Nunc model # 4-42404, Roskilde, Denmark) were

coated with rat anti-mouse antibody (Pierce M-3534, 1:500 in a 20 mM Na<sub>2</sub>HPO<sub>4</sub> (PB), 0.25 ml/well) and incubated at 4 °C overnight. Samples and standards (0.25 ml/well) were then added and the plates were incubated for 2 hr at room temperature. Goat anti-mouse antibody-alkaline phosphatase conjugate (Sigma A-1682, 1:500 in PB, 0.25 ml/well) was added and allowed to incubate for 1 hr at room temperature. p-Nitro phenyl phosphate (Pierce, 4 mg/ml in diethanolamine buffer, pH 9.8, 0.2 ml) was placed in each well and the change in absorbance with time (over 10 min) was monitored via a microplate reader at 405 nm (Spectra Max 250, Molecular Devices, Sunnyvale, CA). Standards were made by diluting a stock 7E3 solution, with PBS, to the appropriate concentration (0, 10, 20, 40, 60, and 75 ng/ml), and by adding rat plasma (Hilltop Laboratories, Scottsdale, PA) to a final concentration of 1% (v/v). Standard curves were linear in this concentration range. Intra-assay variability was approximately 10% at the limit of quantitation (10 ng/ml).

#### *Specific activity of 7E3 preparation*

The fraction of antibody specifically directed against platelets (i.e., the specific activity) was assessed by ELISA. Briefly, 7E3, ~1 µg/ml in PBS, was incubated with ~5 × 10<sup>9</sup>/ml outdated human platelets (American Red Cross, Salt Lake City, UT) for 2 hr, while shaking at room temperature. Samples were centrifuged at 13,000g for 6 min to pellet out the platelets and the platelet-bound 7E3. Supernatant (i.e. unbound) 7E3 concentrations were determined by ELISA. Control mouse IgG, obtained from normal mouse blood, was incubated with platelets as a negative control. The specific activity was defined as the percent of the IgG bound to the platelets.

### *7E3 Binding to Rat Platelets*

**Flow cytometry.** Rat platelets were obtained from the blood of female Sprague-Dawley rats (Harlan Sprague Dawley, Inc., Indianapolis, IN). Blood was obtained either from a jugular vein catheter or via aortal venipuncture into a final concentration of approximately 10 units/ml heparin. Blood was centrifuged at  $\sim 650g$  for 2 min, platelet rich plasma was isolated, and the process was repeated. Platelets were washed with PBS twice, and re-suspended to a final concentration of  $2.2 \times 10^7$ /ml in PBS containing 1% bovine serum albumin (Sigma). 7E3 was added to the platelets and the suspension was incubated at room temperature for 2 hr. The final 7E3 and platelet concentrations were  $\sim 11 \mu\text{g/ml}$  and  $3.7 \times 10^6$ /ml, respectively. After incubation with 7E3, the platelets were washed with PBS and re-suspended in 100  $\mu\text{l}$  of a solution containing an FITC-labeled, anti-mouse IgG antibody (1:10 dilution, Pierce 31569). Following a 1 hr incubation, the platelets were washed, re-suspended in 1 ml PBS, and submitted for analysis by flow cytometry (Flow Cytometry Core Facility, Huntsman Cancer Institute, Salt Lake City, UT). Positive controls consisted of human platelets incubated with 7E3. Negative controls consisted of rat platelets incubated with control mouse IgG.

**Quantitative binding studies.** 7E3 was incubated with rat platelets for 2 hr, at 7E3 concentrations ranging from 3.7-73.9  $\mu\text{g/ml}$ , and a platelet concentration of  $9.76 \times 10^9$ /ml. Samples were centrifuged at  $\sim 3000g$  for 6 min and unbound (i.e., supernatant) 7E3 concentrations were determined using the ELISA. The apparent affinity of binding ( $K_d$ ) and the number of receptors for 7E3 ( $R_t$ ) on rat platelets were determined by fitting the free (i.e., unbound) and bound 7E3 concentration data to the following equation (Taylor

and Insel, 1990):  $[7E3]_b = \frac{[7E3]_f \times R_t \times K_A}{1 + K_A \times [7E3]_f}$ ;  $[7E3]_b$  is the molar concentration of 7E3

bound to the platelets, and  $[7E3]_f$  is the molar concentration of free 7E3. Non-linear least squares regression, using *The Scientist* (MicroMath, Salt Lake City, UT), found the best fit of the data and the resulting parameter values. The standard deviations reported for  $K_A$  and  $R_t$  were obtained from *The Scientist's* fit of the data. Control mouse IgG was incubated with rat platelets to detect possible non-specific binding.

#### *Pharmacokinetic Analysis*

Female Sprague-Dawley rats, 220-250 g, were instrumented with jugular vein cannulas under ketamine/xylazine anesthesia (75/15 mg/kg). Two to three days following surgery, animals were given an i.v. bolus dose of 7E3 (0.8, 4, or 8 mg/kg). Blood samples, 0.3 ml, were collected at 0, 1, 3, 6, 12, 24, 48, 72, 96, and 168 hours, and placed into 50  $\mu$ l of an acid-citrate-dextrose anticoagulant. The blood was then centrifuged at 13,000g for 2 min, and the plasma was isolated and stored at 4 °C until analysis (usually within 3 days). Plasma 7E3 concentrations were determined via ELISA, and the resulting 7E3 concentration values were adjusted for anticoagulant dilution by assuming a hematocrit value of 0.46.

Cannula patency was maintained by flushing the cannulas with ~ 0.15 ml heparinized saline after each blood draw (10 units/ml during the first 24 hr of heavy sampling, and 500 units/ml during daily sampling). In the rare case when cannula patency could not be maintained for the duration of the study, blood (10-20  $\mu$ l) for pharmacokinetic analysis

was taken from the rats' tail. Following the 0.8 mg/kg dose, 7E3 concentrations at 168 hr fell below the limit of quantification of the ELISA, and were not used in the subsequent pharmacokinetic analyses.

Non-compartmental approaches were used to analyze 7E3 concentration versus time data. Clearance (CL) was determined from the dose of 7E3 and the area under the 7E3 plasma

concentration time curve (AUC):  $CL = \frac{Dose}{AUC}$ . Terminal half-life values were determined

from the relationship:  $t_{1/2} = \frac{\ln(2)}{\lambda}$ , where  $\lambda$  is the negative of the slope of the terminal

portion of the ln C versus time plot. The terminal portion of the curve was defined as the

final three time points for each rat. Mean residence times (MRT) were estimated from

the quotient of AUMC and AUC (Gibaldi and Perrier, 1982), where AUMC is the area

under the 7E3 concentration×time vs. time curve. AUC and AUMC values were

determined using the linear trapezoidal method (Gibaldi and Perrier, 1982). Volume of

distribution at steady state ( $V_{ss}$ ) values were determined from the relationship  $V_{ss} =$

$MRT \times CL$  (Gibaldi and Perrier, 1982). Three rats were used for each dose, and the values

for the pharmacokinetic parameters are reported as mean  $\pm$  standard deviation.

### *Pharmacodynamic Analysis*

Three pharmacodynamic measures were chosen to evaluate the effects of 7E3 in the rat:

platelet count nadir values, bleeding time values following a standardized incision in the

tail, and blood volumes lost during the bleeding experiments. Rats (n=3-5 per group)

were dosed with 7E3 as described above. Control rats were given a similar volume of normal saline and were treated in the same manner as the dosed animals.

**Platelet counts.** Platelet counts were determined over the first 24 hr of the study using a Coulter Z1 particle counter. Briefly, an initial 20-fold dilution of blood was made into Coulter Isoton II solution and the solution was centrifuged at ~400g for 5 min. The supernatant was then further diluted with Coulter Isoton II solution and the resulting sample was analyzed using the Coulter counter (70  $\mu\text{m}$  aperture; counting window of 1.478-2.800  $\mu\text{m}$ ). Nadir percent platelet count values were determined from the quotient of the nadir platelet count value and the initial platelet count value for each rat (multiplied by 100).

**Bleeding times.** Bleeding times were determined using a method similar to that described by Booth and coworkers (Booth et al., 1996). Bleeding times were taken 24 hr following the initial dose of 7E3. A 1 cm long $\times$ 1 mm deep, template guided incision was made in the tail of anesthetized rats (25 mg/ml ketamine, titrated i.v.), 1 cm from the tip of the tail, ~45 degrees from the dorsal vein. Tails were immersed in 45 ml of normal saline (37  $^{\circ}\text{C}$ ) and the time until bleeding stopped was measured with a stopwatch. A maximum of 15 min was allowed for bleeding times, as the same animals were being used for the ongoing pharmacokinetic studies. Direct pressure was applied to the cut to stop the bleeding in the animals that bled longer than 15 min.

**Blood volume lost.** The volume of blood lost by each rat during the bleeding time measurement was determined spectrophotometrically (Rybak and Renzulli, 1993). Following the bleeding time experiment, 1 ml of 5% Triton-X 100, in saline, was added to the container with the blood. After ~ 30 min of shaking gently, samples were centrifuged at ~ 6000g for 5 min and analyzed at 546 nm on a Carey UV-Vis spectrophotometer. Standard curves were generated from the blood of each rat, and blood volume lost was determined from a linear regression analysis of the standards.

#### *Statistical Analysis*

The pharmacokinetic parameter values and platelet count nadir values obtained in this study were tested for statistical significance at the  $\alpha = 0.05$  level using one-way ANOVA analyses (*Instat*, GraphPad Software Inc., San Diego, CA). A Dunnett Multiple Comparisons test was used to compare the platelet count nadir values at each dose with the control value.

## **Results**

### *Production, Purification, and Specific Activity of 7E3*

Approximately 1 mg of pure mouse IgG was obtained from each mouse injected with 7E3-producing hybridoma cells. The purity of each IgG preparation was determined by SDS-PAGE. A representative gel comparing the ascitic fluid, the non-retained protein pool from the protein G purification, and the retained protein pool (IgG) is shown in figure 1.

For determination of the specific activity, the purified 7E3 preparation was incubated with human platelets. Following the removal of platelet-bound IgG by centrifugation, 7E3 concentrations in the supernatant were determined, and were 4-10% of the initial values. In similar experiments, recovery of control mouse IgG was complete. These results, taken together, suggest that the specific activity of the 7E3 preparation was 90-96% (90-96 mg of 7E3 per 100 mg total mouse IgG).

### *Binding of 7E3 to Rat Platelets*

Binding of 7E3 to rat platelets was assessed qualitatively using flow cytometry, and resulting histograms of fluorescence intensity verses number of particles are shown in figure 2. The relative median fluorescence intensity of the 7E3 coated rat platelets was ~ 33 (figure 2A), compared to a value of ~ 4 for the mouse IgG negative controls (figure 2B). The relative median fluorescence intensity of the 7E3 coated human platelets (positive control) was ~ 760 (figure 2C).

The binding curve resulting from the quantitative 7E3-rat platelet binding experiment is shown in figure 3. Non-linear least squares fitting of the data resulted in an apparent affinity of  $1.2\pm 0.2\times 10^7 \text{ M}^{-1}$  for the 7E3-rat platelet interaction, and a total receptor concentration of  $5.3\pm 0.5\times 10^{-7} \text{ M}$ , corresponding to  $3.3\pm 0.3\times 10^4$  7E3 binding sites per platelet. No binding of control, polyvalent, mouse IgG to rat platelets was observed.

### *Pharmacokinetic Analysis*

Plasma 7E3 concentration versus time data resulting from initial doses of 0.8, 4, and 8 mg/kg are plotted in figure 4. Table 1 lists the CL,  $V_{ss}$ , and  $t_{1/2}$  parameter values obtained from non-compartmental analyses of the 7E3 pharmacokinetic data. Dose-normalized plots of the 7E3 concentration versus time data did not superimpose, suggesting dose-dependent pharmacokinetics. Clearance decreased with dose, from a mean value of  $1.01\pm 0.08 \text{ ml/hr/kg}$  (0.8 mg/kg) to  $0.64\pm 0.08 \text{ ml/hr/kg}$  (8 mg/kg). This decrease in CL with dose was statistically significant ( $p=0.0043$ ), and is suggestive of concentration-dependent, saturable clearance of 7E3. As a result of this concentration-dependence, the reported CL values should be considered as time-averaged values. The methods employed to estimate MRT and  $V_{ss}$  are based on assumptions of linear disposition; consequently, the values of MRT and  $V_{ss}$  reported should be regarded as rough approximations (Cheng and Jusko, 1988). The disposition of 7E3 will be more completely characterized in future work that will attempt to build a suitable integrated compartmental PK model and PD model of the 7E3-induced thrombocytopenia. Dose-dependencies were not observed for  $V_{ss}$  ( $62\pm 15 \text{ ml/kg}$ ) or for  $t_{1/2}$  ( $61\pm 5 \text{ hr}$ ), with  $p=0.21$  and  $p=0.87$ , respectively.

### *Pharmacodynamic Analysis*

**Platelet counts.** Platelet counts decreased in a dose-dependent fashion upon administration of 7E3, with statistically significant decreases relative to control at each dose (0.8 mg/kg,  $p < 0.05$ ; 4 mg/kg,  $p < 0.01$ ; 8 mg/kg,  $p < 0.01$ ). Platelet count nadirs occurred 1-3 hr after administration of 7E3. Nadir values were  $54 \pm 4$ ,  $22 \pm 8$  and  $18 \pm 4\%$  of the initial platelet counts for the 0.8, 4, and 8 mg/kg doses, respectively (see figure 5). In 7E3 treated rats, absolute platelet counts fell to  $79 \pm 33$ ,  $25 \pm 6$ , and  $17 \pm 2 \times 10^6/\text{ml}$  (0.8, 4, and 8 mg/kg, respectively). Therefore, the 4 and 8 mg/kg doses of 7E3 reduced platelet counts to levels associated with severe thrombocytopenia in humans (i.e.,  $< 30 \times 10^6/\text{ml}$ ). Nadir values for the control group averaged  $67 \pm 10\%$  of initial platelet counts. Plots of the time course of thrombocytopenia following 7E3 administration are shown in figure 6.

**Bleeding times.** Bleeding times increased in a dose-dependent manner (relative to control) after treatment with 7E3 (figure 7). The bleeding times after the 0.8, 4, and 8 mg/kg doses of 7E3 were  $11.5 \pm 4.3$ ,  $14.7 \pm 0.6$ , and  $15 \pm 0$  min, respectively. Due to the ongoing nature of the pharmacokinetic studies on these animals, the maximum allowed bleeding time was set to be 15 min; this accounts for the decrease in the standard deviation of the bleeding time values with increase in dose of 7E3. Control animals bled for  $5.3 \pm 2.9$  min.

**Blood volume lost.** Blood volume lost was assessed from a standard curve relating blood concentration (v/v) to absorbance at 546 nm. Standard curves were created for each individual rat, and were linear from 0 to  $\sim 1$  ml of blood lost ( $r^2$  values typically

>0.999). The blood volume lost versus dose of 7E3 also increased in a dose-dependent fashion (figure 8), with values of  $87\pm46$ ,  $147\pm39$ , and  $349\pm358$   $\mu\text{l}$  for the 0.8, 4, and 8 mg/kg doses of 7E3, respectively. Saline treated animals lost an average of  $30\pm24$   $\mu\text{l}$  blood during the bleeding time experiments.

## Discussion

The main goal of the present work was to develop a quantitative, reproducible, passive immune model of thrombocytopenia in rats that will allow mechanistic evaluation of new therapies for ITP. To accomplish this goal, it was essential to identify a stable, reproducible, well-characterized antibody with reactivity for rat platelet antigens. No anti-rat platelet monoclonal antibody producing cells are commercially available; consequently, a murine anti-human platelet monoclonal antibody, 7E3, was selected and evaluated for use in developing a rat model of ITP.

7E3 is derived from a commercially available hybridoma cell line, is of the IgG<sub>1</sub> isotype, and binds to the platelet membrane GPIIb/IIIa complex, a common target of autoantibodies in patients afflicted with ITP (Fujisawa et al., 1991; Hou et al., 1997). The GPIIb/IIIa complex is present on rat platelets, and is known to have a high degree of amino acid sequence homology with human GPIIb/IIIa. Cieutat et al. report that rat and human GPIIb and GPIIIa share 78% and 92% amino acid sequence homology, respectively (Cieutat et al., 1993). 7E3 was first described in 1985, and bound human platelet GPIIb/IIIa with an apparent affinity of  $2.9 \times 10^8 \text{ M}^{-1}$ . Chimeric Fab fragments derived from the 7E3 antibody are used clinically to treat patients with ischemic cardiovascular disease (Coller, 1985; Mascelli et al., 1998).

Binding of 7E3 to rat platelets was demonstrated using flow cytometry and ELISA. The estimated number of binding sites for 7E3 on rat platelets is similar to the value reported for the number of binding sites for 7E3 on human platelets (n=41,300 for human platelets

(Wagner et al., 1996) vs. 33,000 for rat platelets). However, the apparent affinity of 7E3 for the rat platelet antigens is approximately 24-fold lower than the reported affinity of 7E3 for human platelets ( $K_A=1.2 \times 10^7 \text{ M}^{-1}$  for rat platelets vs.  $2.9 \times 10^8 \text{ M}^{-1}$  for human platelets) (Coller, 1985).

Pharmacokinetic characterization of 7E3 revealed a bi-exponential curve (figure 3), and apparent dose-dependency in 7E3 clearance. The pharmacokinetic parameters and bi-exponential decline in the concentration versus time curve for 7E3 are similar to other reports for mouse IgG pharmacokinetics in the rat (Bazin-Redureau et al., 1997; Caballero et al., 1998). To the authors' knowledge, no previous reports specifically show dose-dependencies in mouse IgG pharmacokinetics in the rat; however, some groups have reported dose-dependent changes in the pharmacokinetics of murine monoclonal antibodies in humans (Trang, 1992).

As introduced above, ITP patients are prone to develop bleeding complications ranging from epistaxis to fatal intracranial hemorrhage. These bleeding complications may be caused by thrombocytopenia and/or by auto-antibody induced changes in platelet aggregation and adhesion (Balduini et al., 1992). In the evaluation of our animal model, we utilized two common surrogates of bleeding tendency: bleeding time and blood volume lost (following a standardized tail-incision). Bleeding time is prolonged by thrombocytopenia or by inhibition of platelets, and is often used as a clinical measure of global bleeding tendency (Lavelle and MacLomhair, 1998). Additionally, some

researchers report blood loss to be a quantitative and reproducible method of determining bleeding (Rybak and Renzulli, 1993).

Although some variability was seen with thrombocytopenia, bleeding time, and blood loss, each clearly showed dose-dependent effects upon administration of 7E3. Part of the observed variability in the bleeding time and blood loss could be due to the use of heparin to keep the cannulas patent. However, every attempt was made to treat the animals as similarly as possible, and the heparin flushes cannot account for the dose-dependent increases in bleeding times and blood lost upon administration of 7E3. In these studies, no attempts were made to determine the extent to which 7E3-induced increases in bleeding are due to 7E3 effects on platelet aggregation as opposed to 7E3 effects on platelet count, and it is probable that both factors contributed to the observed increases in bleeding.

As shown in figure 6, saline treated control animals demonstrated an average nadir platelet count of ~70% of the initial values. This drop in platelet counts in control animals was reproducible, and is of unknown origin. It is possible that volume changes resultant from saline dosing, heavy sampling (3 samples within the first 3 hours), and fluid replacement may contribute to the thrombocytopenia observed in these animals. Additionally, prior to drawing each blood sample for analysis, an initial volume of blood (~0.3 ml) was drawn into a clean syringe to remove heparin from the cannula. After withdrawing the sample, the contents of the first syringe were then re-infused into the rat, to minimize blood loss. Given that others have reported that platelet activation may

result following blood exposure to biomaterials (including Silastic tubing), it is possible that the contact of the blood with the cannula or syringe could lead to platelet aggregation and /or consumption upon the re-infusion blood (Gemmell et al., 1995). Whatever the cause, the degree of thrombocytopenia observed in the control animals is very small compared with that seen following the highest doses of 7E3.

It is important to point out that this acute, passive model of immune thrombocytopenia does not precisely duplicate the human condition of ITP. Most notably, the thrombocytopenia observed in this animal model is produced by exogenous administration of antibody; in the human condition the anti-platelet antibody is produced endogenously. Consequently, this model will not facilitate investigation of therapies that involve inhibition of antibody production. Despite the inability of this model to fully replicate the human condition, 7E3-induced immune thrombocytopenia is consistent with the observed clinical manifestations of ITP, in that 7E3 decreases platelet count and increases measures of bleeding tendency. Consequently, this will be a useful ITP model in that it will allow quantitative assessment of therapies that interfere with anti-platelet antibody induced thrombocytopenia and bleeding.

In summary, this work demonstrates that 7E3, an anti-human GPIIb/IIIa monoclonal antibody, binds to rat platelets with an affinity of  $1.2 \pm 0.2 \times 10^7 \text{ M}^{-1}$ . Additionally, an enzyme-linked immunosorbent assay was developed, which allowed for pharmacokinetic analysis of the disposition of 7E3 in conscious rats. Finally, administration of 7E3 to

Sprague-Dawley rats produces a dose-dependent, reproducible thrombocytopenia, with increases in bleeding time and bleeding volume.

A significant advantage of this model of ITP is that it is produced by a readily available, well-characterized source of anti-platelet antibody, allowing it to be easily adapted for various applications. Because this model provides a unique opportunity to develop quantitative relationships between anti-platelet antibody concentrations and effects, the model is expected to facilitate systematic, mechanistic evaluations of new therapies of ITP.

## References

Agam G and Livne AA (1992) Erythrocytes with covalently bound fibrinogen as a cellular replacement for the treatment of thrombocytopenia. *Eur J Clin Invest* **22**:105-112.

Alves-Rosa F, Stanganelli C, Cabrera J, van Rooijen N, Palermo MS and Isturiz MA (2000) Treatment with liposome-encapsulated clodronate as a new strategic approach in the management of immune thrombocytopenic purpura in a mouse model. *Blood* **96**:2834-2840.

Ashida SI and Abiko Y (1975) Protective effect of pantethine on experimental thrombocytopenia in the rat. *Thromb Diath Haemorrh* **33**:528-539.

Balduini CL, Bertolino G, Noris P, Piovella F, Sinigaglia F, Bellotti V, Samaden A, Torti M and Mazzini G (1992) Defect of platelet aggregation and adhesion induced by autoantibodies against platelet glycoprotein IIIa. *Thromb Haemost* **68**:208-213.

Bazin-Redureau MI, Renard CB and Scherrmann JM (1997) Pharmacokinetics of heterologous and homologous immunoglobulin G, F(ab')<sub>2</sub> and Fab after intravenous administration in the rat. *J Pharm Pharmacol* **49**:277-281.

Booth BP, Jacob S, Bauer JA and Fung HL (1996) Sustained antiplatelet properties of nitroglycerin during hemodynamic tolerance in rats. *J Cardiovasc Pharmacol* **28**:432-438.

Caballero F, Pelegri C, Castell M, Franch A and Castellote C (1998) Kinetics of W3/25 anti-rat CD4 monoclonal antibody. Studies on optimal doses and time-related effects. *Immunopharmacology* **39**:83-91.

Cheng HY and Jusko WJ (1988) Mean residence time concepts for pharmacokinetic systems with nonlinear drug elimination described by the Michaelis-Menten equation. *Pharm Res* **5**:156-164.

Coetzee LM, Pieters H, van Wyk V, Cooper S, Roodt J, De Reys S and Badenhorst PN (2000) The effect of monoclonal anti-human-platelet antibodies on platelet kinetics in a baboon model: IgG subclass dependency. *Thromb Haemost* **83**:148-156.

Coller BS (1985) A new murine monoclonal antibody reports an activation-dependent change in the conformation and/or microenvironment of the platelet glycoprotein IIb/IIIa complex. *J Clin Invest* **76**:101-108.

Fujisawa K, TE OT, Tani P, Loftus JC, Plow EF, Ginsberg MH and McMillan R (1991) Autoantibodies to the presumptive cytoplasmic domain of platelet glycoprotein IIIa in

patients with chronic immune thrombocytopenic purpura. *Blood* **77**:2207-2213.

Gemmell CH, Ramirez SM, Yeo EL and Sefton MV (1995) Platelet activation in whole blood by artificial surfaces; Identification of platelet-derived microparticles and activated platelet binding to leukocytes as material-induced activation events. *J Lab Clin Med* **125**:276-287.

George JN, Woolf SH, Raskob GE, Wasser JS, Aledort LM, Ballem PJ, Blanchette VS, Bussel JB, Cines DB, Kelton JG, Lichtin AE, McMillan R, Okerbloom JA, Regan DH and Warrier I (1996) Idiopathic thrombocytopenic purpura: a practice guideline developed by explicit methods for the American Society of Hematology. *Blood* **88**:3-40.

Gibaldi M and Perrier D (1982) *Pharmacokinetics*, 2 ed, Vol 15 Marcel Dekker, Inc., New York.

Hansen RJ and Balthasar JP (1999) An ELISA for quantification of murine IgG in rat plasma: application to the pharmacokinetic characterization of AP-3, a murine anti-glycoprotein IIIa monoclonal antibody, in the rat. *J Pharm Biomed Anal* **21**:1011-1016.

Harlow E and Lane D (1988) *Antibodies: A Laboratory Manual*. Cold Spring Harbor Laboratory, New York.

Hosono M, Sone N, Endo K, Saga T, Kobayashi H, Hosono MN, Sakahara H, Yasunaga K and Konishi J (1995) Kinetics of platelets in dogs with thrombocytopenia induced by antiglycoprotein IIb/IIIa receptor monoclonal antibody. *Nucl Med Biol* **22**:71-76.

Hou M, Stockelberg D, Kutti J and Wadenvik H (1997) Immunoglobulins targeting both GPIIb/IIIa and GPIb/IX in chronic idiopathic thrombocytopenic purpura (ITP): evidence for at least two different IgG antibodies. *Br J Haematol* **98**:64-67.

Kuter DJ and Rosenberg RD (1995) The reciprocal relationship of thrombopoietin (c-Mpl ligand) to changes in the platelet mass during busulfan-induced thrombocytopenia in the rabbit. *Blood* **85**:2720-2730.

Lavelle SM and MacIomhair M (1998) Bleeding Times and the Antithrombotic Effects of High-Dose Aspirin, Hirudin and Heparins in the Rat. *Ir J Med Sc* **167**:216-220.

Mascelli MA, Lance ET, Damaraju L, Wagner CL, Weisman HF and Jordan RE (1998) Pharmacodynamic profile of short-term abciximab treatment demonstrates prolonged platelet inhibition with gradual recovery from GP IIb/IIIa receptor blockade. *Circulation* **97**:1680-1688.

McMillan R (1997) Therapy for adults with refractory chronic immune thrombocytopenic purpura. *Ann Intern Med* **126**:307-314.

Meade CJ, Heuer H and Kempe R (1991) Biochemical pharmacology of platelet-activating factor (and PAF antagonists) in relation to clinical and experimental thrombocytopenia. *Biochem Pharmacol* **41**:657-668.

Nieswandt B, Bergmeier W, Rackebrandt K, Gessner JE and Zirngibl H (2000) Identification of critical antigen-specific mechanisms in the development of immune thrombocytopenic purpura in mice. *Blood* **96**:2520-2527.

Oyaizu N, Yasumizu R, Miyama-Inaba M, Nomura S, Yoshida H, Miyawaki S, Shibata Y, Mitsuoka S, Yasunaga K, Morii S, Good RA and Ikehara S (1988) (NZW x BXSB)F1 mouse. A new animal model of idiopathic thrombocytopenic purpura. *J Exp Med* **167**:2017-2022.

Raife TJ, Olson JD and Lentz SR (1997) Platelet antibody testing in idiopathic thrombocytopenic purpura. *Blood* **89**:1112-1114.

Rybak EM and Renzulli LA (1993) A liposome based platelet substitute, the plateletsome, with hemostatic efficacy. *Biomater, Art, Cells & Immob Biotech* **21**:101-118.

Taylor P and Insel PA (1990) Molecular Basis of Pharmacologic Selectivity, in *Principles of Drug Action: The Basis of Pharmacology*, 3 ed (Pratt WB and Taylor P eds) pp 1-102, Churchill Livingstone Inc., New York.

Trang JM (1992) Pharmacokinetics and Metabolism of Therapeutic and Diagnostic Antibodies, in *Protein Pharmacokinetics and Metabolism*, , Vol 1 (Ferraiolo BL, Mohler MA and Gloff CA eds) pp 223-270, Plenum Press, New York.

Wagner CL, Mascelli MA, Neblock DS, Weisman HF, Collier BS and Jordan RE (1996) Analysis of GPIIb/IIIa receptor number by quantification of 7E3 binding to human platelets. *Blood* **88**:907-914.

**Footnotes**

This work was presented, in part, at the annual meeting of the American Association of Pharmaceutical Scientists, 1999 (New Orleans, LA).

R.J.H. is a Pre-Doctoral Fellow of the American Foundation for Pharmaceutical Education.

TABLE 1

Pharmacokinetic parameters estimated following 7E3 administration to rats

Dose of 7E3 (mg kg <sup>-1</sup> )	CL (ml hr <sup>-1</sup> kg <sup>-1</sup> )*	V <sub>ss</sub> (ml kg <sup>-1</sup> )	t <sub>1/2</sub> (hr)
0.8	1.01 ± 0.08	78 ± 29	63 ± 26
4	0.86 ± 0.09	57 ± 8	55 ± 17
8	0.64 ± 0.08	50 ± 10	64 ± 24

Non compartmental techniques were used to determine each parameter value. Values are listed as mean ± standard deviation (n=3).

\*Statistically significant differences between the parameter values were found only in the CL (p=0.0043).

## Legends for Figures

Figure 1. SDS-PAGE (non-reducing conditions, 12% gel) analysis of the purity of the IgG pool collected from Protein G chromatography of 7E3-containing ascitic fluid. Lanes 1&2 show proteins in the pre-purified ascitic fluid (20 and 200 fold dilution of ascitic fluid, respectively). Lanes 3 and 4 show the non-retained proteins (non-IgG proteins) collected from protein G chromatography ( $\sim 3.2$  and  $0.2 \mu\text{g}/\text{well}$ , respectively). Lanes 5 and 6 show the retained protein (IgG) from the purification ( $\sim 1.3$  and  $0.069 \mu\text{g}/\text{well}$ , respectively).

Figure 2. Binding of 7E3 to rat platelets by flow cytometry. Histograms of relative fluorescence intensity versus platelet number are plotted. Platelets (rat or human) were incubated with 7E3 or mouse IgG. After washing the platelets to remove unbound IgG, a secondary anti-mouse IgG-FITC antibody was added, and samples were analyzed by flow cytometry. Figure 2A shows the histogram obtained upon incubation of 7E3 and rat platelets. Figure 2B shows the negative control (mouse IgG incubated with rat platelets), and figure 2C shows a positive control (7E3 incubated with human platelets).

Figure 3. Binding curve obtained after incubation of 7E3 with rat platelets. Total platelet concentration was held constant as the 7E3 concentration was increased. Free (i.e., unbound) 7E3 concentrations were determined by ELISA. Data were fit as described in the text. Error reported is the standard deviation estimated by *The Scientist* software.

Figure 4. Plasma 7E3 pharmacokinetics for three i.v. doses of 7E3 (0.8[○], 4[□], and 8[Δ] mg/kg) in rats (n=3/group). 7E3 concentrations were determined via ELISA. Error bars represent the standard deviation about the mean concentration at each time point.

Figure 5. Time course of thrombocytopenia produced by administration of saline (◇), and 0.8 (○), 4 (□), or 8 (Δ) mg/kg doses of 7E3 to rats. Rats were given an i.v. dose of 7E3, and platelet counts were obtained using a Coulter Z1 particle counter. The control and treated groups consisted of 5 and 4 rats respectively. Error bars represent the standard deviation about the mean.

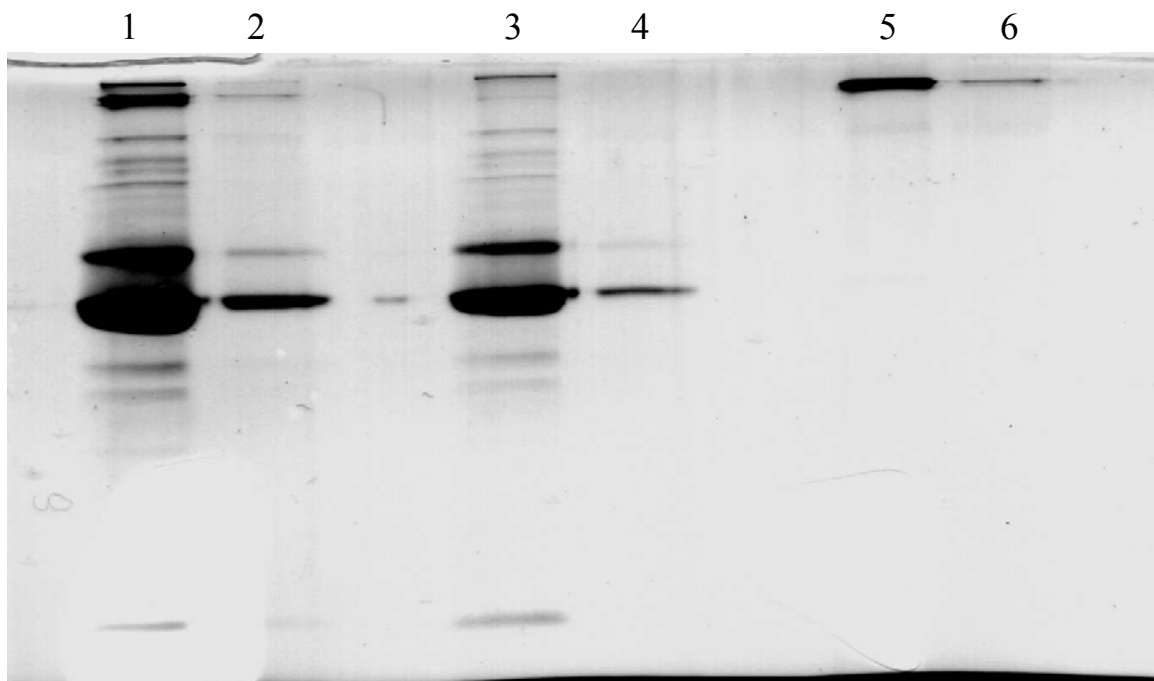
Figure 6. Nadir percent platelet counts obtained after 7E3 (0.8, 4, or 8 mg/kg) administration. Control and treated groups consisted of 5 and 4 rats, respectively. Error bars represent the standard deviation about the mean value. Each dose resulted in statistically significant decreases in platelet counts relative to control.

Figure 7. Bleeding times following a 1mm × 1 cm incision in the tail of the rat. Control and treated groups (0.8, 4, and 8 mg/kg 7E3) consisted of 3-4 rats/group. A maximum of 15 minutes was allowed for the bleeding time studies. Error bars represent the standard deviation about the mean.

Figure 8. Blood loss during bleeding time experiments for control, 0.8, 4, and 8mg/kg 7E3-treated rats. Blood volumes were determined spectrophotometrically, after lysis of

the red blood cells and analysis of absorbance at 546 nm. Error bars represent the standard deviation about the mean.

Figure 1.



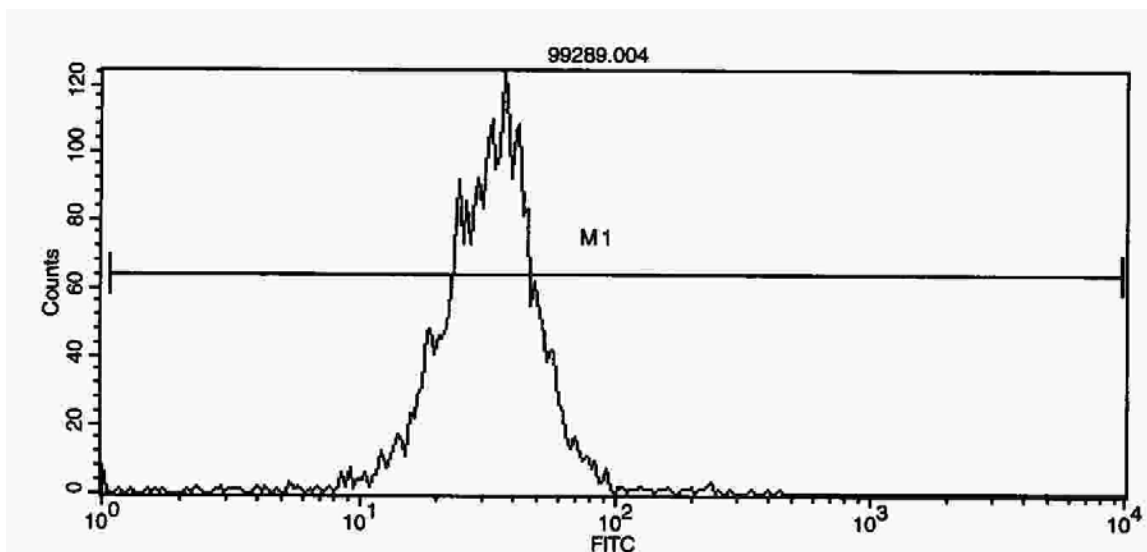


Figure 2A

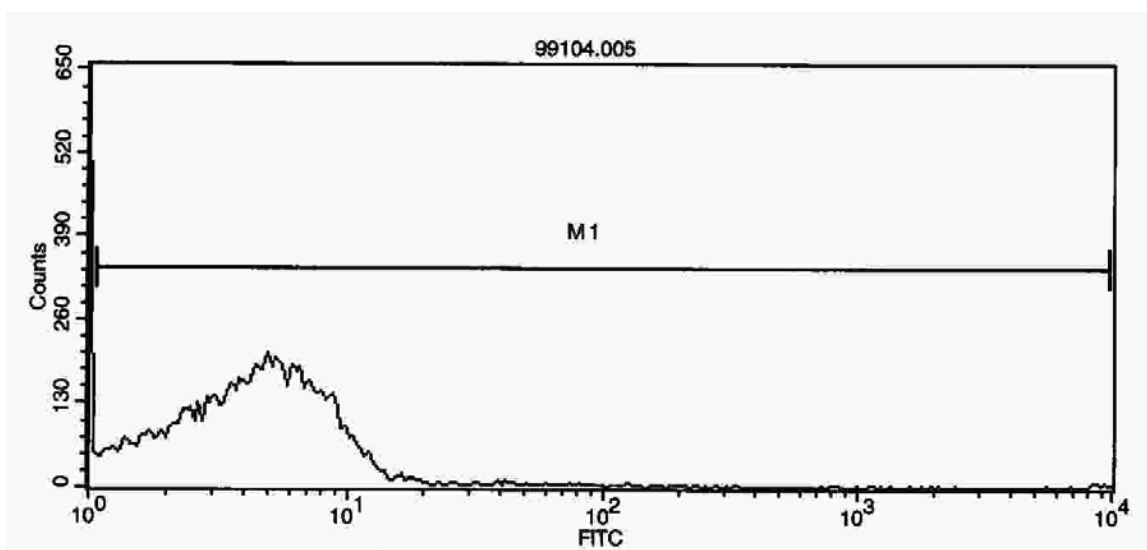


Figure 2B

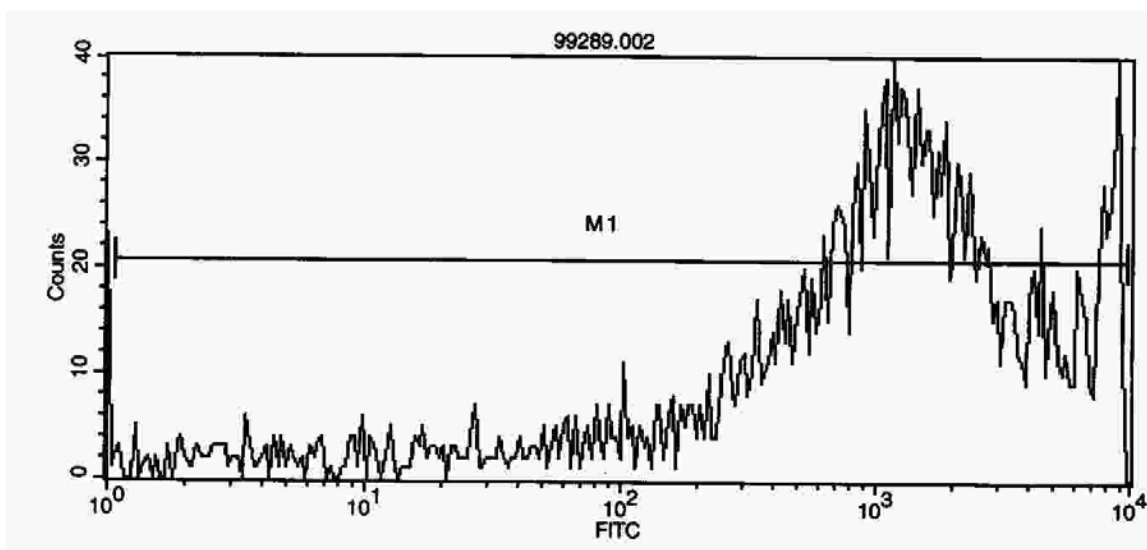


Figure 2C

Figure 3.

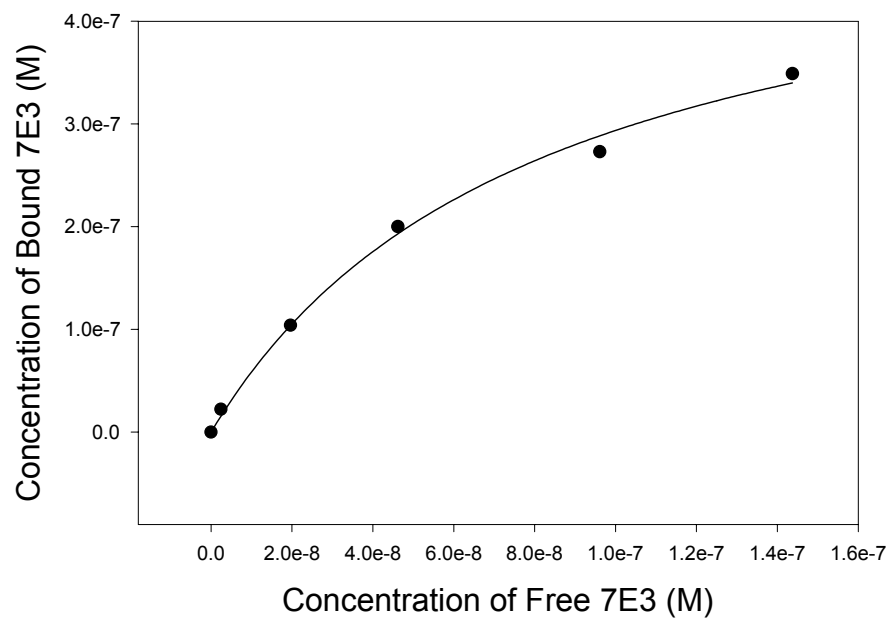


Figure 4.

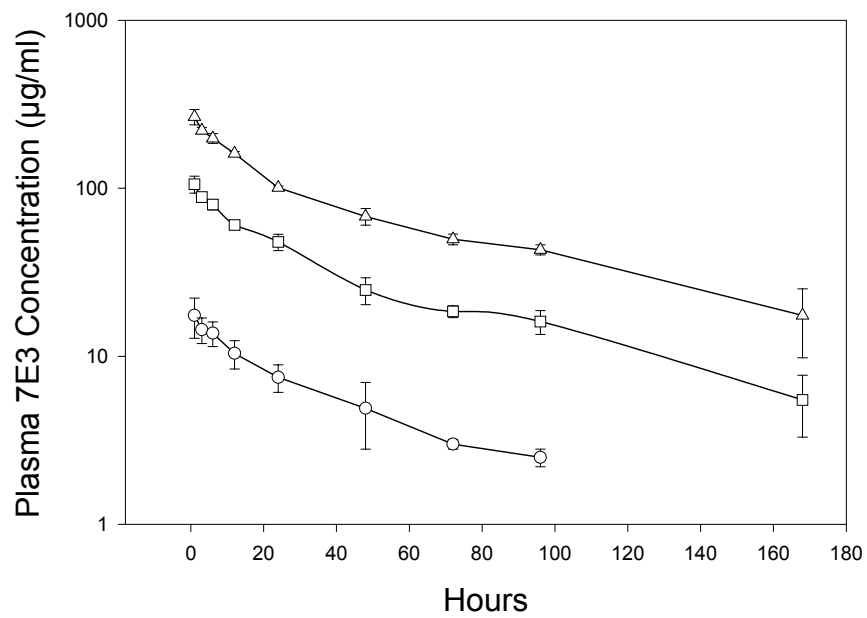


Figure 5.

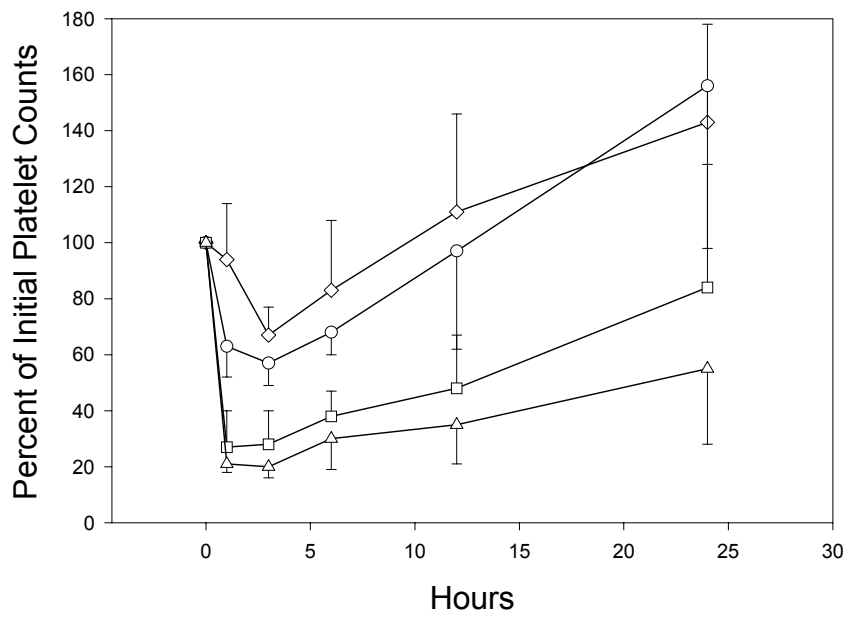


Figure 6.

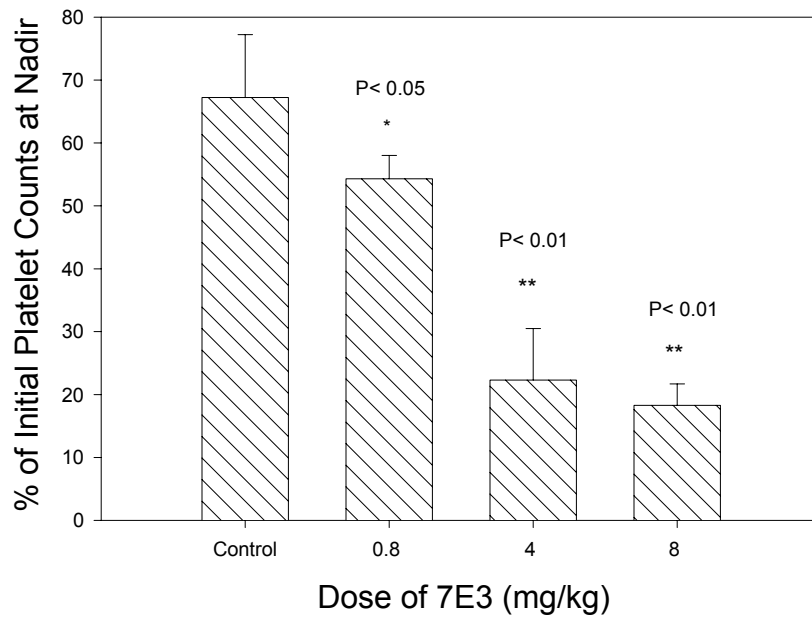


Figure 7.

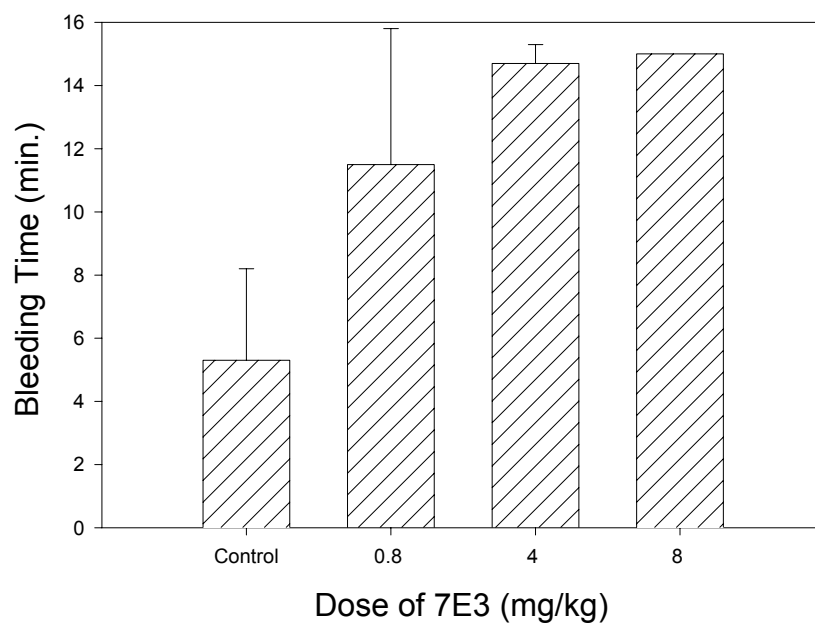
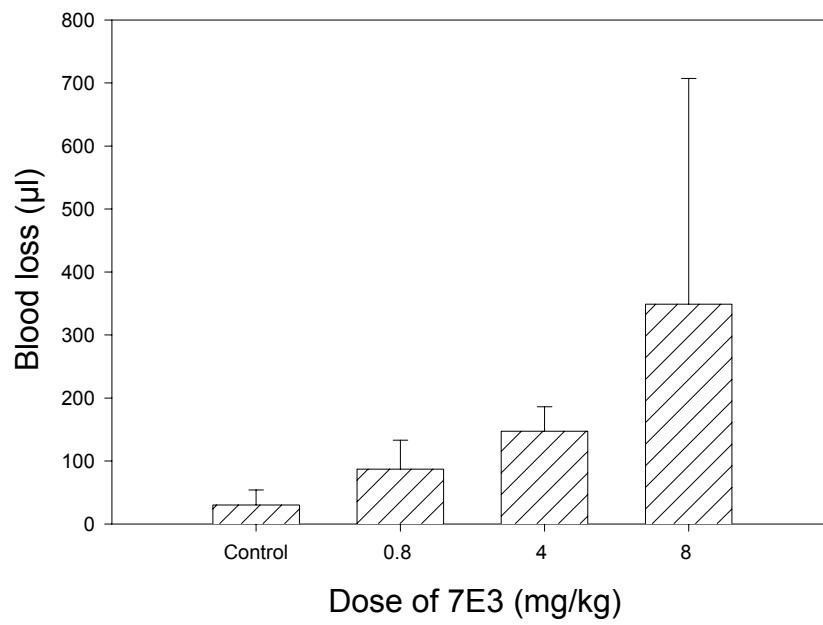


Figure 8.



# CHAPTER FOUR

---

## EFFECTS OF INTRAVENOUS IMMUNOGLOBULIN ON PLATELET COUNT AND ANTI-PLATELET ANTIBODY DISPOSITION IN A RAT MODEL OF THROMBOCYTOPENIA

---

*This work has been submitted for publication in Blood (2001).*

## **Abstract**

Experiments were conducted to investigate the effects of intravenous immunoglobulin (IVIG) in a rat model of immune thrombocytopenia (ITP). Rats were pre-treated with 0-2 g/kg IVIG and then challenged with an anti-platelet antibody (7E3, 8 mg/kg). IVIG effects on 7E3-induced thrombocytopenia and on 7E3 pharmacokinetics were determined. IVIG pre-treatment led to significant changes in the degree and in the time-course of 7E3-induced thrombocytopenia ( $p = 0.031$ ). Nadir percent platelet counts were 121-279% greater in IVIG treated animals (0.4-2 g/kg) than in animals receiving 7E3 alone. IVIG treatment also led to dose-dependent increases in 7E3 clearance ( $p < 0.001$ ), with greater than 2-fold increases in 7E3 clearance seen following the highest dose of IVIG. In vitro experiments showed that IVIG effects on platelet count are not likely due to anti-idiotypic inhibition of 7E3-platelet binding and that IVIG did not directly bind to 7E3. Consequently, IVIG-7E3 binding cannot explain the increase of 7E3 clearance following IVIG treatment. We propose that the observed increase in 7E3 clearance with IVIG therapy is due to saturation of the FcRn salvage receptor for IgG. The importance of the effect of IVIG on 7E3 clearance to the prevention of thrombocytopenia in these animals is unclear at present; nonetheless, these data provide experimental support for a new mechanism of IVIG action in ITP (i.e., IVIG mediated increases in anti-platelet antibody elimination). This model of ITP will be useful for further investigations of IVIG mechanism of action, and for development of new therapies of ITP.

## **Introduction**

In 1981, Imbach and coworkers reported that intravenous administration of large amounts of human immunoglobulin (IVIG) increases platelet counts in children afflicted with immune thrombocytopenia (ITP).<sup>1</sup> The efficacy of IVIG in ITP has been confirmed by a number of additional studies,<sup>2</sup> and IVIG has shown benefit as a treatment for several other autoimmune conditions.<sup>3</sup> Many studies have investigated the mechanisms by which IVIG achieves effects in the treatment of autoimmune diseases.<sup>4</sup> With regard to ITP, early investigations led to the conclusion that IVIG effects are mainly due to blockade of the Fc receptors responsible for phagocytosis of antibody-opsonized platelets.<sup>5</sup> Subsequent studies showed that Fc-depleted IVIG preparations provided increases in platelet counts in some ITP patients, and suggested that some of IVIG effects are non-Fc dependent<sup>6</sup> (e.g., perhaps mediated by anti-idiotypic antibodies).<sup>7,8</sup> Recently, it was reported that IVIG effects are due to stimulation of FcγRIIb expression on macrophage cells, leading to inhibition of platelet phagocytosis.<sup>9</sup> Other proposed effects of IVIG in ITP include: inhibition of anti-platelet antibody production,<sup>10</sup> inhibition of complement mediated platelet destruction,<sup>11</sup> and stimulation of platelet production.<sup>12</sup> Although a number of possible effects of IVIG have been identified, a clear definition of the mechanisms of IVIG action in ITP remains elusive due to analytical difficulties associated with the quantification of IVIG effects in ITP patients. Given the efficacy of IVIG in ITP, it is plausible that delineation of IVIG mechanism of action may facilitate the development of better therapies for the disease.

Recently, our lab reported a new animal model of ITP, produced by administration of an anti-platelet monoclonal antibody (7E3) to rats.<sup>13</sup> This model is unique in that it allows quantification of anti-platelet antibody plasma concentrations as well as quantification of platelet counts. Because of its quantitative nature, this model will facilitate systematic investigations of IVIG effects in ITP, and may provide a foundation for the development and evaluation of new treatments of the disease.

The purpose of the present study was to demonstrate and investigate IVIG effects in our rat model of ITP. In so doing, we quantified IVIG effects on 7E3-induced thrombocytopenia, and on 7E3 pharmacokinetics. We have found that IVIG treatment led to dose-dependent increases both in platelet counts and in the clearance of anti-platelet antibody. The latter effect is a finding that, to our knowledge, has not been previously reported. The relationship between IVIG effects on anti-platelet antibody clearance and IVIG effects on thrombocytopenia is not clear at present; however, our results suggest that this animal model may be used to perform quantitative evaluations of this, and other, proposed mechanisms of IVIG action.

## Methods

*Animals and Reagents.* Female Sprague-Dawley rats, 200-225g, were used for the *in vivo* analyses. Rats were instrumented with jugular vein catheters 2 days prior to treatment. 7E3, a murine anti-GPIIb/IIIa monoclonal antibody, was produced from hybridoma cells obtained from American Type Culture Collection (Manassas, VA). Hybridoma cells were grown in serum free media (Life Technologies, Inc., Rockville, MD) and antibodies were purified from the media using protein G chromatography, as reported previously.<sup>13</sup> Intravenous immunoglobulin (IVIG) preparations were obtained from Baxter Healthcare Corporation (Hyland Division, Glendale, CA) and Bayer Corporation (Pharmaceutical Division, Elkhart, IN). Both IVIG preparations are solvent /detergent-treated and are manufactured via cold ethanol fractionation of human plasma. Outdated human platelets were obtained from the American Red Cross (Buffalo, NY and Salt Lake City, UT). A murine anti-methotrexate IgG<sub>1</sub> monoclonal antibody (AMI) was generated and purified in our laboratory. Goat anti-human IgG (no cross reactivity to goat and mouse serum proteins) and alkaline phosphatase conjugated goat anti-mouse IgG (no cross reactivity to goat and human serum proteins) were both obtained from Rockland (Gilbertsville, PA). Mouse anti-human IgG, FITC-labeled anti-mouse IgG, and p-nitro phenyl phosphate were from Pierce (Rockford, Illinois). Bovine serum albumin (BSA) and buffer reagents were obtained from Sigma (St. Louis, MO). Buffers were phosphate-buffered saline (pH 7.4, PBS), 0.02 M Na<sub>2</sub>HPO<sub>4</sub> (PB), and PB + 0.05% Tween-20 (PB-Tween).

*IVIG effects on 7E3-mediated thrombocytopenia and 7E3 kinetics.* Rats were dosed with IVIG (0.4, 1, or 2 g/kg) via the jugular vein catheter. Following IVIG dosing, a blood

sample (0.15 ml) was withdrawn for a baseline measurement of platelet counts. Rats were then dosed with 7E3, 8 mg/kg, and platelet counts were taken over 24 h, using a Cell-Dyne 1700 multi-parameter hematology analyzer (Abbott Laboratories, Abbott Park, IL). Control animals were dosed with saline, followed by 7E3. The platelet nadir for each animal was the lowest observed platelet count. Platelet count data was normalized by the initial platelet count because of large inter-animal variability in initial platelet counts. By normalizing the data, the effects of 7E3 and IVIG can be better compared between animals.

Blood samples (0.15 ml) were taken for pharmacokinetic analysis at 1, 3, 6, 12, 24, 48, 96, and 168 h after 7E3 dosing. 7E3 plasma concentrations were determined using an ELISA.<sup>13,14</sup> Standard non-compartmental pharmacokinetic techniques were used to estimate 7E3 clearance and terminal half-life following IVIG administration, as previously reported.<sup>13</sup> Catheters were kept patent by flushing with 0.1 ml heparin (50 units/ml) between blood draws. Each group consisted of 4 rats.

*Binding of IVIG to 7E3.* Goat anti-human IgG (diluted 1:500 in PB, 0.25 ml/well) was added to the wells of a Nunc Maxisorp 96 well microplate (Nunc model # 4-42404, Roskilde, Denmark), and the plate was allowed to incubate at 4°C, overnight. IVIG (25 mg/ml) and 7E3 (0, 0.01, 0.05, and 0.10 mg/ml) were combined in test tubes and allowed to incubate for 2 h at 37°C. Positive control samples consisted of IVIG incubated with mouse anti-human IgG (Pierce, #31137), at the same concentrations as indicated for 7E3. Samples and controls were diluted by 1000 into 1% BSA, in PBS, and then added to the

microplate (0.25 ml/well) and allowed to incubate for 2 h at room temperature. Alkaline phosphatase-labeled anti-mouse IgG (diluted 1:500 in PB, 0.25 ml/well) was then added to the plate, and allowed to incubate for 45 min, also at room temperature. Finally, p-nitro phenyl phosphate (4 mg/ml in diethanolamine buffer, pH 9.8) was added, 0.2 ml/well, and the plate was read at 405 nm on a plate-reader (Spectra Max 340PC, Molecular Devices, Sunnyvale, CA). The plate was read over a period of 10 minutes, and the slopes of the absorbance verses time curves were used to assess assay response (dA/dt). Each sample was assayed in triplicate, and responses are shown as mean  $\pm$  standard deviation. Between each step of the assay, the wells of the microplate were washed 3 times with PB-Tween.

*IVIG effects on AMI pharmacokinetics.* Rats (n=3 per group) were dosed via the jugular vein cannula with 2 g/kg IVIG (or saline for controls), followed by AMI (8 mg/kg). Blood samples were taken over 1 week, and plasma was analyzed for AMI concentrations via ELISA. Pharmacokinetic analyses were performed as described above for 7E3.

*IVIG effects on 7E3-PLT binding.* Both qualitative and quantitative studies were performed to determine if IVIG could inhibit the binding of 7E3 to human platelets. In a qualitative study, 10  $\mu$ g/ml 7E3 was incubated for 1.5 h with human platelets ( $1 \times 10^7$  PLT/ml) in the presence or absence of IVIG (2.5 mg/ml). Control mouse IgG was a negative control. The samples were centrifuged at 4000 rpm for 6 min, washed with PBS (twice), and then incubated for 45 min with 100  $\mu$ l of a 1:10 dilution (in PBS) of FITC-labeled anti-mouse IgG solution. Samples were washed again, re-suspended in PBS, and

submitted for analysis by flow cytometry (Flow Cytometry Core Facility, Huntsman Cancer Institute, Salt Lake City, UT).

In quantitative inhibition studies, the potential for IVIG inhibition of 7E3-platelet binding was studied in greater detail. Human platelets ( $8.2 \times 10^8/\text{ml}$ ) were incubated with 7E3 (4.8-72.5  $\mu\text{g}/\text{ml}$ ) in the presence or absence of IVIG (25  $\text{mg}/\text{ml}$ ), for 2 h. Samples were then centrifuged at  $\sim 3000g$  for 6 min to obtain a platelet pellet. A portion of each supernatant was obtained and assayed for unbound 7E3 concentration. Binding of 7E3 to platelets, in the presence and absence of 7E3, was analyzed by fitting the data to the

following binding curve: 
$$F_f = \frac{[7E3]_f \times K_a + 1}{1 + K_a \times [7E3]_f + K_a \times R_t}$$

In the above equation,  $F_f$  is the free fraction of 7E3,  $K_A$  is the apparent affinity for 7E3-platelet binding,  $[7E3]_f$  is the unbound molar 7E3 concentration, and  $R_t$  is the total receptor concentration. Micromath Scientist was used to generate non-linear least squares analyses of the data, and parameter values and reported standard deviations are from the software output.

*Statistical Analysis.* Differences in the time course of platelet counts for the treatment groups were tested for statistical significance using a two-way, repeated measures ANOVA. Analysis of statistically significant differences between platelet nadir values was performed using a Kruskal-Wallis one-way ANOVA on rank, with a Dunnett multiple comparisons test to compare treatment groups to control. A non-parametric ANOVA was used because the variance between the groups differed statistically. To compare 7E3 clearance and terminal  $t_{1/2}$  values between treatment groups, one-way

ANOVAs, with Tukey multiple comparisons procedures, were used. A t-test was used to compare AMI clearance between groups. One way ANOVA's (with Dunnett post tests) were also used to test for significant 7E3-IVIG and control IgG-IVIG binding. Statistical analyses were accomplished using SigmaStat 2.0 (SPSS Science, Chicago, IL), and the level of significance for each test was  $\alpha=0.05$ .

## Results

*IVIG effects on 7E3-mediated thrombocytopenia and 7E3 kinetics.* At a dose of 8 mg/kg, 7E3 caused rapid and severe thrombocytopenia in the rats. As can be seen in figure 1, pretreatment of rats with IVIG significantly altered the platelet count time course following the dose of 7E3 ( $p=0.031$ ). Statistically significant differences from control ( $p<0.01$ ) were seen in platelet counts at 1 and 3 hr for the 2 g/kg IVIG group, and at 3 hr for the 1 g/kg IVIG group. Percent platelet counts were used to assess the effects of 7E3 in this model because of the large degree of variability in initial absolute platelet counts. However, each group had comparable mean initial platelet counts, with control, 0.4, 1 and 2g/kg IVIG groups having absolute initial counts of  $326\pm62$ ,  $323\pm137$ ,  $272\pm111$ , and  $301\pm69 \times 10^9$  platelets/l, respectively. Because absolute platelet count may be important in assessing bleeding risk, we also looked at platelet count nadir values as a metric to determine IVIG effects in this model. After 7E3 treatment alone, the animals reached an absolute platelet nadir of  $48\pm28 \times 10^9$  platelets/l, which corresponded to an average of  $14\pm8\%$  of initial counts. With IVIG pretreatment, a 121-279% increase in the nadir percent platelet count (compared to control) was observed ( $p=0.044$ ), with values of  $31\pm26$ ,  $44\pm24$ , and  $53\pm27\%$  for the 0.4, 1, and 2 g/kg IVIG doses, respectively. Each IVIG treated group differed significantly from the control ( $p<0.05$ ). However, IVIG was not completely effective at blocking thrombocytopenia, even at the highest doses. The percentage of rats reaching a threshold value of thrombocytopenia ( $<30\%$  of initial counts) decreased with dose for animals pre-treated with IVIG, with 75%, 50%, and 25% of rats in the 0.4, 1, and 2 g/kg IVIG groups having nadir platelet counts less than 30% of initial.

IVIG effects on 7E3 pharmacokinetics were determined by measuring 7E3 plasma concentrations following pretreatment of the rats with IVIG. IVIG enhanced the clearance of 7E3, as can be seen from figure 2 and table 1. An ANOVA revealed highly significant differences between the CL values calculated for the 4 treatment groups ( $P < 0.001$ ). Differences in 7E3 clearance were shown to be statistically significant for all pairs of treatment groups, except for the comparison of data from animals receiving 0.4 versus 1 g/kg IVIG (Tukey multiple comparisons test). Significant differences from control were seen in 7E3 concentrations at each time point  $\geq 12$  h for the 2 g/kg IVIG group, and  $\geq 48$  hr for the 0.4 and 1 g/kg IVIG groups.

*Binding of IVIG to 7E3.* Binding of 7E3 to IVIG, in vitro, could not be detected in this study. Figure 3 shows the results obtained from the experiment designed to detect 7E3-IVIG binding. IVIG and 7E3 were incubated, in vitro, at 37°C, for 2 hr. Following this incubation, the samples were diluted and added to a microplate coated with anti-human IgG. Thus, if 7E3 did bind to IVIG, a secondary anti-mouse IgG would detect the presence of 7E3. There were no statistically significant differences between assay responses for 7E3-containing samples versus the negative control (IVIG alone), with  $p = 0.164$ . However, there were significant differences in assay responses (at each concentration) for the positive control antibody, with  $p < 0.001$ . The concentration ratios of 7E3:IVIG in this experiment were designed to be similar to what would be expected in the in vivo experiments.

*IVIG effects on AMI pharmacokinetics.* Figure 2 showed that IVIG increased the clearance of the anti-platelet antibody, 7E3. To determine if this effect of IVIG was specific for 7E3, we characterized the pharmacokinetics of a second monoclonal antibody, AMI, in the presence and absence of IVIG. Figure 4 demonstrates that IVIG also increased the clearance of AMI, with AMI clearance increasing from  $0.44 \pm 0.05$  to  $1.17 \pm 0.05 \text{ ml hr}^{-1} \text{ kg}^{-1}$  from the control to the IVIG treated group ( $p < 0.001$ ). Furthermore, the relative degree of increased clearance due to IVIG treatment was similar between groups, with a 2.37-fold increase in clearance seen for 7E3, and a 2.66-fold increase in clearance seen for AMI, following 2 g/kg IVIG treatment.

*IVIG effects on 7E3-PLT binding.* Qualitative and quantitative studies were performed to determine the effect of IVIG on binding of 7E3 to human platelets. Results of the qualitative flow cytometric analyses are shown in figure 5. No shift in the fluorescence histogram was observed in the presence of IVIG. In quantitative studies, the platelet concentration was kept constant as the 7E3 concentrations varied, either in the absence or presence of IVIG. One might expect that anti-idiotypic antibodies in the IVIG preparation would lead to a decrease in the apparent affinity of 7E3-platelet binding. Results from the quantitative studies are shown in figure 6. Binding curves are nearly identical in the presence and absence of IVIG. No significant difference was found in the binding parameters  $K_A$ , and  $R_t$ . Without IVIG present,  $K_A$  was  $4.9 \pm 0.7 \times 10^8 \text{ M}^{-1}$ , and  $R_t$  was  $7.5 \pm 0.4 \times 10^{-8} \text{ M}$  ( $55000 \pm 3000 \text{ GP/platelet}$ ). With IVIG,  $K_A$  was  $5.5 \pm 1.2 \times 10^8 \text{ M}^{-1}$ , and  $R_t$  was  $7.6 \pm 0.7 \times 10^{-8} \text{ M}$  ( $56000 \pm 5000 \text{ GP/platelet}$ ).

## **Discussion**

The present study was designed to evaluate the efficacy of IVIG in a rat model of ITP, and to gain insight into the mechanism of IVIG action in this model. Rats were pretreated with IVIG, 0-2 g/kg, and then challenged with a short infusion of anti-platelet antibody (7E3). As evidenced by figure 1, pre-treatment of the rats with IVIG attenuated 7E3-induced thrombocytopenia. IVIG pre-treatment reduced the average degree of thrombocytopenia achieved after 7E3 treatment (as measured by average percent platelet count at nadir), and decreased the fraction of animals demonstrating severe thrombocytopenia.

The definition of severe thrombocytopenia used in this study (i.e., platelet nadir values less than 30% of initial platelet counts) was selected based on the results of previous studies of 7E3-treated rats.<sup>13</sup> In these studies, animals receiving 8 mg/kg 7E3 demonstrated an average percent nadir platelet count of 18%, with a 99% confidence interval of 6.3-30%. As such, we could expect that 99.5% of the 7E3 treated rats would demonstrate a nadir platelet count less than 30% (i.e., in the absence of an IVIG effect). It is interesting to note that some animals developed severe thrombocytopenia, even at the highest doses of IVIG.

To date, few published reports have shown IVIG effects in animal models of thrombocytopenia; and, to our knowledge, no reports have shown dose-dependencies in IVIG effects. Recently, Samuelsson et al.<sup>9</sup> published an interesting report demonstrating IVIG efficacy in a mouse model of ITP, but results were shown only for one dose of

IVIG. Because dose-dependent effects of IVIG were seen in our rat model of ITP, it might be reasonable to expect that similar results would be seen in humans with ITP. However, few studies have investigated optimal dosing strategies for IVIG in ITP, and dose-dependencies in IVIG effects have not been thoroughly investigated in man.<sup>15,16</sup>

Some researchers have proposed that anti-idiotypic antibodies present within IVIG preparations may mediate IVIG effects in ITP, via specific inhibition of anti-platelet antibody binding to platelets.<sup>7,8</sup> Given the possibility of an idiotype – anti-idiotype interaction, we conducted binding experiments to evaluate whether anti-idiotype antibodies may contribute to the IVIG effects observed in our rat model of ITP. No differences were seen between the 7E3-platelet binding curves generated in the presence or absence of IVIG. These quantitative results were confirmed by qualitative flow cytometry experiments, which also showed no decrease in 7E3 binding to platelets in the presence of IVIG. Thus, it is unlikely that the *in vivo* effects in this model are due to inhibition of 7E3 binding to the platelets.

An intriguing finding of this work is that IVIG altered the pharmacokinetics of 7E3. Our data demonstrated a trend toward a reduction of 7E3 terminal half-life with IVIG administration ( $p=0.06$ ), with statistical significance reached in the comparison of half-life in control animals to that seen in animals receiving 1 g/kg IVIG ( $p < 0.05$ ). More importantly, IVIG was found to induce a dramatic increase in the clearance of the anti-platelet antibody ( $p < 0.001$ ). Clearance, which serves as a time and concentration-averaged measure of 7E3 elimination, is a better metric for evaluation of IVIG effects on

7E3 elimination, as IVIG effects on elimination rate (and half-life) may be expected to decrease with time following IVIG administration. To our knowledge, this IVIG effect on anti-platelet antibody elimination has not been previously reported in humans or in animal models of ITP. We performed further experiments to determine whether this pharmacokinetic effect was a specific effect (i.e., mediated by IVIG binding to 7E3 and increasing clearance), or a general effect (e.g., saturation of the Fc receptor responsible for protecting IgG from catabolism) of IVIG.

Using an in vitro assay, we were unable to detect binding of IVIG to 7E3. This lack of detection of binding could be due to at least two factors: (i) IVIG may not bind to 7E3, or (ii) the assay may not be sensitive enough to detect the small amount of binding that might occur. Using a standard curve based on the positive control antibody, and the highest assayed quantity of 7E3-IVIG binding, we estimate that less than 2% of 7E3 bound to IVIG. Although some literature suggests that IVIG preparations contain anti-mouse antibodies,<sup>17</sup> the levels of anti-mouse antibody are likely very low, and may vary greatly from batch to batch. Our observation of the lack of 7E3-IVIG binding in vitro, together with the observed effect of IVIG on AMI clearance, suggests that the change in 7E3 clearance following IVIG treatment is not due to specific 7E3-IVIG interactions, but is likely due to a more general effect.

It is well known that IgG clearance increases with increasing plasma concentrations of IgG, and it is accepted that this phenomenon is due to the saturation of a salvage receptor for IgG (FcRn).<sup>18,19</sup> This receptor is found both in rodents and humans.<sup>20</sup> Additionally,

FcRn is widely distributed throughout the body, and is present in the diverse sites thought to be associated with IgG catabolism, including the endothelial cells of muscle vasculature and hepatic sinusoids<sup>19,21</sup>. Normally, proteins taken into cells by pinocytosis are rapidly catabolized upon fusion of the endosome with the lysosome. However, in the case of IgG, the FcRn receptor binds IgG with high affinity in the more acidic environment of the endosome, prevents release of the IgG into the lysosome, and eventually returns the IgG to the plasma. It has been reported that a doubling of plasma IgG concentration (similar to what might be expected following 1g/kg IVIG therapy) results in an increase in fractional IgG catabolism rate to 180% of its normal value.<sup>22,23</sup> In our studies, administration of 1g/kg IVIG resulted in a  $7E3$  clearance value that was 176% of the control value. It is probable that the observed increase in  $7E3$  clearance with increasing doses of IVIG is due to saturation of this salvage receptor by the IVIG, leaving a greater fraction of the  $7E3$  available for catabolism. A schematic representation of this proposed hypothesis for IVIG effects is shown in figure 7.

Several authors have suggested that IVIG therapy may lead to alterations in auto-antibody concentrations in blood. For example, Tsubakio et al.<sup>24</sup> reported in 1983 that IVIG treatment led to decreased auto-antibody titers in a small number of patients. However, the authors attributed these effects to decreases in antibody production. In 1993, Masson<sup>23</sup> first proposed that IVIG administration may lead to an increased rate of elimination of pathogenic auto-antibodies, and suggested that this mechanism may explain some of the effects observed following IVIG therapy in autoimmune conditions. Additionally, Pierangeli et al.<sup>25</sup> proposed that IVIG might increase the rate of

elimination of autoantibodies present in the antiphospholipid antibody syndrome. Others have mentioned this possible mechanism of action for other specific diseases.<sup>26-28</sup> With this report, we provide experimental evidence that IVIG is able to increase the elimination rate of a specific anti-platelet antibody, in a rat model of ITP.

It is reasonable to imagine that decreases in plasma antibody levels would lead to decreases in the degree of platelet opsonization and decreases in the rate of platelet elimination. Because of the non-linear nature of receptor-antibody binding, it is expected that some patients would benefit much more than other patients from an increase in antibody clearance, depending on their respective initial plasma auto-antibody concentrations. Based on our observations of IVIG effects on anti-platelet antibody clearance, and on the relationship between IgG concentrations and IgG clearance in humans, we hypothesize that IVIG effects in ITP are achieved, in part, via IVIG-mediated increases in the rate of anti-platelet antibody elimination.

It is important to note that the relationship between the effects of IVIG on 7E3 clearance to IVIG effects on thrombocytopenia in 7E3 treated animals is uncertain at present. For example, as shown in figure 2, most of the change in 7E3 plasma concentrations following IVIG treatment occurs after 12-24 h. In this acute model, platelet counts were only recorded over the first 24 h, with the most dramatic effects on platelet count occurring within ~3 h, where the changes in 7E3 kinetics were less dramatic. However, if IVIG has the ability to accelerate anti-platelet antibody clearance in a chronic ITP situation (i.e., the human ITP condition, where pathogenic IgG is slowly synthesized

rather than rapidly infused), this increased antibody clearance could conceivably account for some of the beneficial effects seen following IVIG treatment.

Because the effects of IVIG in 7E3-treated rats are not likely due solely to pharmacokinetic or anti-idiotypic effects, it is likely that the IVIG effects in these experiments are also due to factors more directly controlling platelet destruction (i.e., interference with Fc- or complement mediated platelet destruction). These hypotheses were not the subject of this investigation, and will be further investigated in future studies. Currently, mathematical models are being developed that relate anti-platelet antibody concentrations to their effects on thrombocytopenia. With these models, we will be able to obtain a quantitative estimate of the importance of increased antibody clearance relative to the other effects that IVIG might have. Furthermore, this animal model is being used to develop novel therapies of ITP, which are related to the possible effects of IVIG in this model (e.g., a method to specifically increase anti-platelet antibody clearance).

In conclusion, two new findings are reported in this work. First, IVIG was able to attenuate the effects of an anti-platelet antibody in a rat model of ITP, in a dose-dependent manner. This finding, and further studies using this animal model, may provide a means to suggest a rationally designed, optimal dosing strategy for IVIG in ITP. The second important finding was that IVIG had a dramatic, and apparently non-specific, effect on anti-platelet antibody clearance. Thus this work provides experimental

evidence to support the hypothesis that IVIG may achieve effects by increasing the elimination of pathogenic antibodies.

## References

1. Imbach P, Barandun S, d'Apuzzo V, et al. High-dose intravenous gammaglobulin for idiopathic thrombocytopenic purpura in childhood. *Lancet*. 1981;1:1228-1231.
2. Bussel JB, Hilgartner MW. Intravenous immunoglobulin therapy of idiopathic thrombocytopenic purpura in childhood and adolescence. *Hematol Oncol Clin North Am*. 1987;1:465-482.
3. Ballow M. Mechanisms of action of intravenous immunoglobulin therapy and potential use in autoimmune connective tissue diseases. *Cancer*. 1991;68:1430-1436.
4. Ballow M. Mechanisms of action of intravenous immune serum globulin in autoimmune and inflammatory diseases. *J Allergy Clin Immunol*. 1997;100:151-157.
5. Fehr J, Hofmann V, Kappeler U. Transient reversal of thrombocytopenia in idiopathic thrombocytopenic purpura by high-dose intravenous gamma globulin. *N Engl J Med*. 1982;306:1254-1258.
6. Tovo PA, Miniero R, Fiandino G, Saracco P, Messina M. Fc-depleted vs intact intravenous immunoglobulin in chronic ITP. *J Pediatr*. 1984;105:676-677.

7. Berchtold P, Dale GL, Tani P, McMillan R. Inhibition of autoantibody binding to platelet glycoprotein IIb/IIIa by anti-idiotypic antibodies in intravenous gammaglobulin. *Blood*. 1989;74:2414-2417.
8. Mehta YS, Badakere SS. In-vitro inhibition of antiplatelet autoantibodies by intravenous immunoglobulins and Rh immunoglobulins. *J Postgrad Med*. 1996;42:46-49.
9. Samuelsson A, Towers TL, Ravetch JV. Anti-inflammatory activity of IVIG mediated through the inhibitory Fc receptor. *Science*. 2001;291:484-486.
10. Bussel J, Pahwa S, Porges A, et al. Correlation of in vitro antibody synthesis with the outcome of intravenous gamma-globulin treatment of chronic idiopathic thrombocytopenic purpura. *J Clin Immunol*. 1986;6:50-56.
11. Basta M, Langlois PF, Marques M, Frank MM, Fries LF. High-dose intravenous immunoglobulin modifies complement-mediated in vivo clearance. *Blood*. 1989;74:326-333.
12. Grossi A, Vannucchi AM, Casprini P, Morfini M, Ferrini PR. Effects of high-dose intravenous gammaglobulin on kinetic parameters of <sup>51</sup>Cr-labelled platelets

in chronic ITP. *Haematologica*. 1986;71:123-127.

13. Hansen RJ, Balthasar JP. Pharmacokinetics, pharmacodynamics, and platelet binding of an anti-glycoprotein IIb/IIIa monoclonal antibody (7E3) in the rat: A quantitative rat model of immune thrombocytopenic purpura. *J Pharm Exp Ther*. 2001;298:1-7.
14. Hansen RJ, Balthasar JP. An ELISA for quantification of murine IgG in rat plasma: application to the pharmacokinetic characterization of AP-3, a murine anti-glycoprotein IIIa monoclonal antibody, in the rat. *J Pharm Biomed Anal*. 1999;21:1011-1016.
15. Godeau B, Lesage S, Divine M, Wirquin V, Farcet J, Bierling P. Treatment of Adult Chronic Autoimmune Thrombocytopenic Purpura With Repeated High-Dose Intravenous Immunoglobulin. *Blood*. 1993;82:1415-1421.
16. Godeau B, Caulier M, Decuypere L, Rose C, Schaeffer A. Intravenous immunoglobulin for adults with autoimmune thrombocytopenic purpura: results of a randomized trial comparing 0.5 and 1 g/kg b.w. *Br J Haematol*. 1999;107:716-719.

17. Perosa F, Rizzi R, Pulpito V, Dammacco F. Soluble CD4 antigen reactivity in intravenous immunoglobulin preparations: is it specific? *Clin Exp Immunol.* 1995;99:16-20.
18. Brambell F, Hemmings W, Morris I. A theoretical model of gamma-globulin catabolism. *Nature.* 1964;203:1352-1355.
19. Junghans RP, Anderson CL. The protection receptor for IgG catabolism is the beta2-microglobulin-containing neonatal intestinal transport receptor. *Proc Natl Acad Sci U S A.* 1996;93:5512-5516.
20. Yu Z, Lennon VA. Mechanism of intravenous immune globulin therapy in antibody-mediated autoimmune diseases. *N Engl J Med.* 1999;340:227-228.
21. Ghetie V, Ward ES. FcRn: the MHC class I-related receptor that is more than an IgG transporter. *Immunol Today.* 1997;18:592-598.
22. Schultze HE, Heremans JF. Turnover of the Plasma Proteins. In: *Molecular Biology of Human Proteins.* Vol. 1. Amsterdam: Elsevier Publishing Company; 1966:481-487

23. Masson PL. Elimination of infectious antigens and increase of IgG catabolism as possible modes of action of IVIg. *J Autoimmun.* 1993;6:683-689.
24. Tsubakio T, Kurata Y, Katagiri S, et al. Alteration of T cell subsets and immunoglobulin synthesis in vitro during high dose gamma-globulin therapy in patients with idiopathic thrombocytopenic purpura. *Clin Exp Immunol.* 1983;53:697-702.
25. Pierangeli SS, Espinola R, Liu X, Harris EN, Salmon JE. Identification of an Fc gamma receptor-independent mechanism by which intravenous immunoglobulin ameliorates antiphospholipid antibody-induced thrombogenic phenotype. *Arthritis Rheum.* 2001;44:876-883.
26. Urbaniak SJ, Duncan JI, Armstrong-Fisher SS, Abramovich DR, Page KR. Transfer of anti-D antibodies across the isolated perfused human placental lobule and inhibition by high-dose intravenous immunoglobulin: a possible mechanism of action. *Br J Haematol.* 1997;96:186-193.
27. Pottier Y, Pierard I, Barclay A, Masson PL, Coutelier JP. The mode of action of treatment by IgG of haemolytic anaemia induced by an anti-erythrocyte monoclonal antibody. *Clin Exp Immunol.* 1996;106:103-107.

28. Sater RA, Rostami A. Treatment of Guillain-Barre syndrome with intravenous immunoglobulin. *Neurology*. 1998;51:S9-15.

## Figure Legends

**Figure 1. IVIG effects on the time course of 7E3-induced thrombocytopenia.** Rats received IVIG (or saline) followed by 8 mg/kg 7E3. Panel A. Individual raw platelet count versus time data for animals given saline (1), 0.4 g/kg IVIG (2), 1 g/kg IVIG (3), or 2 g/kg IVIG (4). Panel B. Average percent of initial platelet count data. Symbols represent IVIG treatment groups (n=4 rats/group): saline (●), 0.4 g/kg (■), 1 g/kg (▲), and 2 g/kg (◆). IVIG and 7E3 were given intravenously, and platelet counts were obtained using a Cell-Dyne 1700 multi-parameter hematology analyzer. Error bars represent the standard deviation about the mean. IVIG attenuated the time-course of thrombocytopenia in a dose-dependent manner. Treatments differences were statistically significant (p=0.031).

**Figure 2. Plasma 7E3 pharmacokinetics following IVIG treatment.** Rats (3-4 per group) were dosed intravenously with IVIG (0-2 g/kg) followed by 7E3 (8 mg/kg). Panel A shows plasma 7E3 pharmacokinetic data for each animal given saline (1), 0.4 g/kg IVIG (2), 1 g/kg IVIG (3), or 2 g/kg IVIG (4). Panel B. Average plasma pharmacokinetic data for animals receiving 7E3 and IVIG. Treatment groups are designated as follows: saline (●), 0.4 g/kg (■), 1 g/kg (▲), and 2 g/kg (◆). 7E3 concentrations were determined via ELISA. Error bars represent the standard deviation about the mean concentration at each time point. IVIG treatment significantly increased the clearance of 7E3 (p<0.001), calculated from the concentration vs. time profiles shown in this figure.

**Figure 3. IVIG does not directly bind 7E3.** 7E3 (or control IgG) and IVIG were combined in vitro, at a constant IVIG concentration (25 mg/ml) and varying 7E3 concentrations (0-0.1 mg/ml). The positive control was a mouse anti-human IgG. Samples were then added to a microplate coated with anti-human IgG. Murine IgG binding was visualized using a secondary anti-mouse IgG-alkaline phosphatase conjugate. p-Nitro phenyl phosphate was added, and the plates were read at 405 nm (kinetic assay, over 10 min). Assay response to 7E3 did not differ from control ( $p=0.164$ ), whereas the positive control differed significantly from control ( $p<0.001$ ).

**Figure 4. Plasma AMI pharmacokinetics following IVIG treatment.** Rats (3 per group) were dosed intravenously with saline (●) or 2 g/kg (◆) IVIG, followed by AMI (8 mg/kg). AMI concentrations were determined via ELISA. Error bars represent the standard deviation about the mean concentration at each time point. IVIG treatment significantly increased the clearance of AMI ( $p<0.001$ ), calculated from the concentration vs. time profiles shown in this figure. IVIG's effects on antibody pharmacokinetics are not specific for 7E3.

**Figure 5. IVIG effects on 7E3-platelet binding as determined by flow cytometry.** 7E3 was incubated with human platelets in the presence or absence of IVIG. The histograms plot platelet count versus relative fluorescence intensity. The bottom panel shows the fluorescence histogram obtained for control mouse IgG incubated with platelets (median fluorescence intensity (MFI) was 1.3). The middle panel shows 7E3 incubated with platelets (MFI=246), and the top panel shows 7E3 incubated with platelets

in the presence of IVIG (MFI=284). No decrease in MFI was observed for 7E3 binding to platelets in the presence of IVIG.

**Figure 6. IVIG effects on the 7E3-platelet binding curve.** Total platelet concentration was held constant as the 7E3 concentration was increased, in the presence (○) or absence (▽) of IVIG. Free (i.e., unbound) 7E3 concentrations were determined by ELISA. Data were fit as described in the text. The lines represent the best fits of the data sets (solid line = IVIG, broken line = no IVIG), and are essentially superimposed. Parameters ( $K_A$  and  $R_t$ ) obtained from the fits did not differ significantly. Without IVIG present,  $K_A$  was  $4.9 \pm 0.7 \times 10^8 \text{ M}^{-1}$ , and  $R_t$  was  $7.5 \pm 0.4 \times 10^{-8} \text{ M}$  ( $55000 \pm 3000 \text{ GP/platelet}$ ). With IVIG,  $K_A$  was  $5.5 \pm 1.2 \times 10^8 \text{ M}^{-1}$ , and  $R_t$  was  $7.6 \pm 0.7 \times 10^{-8} \text{ M}$  ( $56000 \pm 5000 \text{ GP/platelet}$ ). IVIG does not prevent 7E3 from binding to platelets.

**Figure 7. A proposed mechanism for IVIG effects on increased anti-platelet antibody clearance.** (1) IVIG (black IgG's) and 7E3 (white IgG's) are taken into the cell by pinocytosis. (2) At physiologic pH, IgG has low affinity for the FcRn receptor, but as the pH decreases following endocytosis, the affinity of IgG for the FcRn receptor increases and the IgG binds to the receptor. Because of the much greater concentrations of IVIG relative to 7E3, IVIG is bound preferentially to the receptor. (3) Bound IgG molecules are protected from release into the lysosome, and (4) eventually returned to the circulation. (5) Unbound IgG proceeds to the lysosome (6) where it is catabolized by proteases.

TABLE 1

Effect of IVIG on the elimination of 7E3

Dose of IVIG (g kg <sup>-1</sup> )	CL of 7E3 (ml hr <sup>-1</sup> kg <sup>-1</sup> ) <sup>a</sup>	t <sub>1/2</sub> (hr) <sup>b</sup>
0	0.78±0.09	79±11
0.4	1.28 ± 0.19*	68 ± 6
1	1.37 ± 0.28**	54 ± 17*
2	1.85 ± 0.19**	56 ± 10

Non compartmental techniques were used to determine each parameter value. Values are listed as mean ± standard deviation (n=3-4).

a: ANOVA, p < 0.001

b: ANOVA, p =0.06

\*: Dunnett post-test, p < 0.05 relative to control

\*\* : Dunnett post-test, p < 0.01 relative to control

Figure 1A.

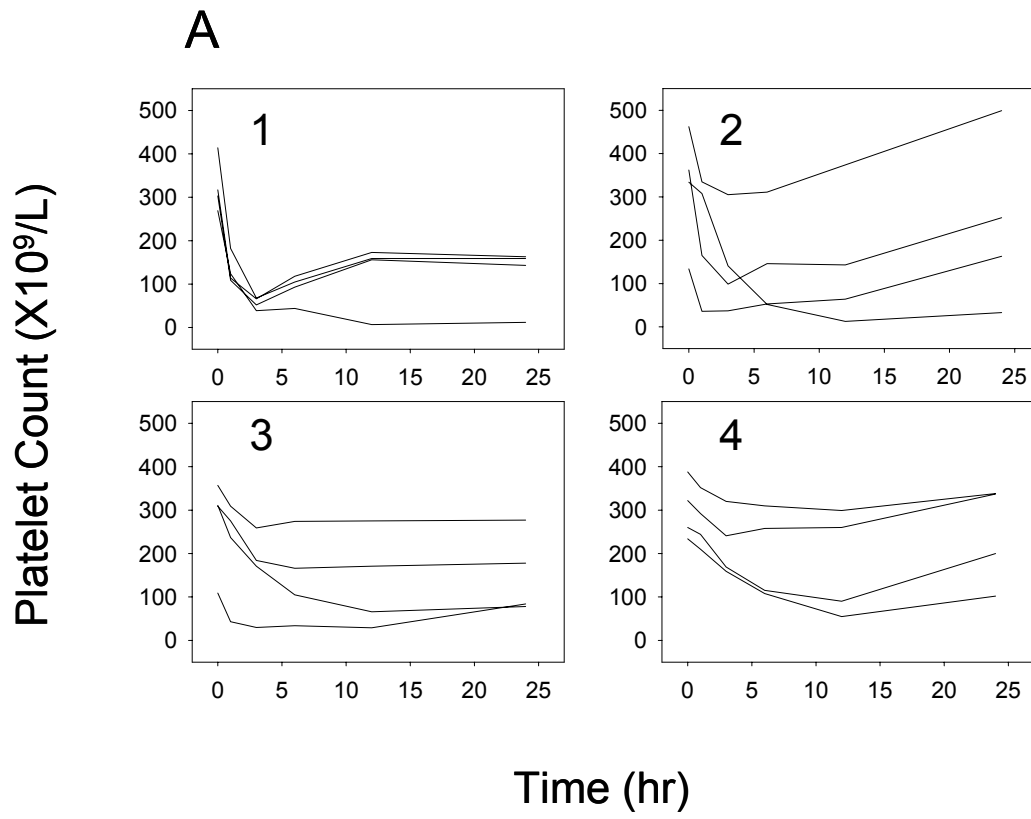


Figure 1B.

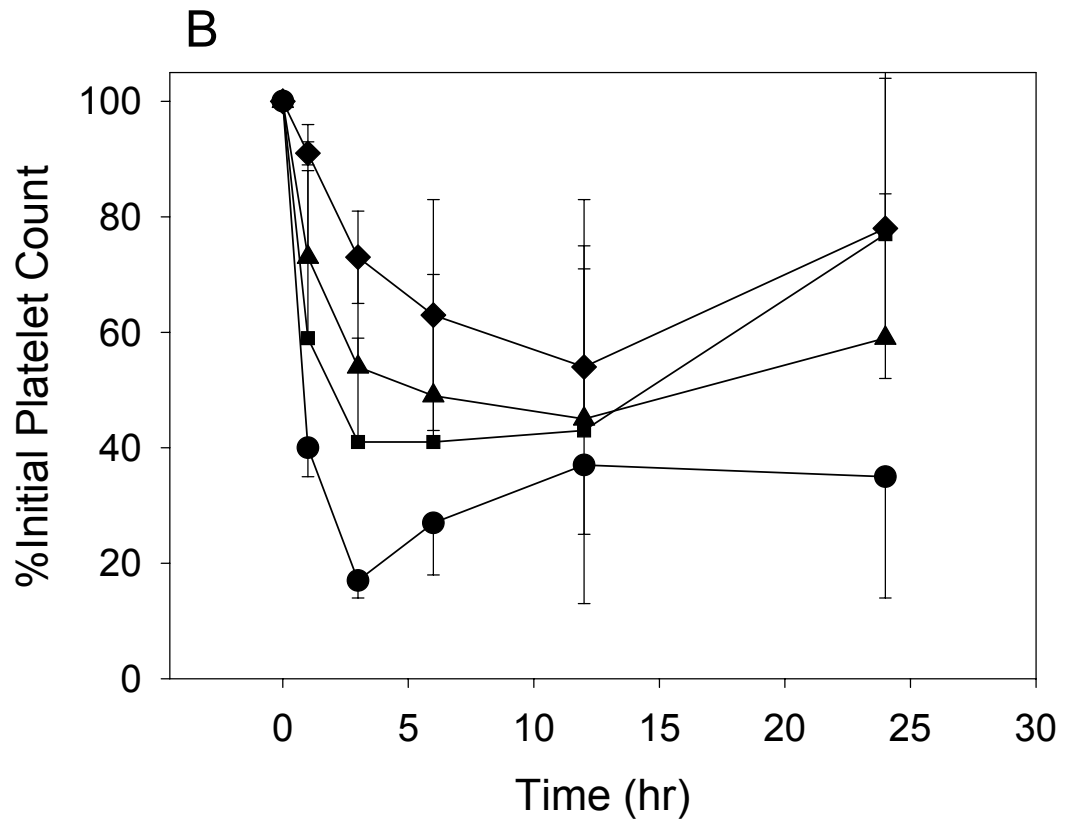


Figure 2A.

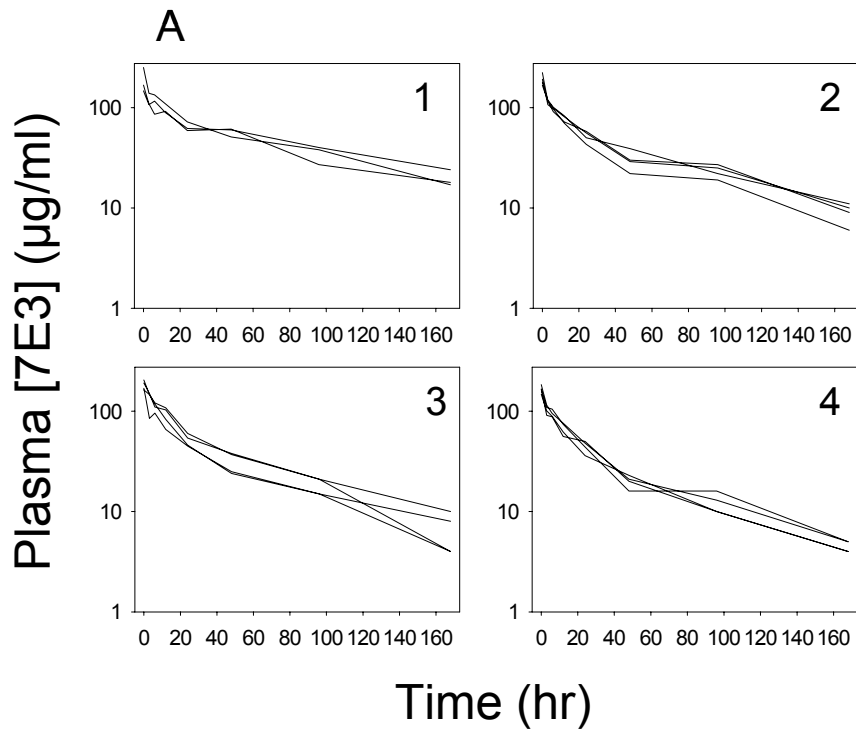


Figure 2B.

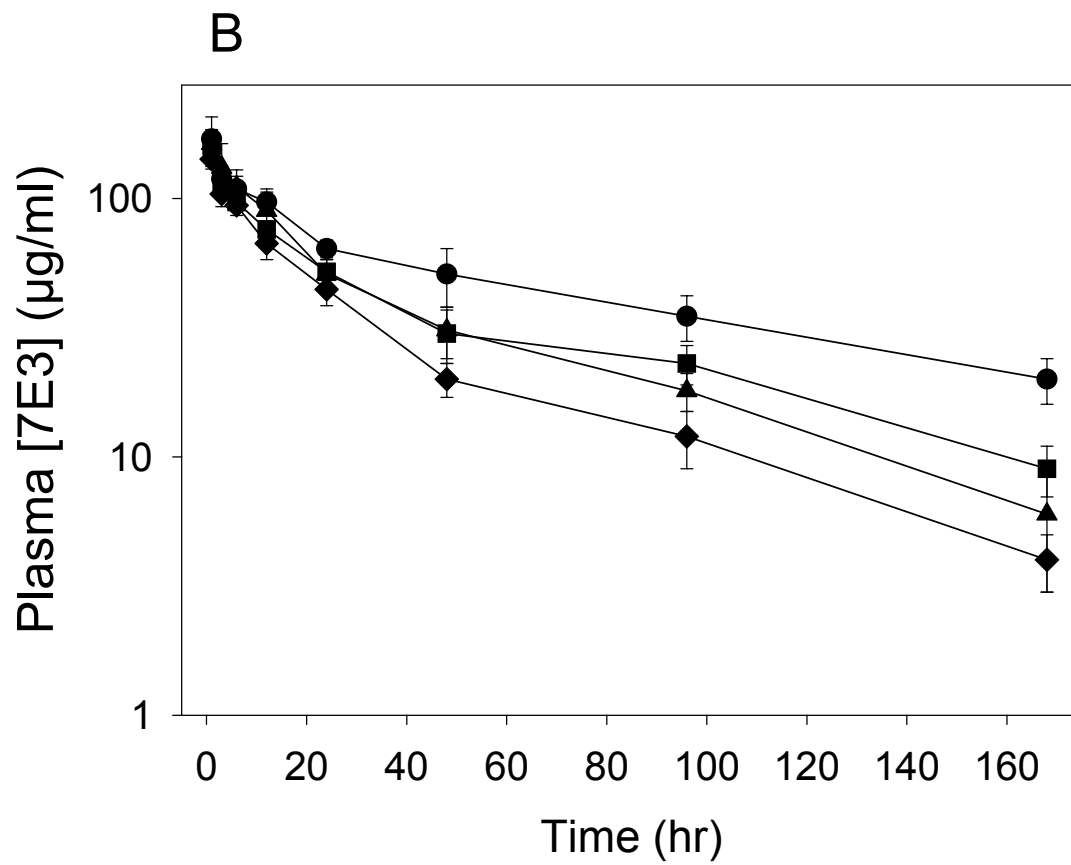


Figure 3.

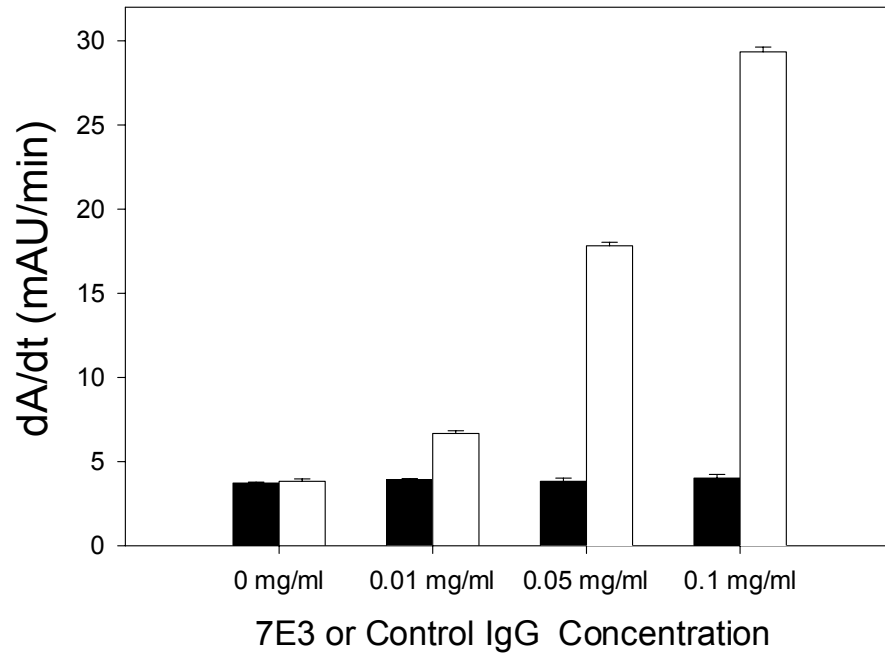


Figure 4.

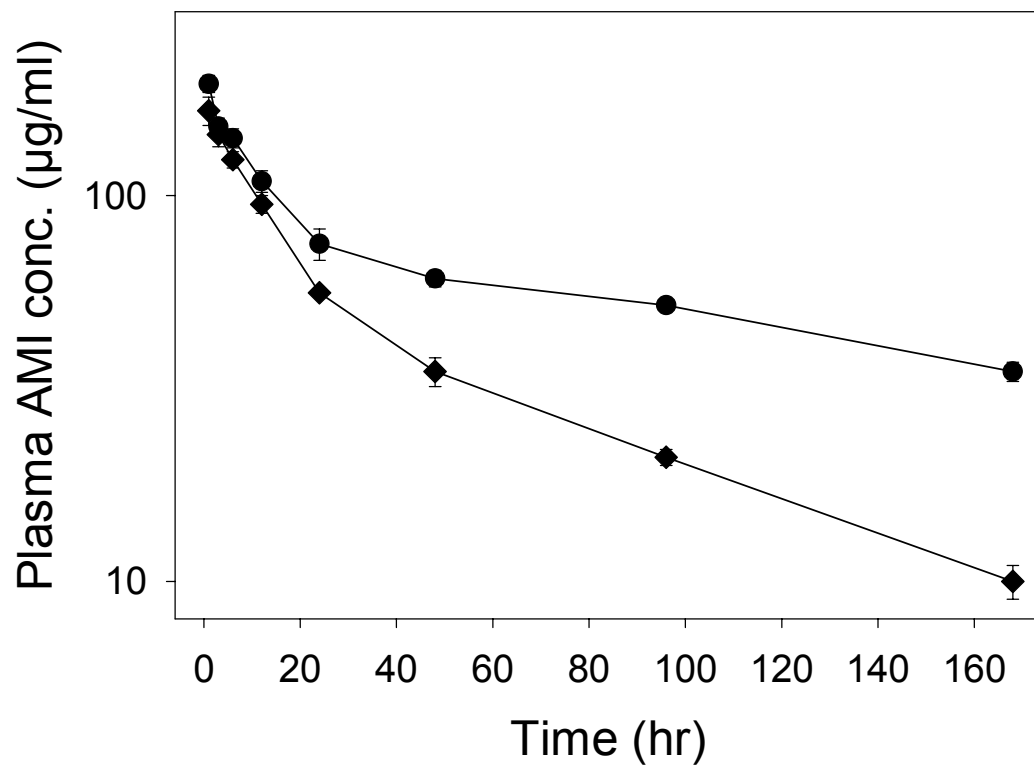


Figure 5.

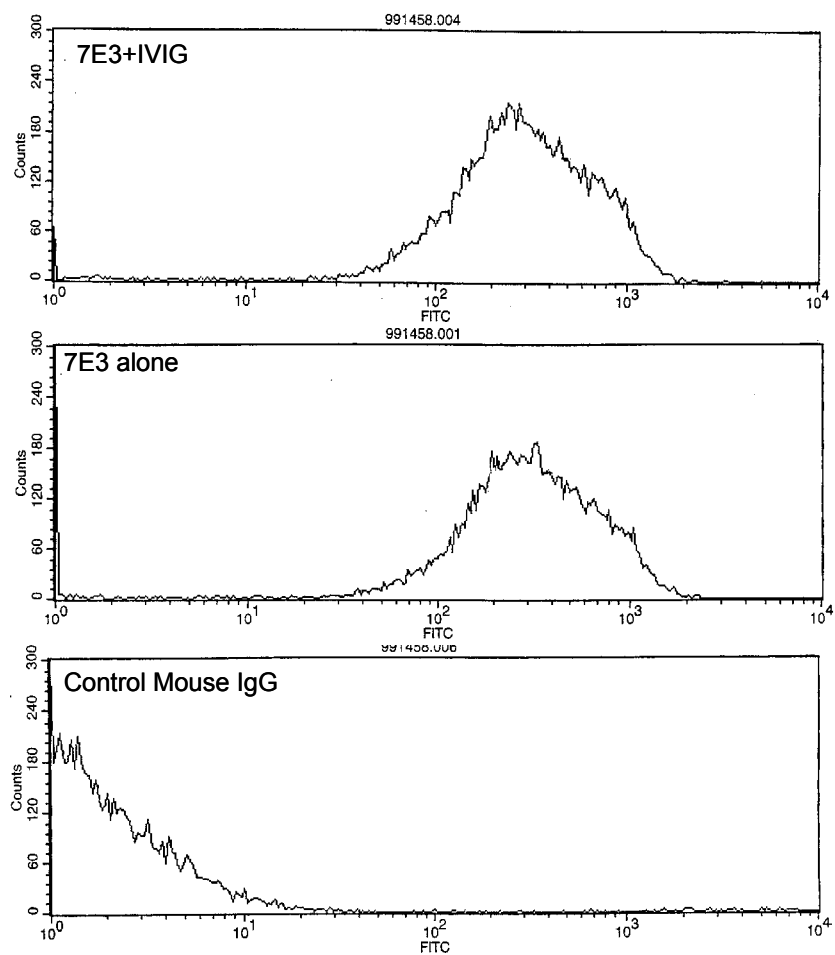


Figure 6.

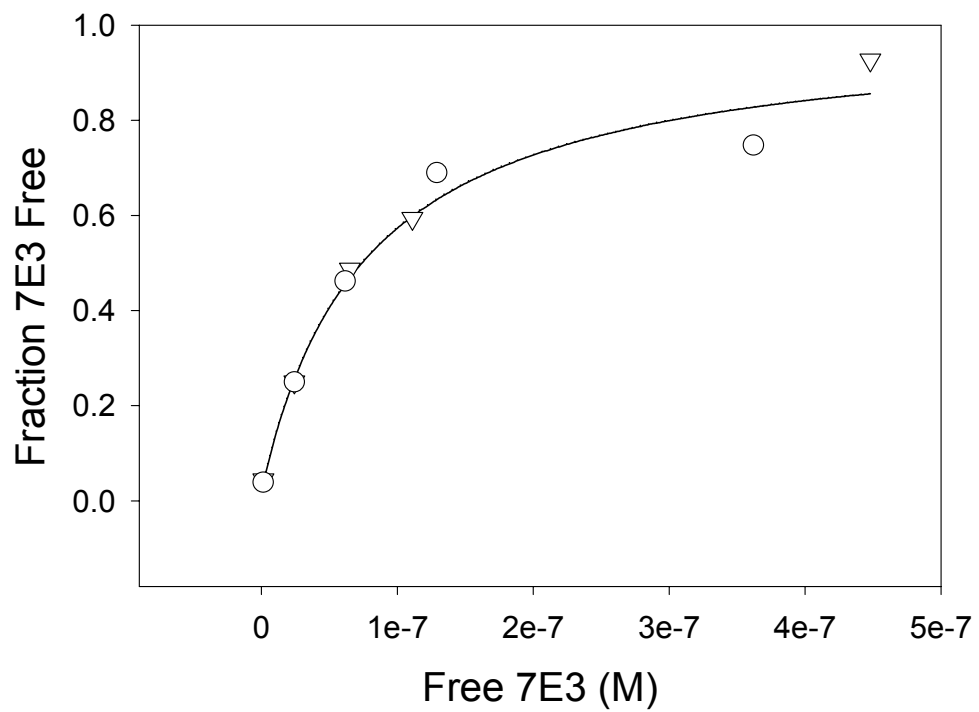
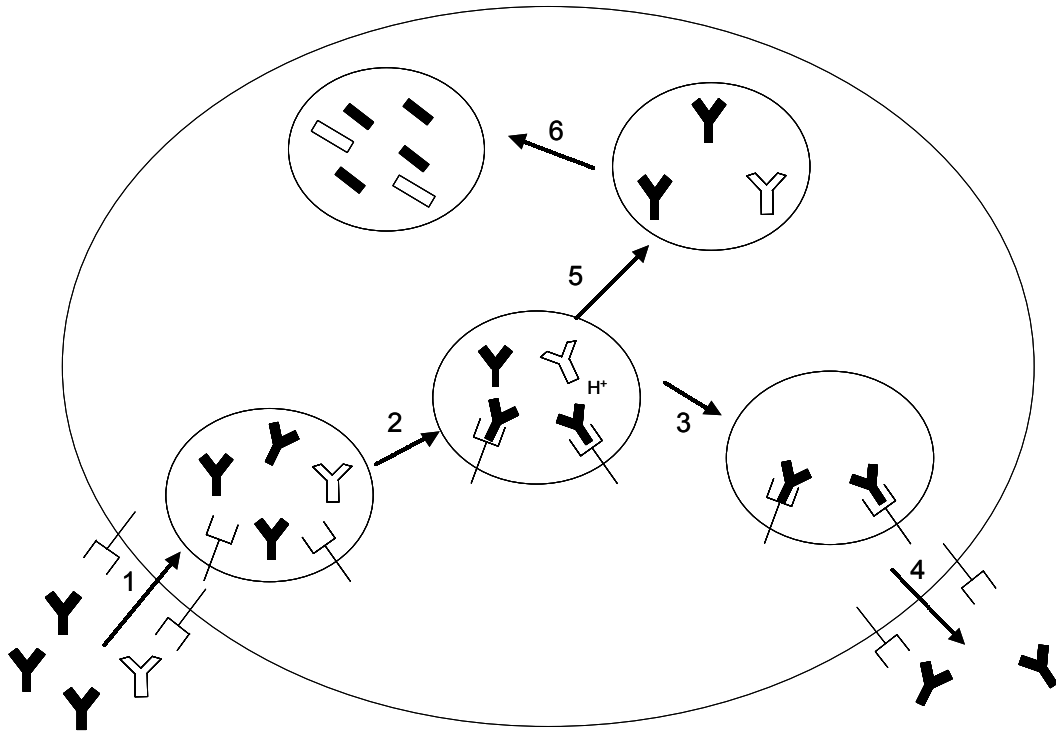


Figure 7.



# CHAPTER FIVE

---

## INTRAVENOUS IMMUNOGLOBULIN MEDIATES AN INCREASE IN ANTI-PLATELET ANTIBODY CLEARANCE VIA THE FcRn RECEPTOR

---

*This work has been submitted for publication in Blood (2002).*

## **Abstract**

Recent studies in our laboratory have shown that intravenous immunoglobulin (IVIG) therapy leads to an increased rate of anti-platelet antibody clearance in an animal model of immune thrombocytopenia. The present study was performed to confirm the importance of the FcRn receptor in mediating this effect of IVIG. The pharmacokinetics of an anti-platelet antibody, 7E3, were studied in mice lacking expression of FcRn and in control mice, both in the presence and absence of IVIG. IVIG increased the clearance of 7E3 in mice with functioning FcRn receptors, with an average clearance value of  $14.4 \pm 1.4$  ml/d/kg in IVIG treated mice versus  $5.2 \pm 0.3$  ml/d/kg in control mice ( $P < 0.001$ ). In mice lacking expression of FcRn, IVIG treatment did not increase the clearance of 7E3 ( $61.0 \pm 3.6$  ml/d/kg in IVIG treated mice vs.  $71.5 \pm 4.0$  ml/d/kg in control mice). Thus, FcRn appears to be the key receptor mediating the increase of 7E3 clearance following IVIG treatment.

Intravenous immunoglobulin (IVIG) therapy is a standard therapy of immune thrombocytopenia, and has shown efficacy for many other autoimmune conditions.<sup>1-3</sup> Recently, our laboratory demonstrated that intravenous immunoglobulin (IVIG) treatment increases anti-platelet antibody clearance in a rat model of immune thrombocytopenia (ITP).<sup>4</sup> We, and others, have suggested that increased autoantibody clearance may be an important mechanism by which IVIG achieves effects in various autoimmune conditions.<sup>4-9</sup>

IVIG effects on autoantibody clearance have been postulated to occur via competition of IVIG with autoantibodies for occupancy of the FcRn receptor.<sup>4-6,9</sup> The FcRn receptor is widely believed to be responsible for protecting IgG from catabolism, leading to the prolonged half-life of IgG (i.e., relative to other plasma proteins).<sup>10</sup> Although it has been hypothesized that IVIG treatment increases autoantibody clearance via competitive inhibition of the FcRn receptor, the link between FcRn and IVIG effects has not been explicitly demonstrated. In the present study, this hypothesis was tested by examining IVIG effects on the pharmacokinetics of an anti-platelet antibody in ‘wild-type’ mice, and in ‘knockout’ mice lacking expression of the FcRn receptor.

## Study Design

*Animals and reagents.*  $\beta$ -2-microglobulin knockout mice (lacking FcRn expression) and C57BL/6 control mice, 21-28 g, were obtained from Jackson Laboratories (Bar Harbor, ME). 7E3, an anti-platelet monoclonal antibody, was purified in our laboratory.<sup>11</sup> Intravenous immunoglobulin was obtained from Bayer (Pharmaceutical Division, Elkhart, IN). Mice were instrumented with jugular vein cannulas, and allowed to recover for 3-4 days prior to initiation of experiments. Human GPIIb/IIIa was obtained from Enzyme Research Laboratories (South Bend, IN). p-nitro phenyl phosphate was obtained from Pierce (Rockford, Illinois). Bovine serum albumin (BSA), goat anti-mouse IgG-alkaline phosphatase conjugate (Fab specific), and buffer reagents were obtained from Sigma (St. Louis, MO). Buffers were phosphate-buffered saline (pH 7.4, PBS), 0.02 M  $\text{Na}_2\text{HPO}_4$  (PB), PB + 0.05% Tween-20 (PB-Tween), and diethanolamine (pH 9.8, DEA).

*7E3 assay.* An antigen specific, enzyme-linked immunosorbent assay (ELISA) was developed to measure 7E3 concentrations in mouse plasma. Human GPIIb/IIIa was diluted 1:500 in PB, and added to Nunc Maxisorp plates (0.25 ml/well). Plates were incubated overnight at 4°C. Standards and samples were then added to the plate (0.25 ml/well) and allowed to incubate for 2 h at room temperature. Goat anti-mouse IgG-alkaline phosphatase conjugate, diluted 1:500, was added to the wells, and allowed to incubate for 45 min at room temperature. Finally, p-nitro phenyl phosphate was added (4 mg/ml in DEA) and the change in absorbance verses time was recorded with a SpectraMax Microplate reader (Molecular Devices, Sunnyvale, CA). Plates were washed 3 times with PB-Tween between each step of the assay. Standards were made to final

concentrations of 0, 1, 2.5, 5, 10 and 20 ng/ml 7E3 in 1% mouse plasma. Standard curves were linear over this concentration range. Intra-assay variability was < 15% for quality control samples within the standard curve range.

*Pharmacokinetic studies.* Mice, 3-5 per group, were dosed via the jugular vein cannula with either IVIG (1 g/kg) or saline, followed by 8 mg/kg 7E3. Blood samples, 20 µl per time point, were obtained from the saphaneous vein of the mice over the course of 4 days for the knockout mice, and over the course of 30-60 days for the control mice. Plasma 7E3 concentrations were determined via ELISA. Standard non-compartmental pharmacokinetic analyses were performed to determine the clearance and terminal half-life of 7E3 for the various treatment groups,<sup>11</sup> using WinNonlin software (Pharsight Corporation, Palo Alto, CA). Statistical analyses were performed using GraphPad InStat (GraphPad Software, Inc., San Diego, CA).

## Results and Discussion

Based on the observation that the fractional catabolic rate of IgG increases with increases in IgG concentration, Brambell et al. first proposed that a receptor-mediated transport system protects IgG from catabolism.<sup>12</sup> It has been suggested that the supposed protective receptor, often referred to as the Brambell receptor, limits that rate of IgG elimination and is responsible for the long half-life associated with IgG. Additionally, Brambell et al. proposed that the protective receptor might be saturated at high concentrations of IgG, thereby providing a mechanistic explanation for the observed increase in fractional IgG catabolism with increasing plasma IgG concentrations. Over thirty years after Brambell's initial hypothesis, this protective receptor was shown to be FcRn, which is also responsible for transporting IgG across the intestine of neonates.<sup>13-15</sup>

FcRn, a heterodimer consisting of an MHC class 1-like heavy chain and a  $\beta$ -2-microglobulin light chain, is widely expressed in adult tissues. Studies have demonstrated that  $\beta$ -2-microglobulin knockout mice do not express FcRn, and have low IgG levels, increased IgG catabolism, and decreased transport of IgG across the gut.<sup>7,10,14</sup> Catabolism of other plasma proteins (e.g., IgA and albumin) is unchanged in these knockout mice.<sup>14,16</sup>

Because of the known role of FcRn in protecting IgG from catabolism, several groups have postulated that IVIG increases autoantibody elimination by saturating this protective receptor.<sup>4-9</sup> However, FcRn has never been explicitly identified as the key receptor

mediating IVIG effects on autoantibody clearance. In this work, we tested the hypothesis that IVIG achieves this beneficial effect on anti-platelet antibody clearance via the FcRn receptor.

IVIG effects on 7E3 pharmacokinetics in  $\beta$ -2-microglobulin knockout and control C57BL/6 mice are shown in figure 1. As expected from our previous rat studies, IVIG increased the clearance of 7E3 in control mice ( $P < 0.001$ ). Additionally, consistent with the hypothesis that this effect is mediated via saturation of FcRn, IVIG treatment failed to increase the clearance of 7E3 in the mice lacking FcRn expression (see table 1). In fact, 7E3 clearance was slightly decreased in the presence of IVIG in the knockout mice. This may be due to saturation of catabolic processes at high IgG concentration.

This study confirms the hypothesis that IVIG effects on anti-platelet antibody clearance are mediated via the FcRn receptor. It is reasonable to suspect that IVIG may achieve therapeutic benefit in ITP via this mechanism; as such, FcRn may be an attractive target for the development of new therapies for ITP and for other humoral autoimmune conditions.

## **Acknowledgements**

We are grateful to David Soda for performing the mice cannulation surgeries, and to Zia Tayab for his laboratory assistance.

## References

1. George JN, Woolf SH, Raskob GE, et al. Idiopathic thrombocytopenic purpura: a practice guideline developed by explicit methods for the American Society of Hematology. *Blood*. 1996;88:3-40.
2. Knapp MJ, Colburn PA. Clinical uses of intravenous immune globulin. *Clin Pharm*. 1990;9:509-529.
3. Krause I, Blank M, Kopolovic J, et al. Abrogation of experimental systemic lupus erythematosus and primary antiphospholipid syndrome with intravenous gamma globulin. *J Rheumatol*. 1995;22:1068-1074.
4. Hansen RJ, Balthasar JP. Intravenous immunoglobulin effects on platelet count and anti-platelet antibody disposition in a rat model of immune thrombocytopenia. *Blood*. 2001; Submitted.
5. Bleeker WK, Teeling JL, Hack CE. Accelerated autoantibody clearance by intravenous immunoglobulin therapy: studies in experimental models to determine the magnitude and time course of the effect. *Blood*. 2001;98:3136-3142.
6. Pierangeli SS, Espinola R, Liu X, Harris EN, Salmon JE. Identification of an Fc gamma receptor-independent mechanism by which intravenous immunoglobulin

ameliorates antiphospholipid antibody-induced thrombogenic phenotype. *Rheum Arthritis*. 2001;44:876-883.

7. Sater RA, Rostami A. Treatment of Guillain-Barre syndrome with intravenous immunoglobulin. *Neurology*. 1998;51:S9-15.
8. Masson PL. Elimination of infectious antigens and increase of IgG catabolism as possible modes of action of IVIg. *J Autoimmun*. 1993;6:683-689.
9. Yu Z, Lennon VA. Mechanism of intravenous immune globulin therapy in antibody-mediated autoimmune diseases. *N Engl J Med*. 1999;340:227-228.
10. Telleman P, Junghans RP. The role of the Brambell receptor (FcRB) in liver: protection of endocytosed immunoglobulin G (IgG) from catabolism in hepatocytes rather than transport of IgG to bile. *Immunology*. 2000;100:245-251.
11. Hansen RJ, Balthasar JP. Pharmacokinetics, pharmacodynamics, and platelet binding of an anti-glycoprotein IIb/IIIa monoclonal antibody (7E3) in the rat: A quantitative rat model of immune thrombocytopenic purpura. *J Pharm Exp Ther*. 2001;298:1-7.

12. Brambell F, Hemmings W, Morris I. A theoretical model of gamma-globulin catabolism. *Nature*. 1964;203:1352-1355.
13. Ghetie V, Hubbard JG, Kim JK, Tsen MF, Lee Y, Ward ES. Abnormally short serum half-lives of IgG in beta 2-microglobulin-deficient mice. *Eur J Immunol*. 1996;26:690-696.
14. Junghans RP, Anderson CL. The protection receptor for IgG catabolism is the beta2-microglobulin-containing neonatal intestinal transport receptor. *Proc Natl Acad Sci U S A*. 1996;93:5512-5516.
15. Israel EJ, Wilsker DF, Hayes KC, Schoenfeld D, Simister NE. Increased clearance of IgG in mice that lack beta 2-microglobulin: possible protective role of FcRn. *Immunology*. 1996;89:573-578.
16. Ghetie V, Ward ES. FcRn: the MHC class I-related receptor that is more than an IgG transporter. *Immunol Today*. 1997;18:592-598.

TABLE 1

Effect of IVIG on the elimination of 7E3 in control and FcRn-deficient mice

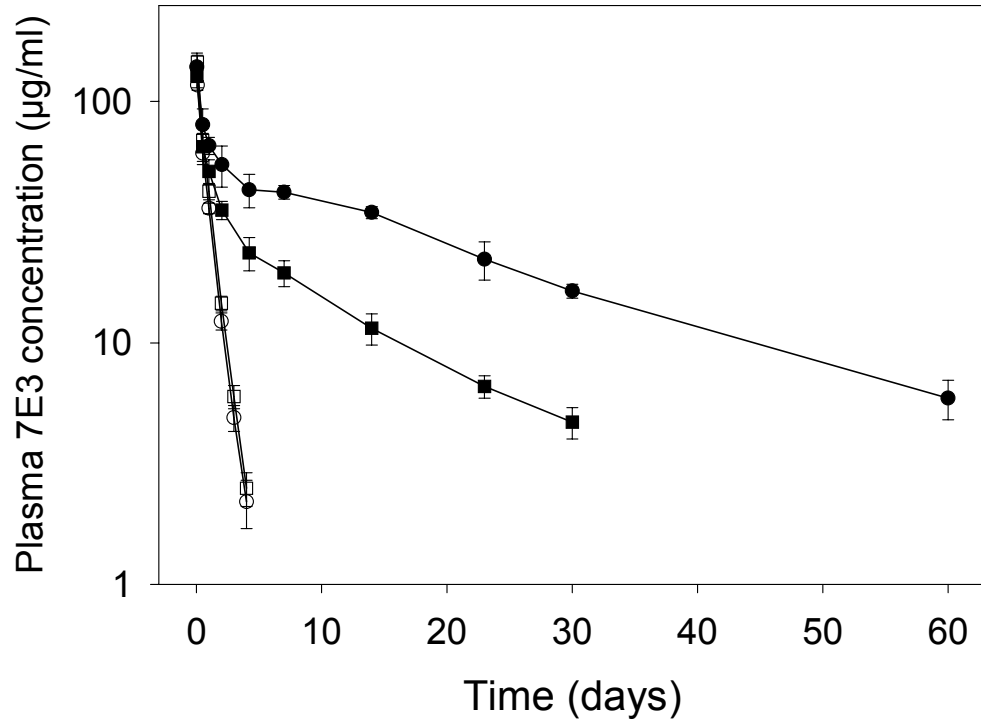
Group	CL of 7E3 (ml d <sup>-1</sup> kg <sup>-1</sup> )	t <sub>1/2</sub> (d)
Control mice-7E3 alone	5.2±0.3	20±2
Control mice-7E3+IVIG	14.4 ± 1.4	12 ± 2
knockout mice – 7E3 alone	72.5 ± 4.0	0.78 ± 0.07
knockout mice – 7E3+IVIG	61.0 ± 3.6	0.75 ± 0.05

Non compartmental techniques were used to determine each parameter value. Values are listed as mean ± standard deviation (n=3-5).

**Figure legends.**

**Figure 1. 7E3 pharmacokinetics following IVIG treatment in control and FcRn-deficient mice.** Mice (3-5 per group) were dosed intravenously with IVIG (1 g/kg) followed by 7E3 (8 mg/kg). Treatment groups are designated as follows: 7E3+saline in control mice (●); 7E3+IVIG in control mice (■); 7E3+saline in knockout mice (○); and 7E3+IVIG in knockout mice (□). 7E3 concentrations were determined via ELISA. Error bars represent the standard deviation about the mean concentration at each time point. IVIG treatment significantly increased the clearance of 7E3 in control mice ( $p < 0.001$ ), but not in FcRn-deficient mice.

Figure 1.



# CHAPTER SIX

---

INTRAVENOUS IMMUNOGLOBULIN EFFECTS ON ANTI-  
PLATELET ANTIBODY SECRETION AND HYBRIDOMA  
PROLIFERATION, IN VITRO

---

## **Abstract**

Several groups have shown that intravenous immunoglobulin (IVIG) therapy leads to an inhibition of antibody production from pokeweed mitogen-stimulated peripheral blood mononuclear cells, *ex vivo*. Additionally, it has been suggested that IVIG may specifically inhibit anti-platelet antibody production via specific (i.e., anti-idiotypic) interaction with the B-cell receptor of cells secreting anti-platelet antibodies. This present study investigates IVIG effects on anti-platelet antibody secretion and on cellular proliferation, *in vitro*. Two anti-platelet antibody-producing hybridoma cell lines, 7E3 and AP-3, and one control hybridoma cell line, 1B7.11, were grown in the presence of IVIG (0-50 mg/ml), in static culture. IVIG treatment led to concentration-dependent decreases in the apparent rates of cell growth and antibody production for each cell line. A mathematical model was developed to characterize IVIG effects. Each cell line exhibited similar sensitivity to IVIG, with IC<sub>50</sub> values of  $2.9 \pm 0.6$ ,  $6.4 \pm 1.5$ , and  $4.1 \pm 1.8$  mg/ml for inhibition of the proliferation of 7E3, AP-3, and 1B7.11, respectively. Thus, IVIG was found to inhibit antibody secretion *in vitro*; however, similar effects were observed for each cell line (i.e., specific anti-idiotypic effects were not apparent in this study). Further studies regarding IVIG suppression of anti-platelet antibody production, *in vivo*, are warranted.

## **Introduction**

Intravenous immunoglobulin (IVIG) was introduced as a treatment for immune thrombocytopenia (ITP) in 1981,<sup>1</sup> and has since become one of the standard treatments for this disease.<sup>2, 3</sup> Although much research has focused on defining the mechanisms of IVIG action in ITP, a complete understanding of these effects has remained elusive.

IVIG may possibly achieve beneficial effects in ITP, and other autoimmune conditions, through inhibition of autoantibody production. Inhibition of antibody secretion may occur as a general effect (i.e., affecting all antibody-producing cells) or as a specific effect (i.e., selectively affecting cells producing autoantibodies). In support of the hypothesis that IVIG produces a general inhibition of antibody production, several groups have shown that IVIG therapy leads to a general inhibition of antibody secretion from isolated peripheral blood mononuclear cells, *ex vivo*.<sup>4-8</sup> However, in addition to these general effects on antibody production, IVIG may have specific effects on autoantibody production (e.g., via specific anti-idiotypic inhibition). To our knowledge, specific effects of IVIG on anti-platelet antibody production have not been investigated.

This study presents the effects of IVIG on the apparent rate of cell growth of anti-platelet antibody producing cells, and on the apparent rate of antibody production from those cells. Mathematical models were developed to gain insight into the mechanisms of IVIG action, and to quantify cellular sensitivity to IVIG exposure.

## Methods

*Cell lines and IVIG preparation.* Two hybridomas producing antibodies directed against human platelets (7E3, ATCC #HB-8832; AP-3, ATCC #HB-242) and one control cell line (producing anti-TNP antibodies, 1B7.11, ATCC #TIB-191) were obtained from the American Type Culture Collection (Rockville, MD). Each cell line produces IgG1 antibodies, and each line was obtained by fusion of spleen cells with P3X63Ag8.653 myeloma cells from Balb/C mice. Cells were maintained in RPMI 1640:fetal bovine serum (90:10) medium (Life Technologies, Rockville, MD), with fluid renewal every 2-3 days. A stock solution of intravenous immunoglobulin (Polygam, Baxter Healthcare Corporation, Glendale, CA) was made by reconstituting the intravenous immunoglobulin product in media to a final IgG concentration of 200 mg/ml.

*IVIG effects on apparent rate of cell growth.* To determine IVIG effects on apparent cell growth, ~25,000 cells were added to media containing 0, 0.25, 2.5, or 25% of the IVIG solution (corresponding to 0, 0.5, 5, and 50 mg/ml IgG), and an appropriate volume of pH-adjusted media to bring the total volume of each culture to 10 ml, and a final pH of 7.2. Cells were counted at 0, 24, 48, 72, 96, 120 and 168 h using a Coulter Z1 particle counter. Cells were maintained in an incubator (37 °C, 5% CO<sub>2</sub>), without media replacement, for the duration of the experiment. Experiments were performed in triplicate, except for the 50 mg/ml treatment of AP-3 cells which was performed in duplicate. Inhibition of cell growth was determined at 120 h, and was defined as %I = (Control cell number – Treated cell number) × 100 / Control cell number. ANOVA were

used to determine statistically significant differences in absolute cell concentrations at 120 h.

*IVIG effects on antibody production.* IgG concentrations were measured at 0, 24, 48, 72, 96, 120, and 168 h in the cell cultures, using a sandwich ELISA developed for mouse IgG.<sup>9, 10</sup> Briefly, experiments were performed in Nunc Immuno Maxisorp plates, with rat anti-mouse IgG (Pierce M-3534, 1:500 in a 20 mM Na<sub>2</sub>HPO<sub>4</sub> buffer (PB), 0.25 ml/well) used as the capture antibody, and goat anti-mouse IgG alkaline phosphatase (Sigma A-1682, 1:500 in PB, 0.25 ml/well) the secondary antibody. Standard curves were linear up to 75 ng/ml. Sample sizes are as described above. Inhibition of antibody production, defined at 120 h, was determined as described for cell growth.

*Mathematical modeling.* A mathematical model was developed to characterize the apparent growth rates of the hybridoma cells, the apparent rates of antibody production, and the effects of IVIG on cell growth and antibody production. A schematic representation of the model is shown in scheme 1. Differential equations used to characterize cell numbers are shown below:

$$\frac{dCell}{dt} = kg(t) \times \left( 1 - \frac{I_{max} \times IVIG}{IC50 + IVIG} \right) \times Cell$$

$$kg(t) = a \times t \times \left( 1 - \frac{Cell}{Cell_{max}} \right)$$

In the above equations, Cell represents cell concentration (cells/ml), kg(t) is a first-order, time and cell concentration-dependent apparent growth rate function (hr<sup>-1</sup>), IVIG is the

human IgG concentration (mg/ml),  $I_{max}$  represents the maximum inhibition of the apparent growth rate function by IVIG (fixed at 1),  $IC_{50}$  (mg/ml) is the concentration of human IgG that produces 50% inhibition of the apparent cell growth rate function. The two parameters of the  $kg(t)$  equation,  $a$  ( $hr^{-2}$ ) and  $Cell_{max}$  (cells/ml), allow the apparent growth rate function to increase with time and decrease with cell number, as was necessary to characterize the data. The equations used to characterize antibody production are as follows:

$$\frac{dIgG}{dt} = K_{igg}(t) \times Cell$$

$$K_{igg}(t) = b \times t \times \left( 1 - \frac{IgG}{IgG_{max}} \right)$$

In these equations, IgG represents IgG concentration (ng/ml) in the cell cultures,  $K_{igg}(t)$  is a zero-order function describing antibody production (ng/hr/cell), that is time and IgG concentration dependent, as was required to characterize the data. The two  $K_{igg}(t)$  parameters,  $b$  (ng/hr<sup>2</sup>/cell) and  $IgG_{max}$  (ng/ml), allow the input function to both increase with time and decrease with concentration. These equations were fit to the cell number and antibody concentration data using non-linear least squares regressions analysis, accomplished using The Scientist software. The data were weighted by  $1/y^2$ . Cell growth parameters were obtained by simultaneously fitting the 0, 0.5, and 5 mg/ml IgG curves. IgG production parameters were obtained from simultaneously fitting the 3 data sets to the IgG production equations. Parameters are reported as mean +/- standard deviation, as reported by the software. The 50 mg/ml IVIG data were not used in the modeling because of concern of potential confounding factors (see discussion).

## Results

Incubation of hybridoma cells in the presence of IVIG led to a concentration-dependent inhibition of cell growth for each cell line. Inhibition of cell growth, measured at 120 h, was determined for each cell line. At 0.5 mg/ml, IVIG treatment resulted in  $21.5 \pm 4.7$ ,  $3.2 \pm 9.2$ , and  $38.9 \pm 3.2\%$  reductions in cell concentration for the 7E3, AP-3, and 1B7.11 cells, respectively. At 5 mg/ml, IVIG treatment resulted in  $52.1 \pm 5.7$ ,  $45.4 \pm 6.0$ , and  $77.9 \pm 4.2\%$  reductions in cell number for the 7E3, AP-3, and 1B7.11 cells, respectively. At 50 mg/ml, IVIG treatment resulted in  $73.2 \pm 8.6$ ,  $96.7 \pm 0.3$ , and  $90.0 \pm 4.3\%$  reductions in cell number for the 7E3, AP-3, and 1B7.11 cells, respectively.

Similarly, IVIG treatment led to concentration dependent inhibition of antibody production from each cell line. Differences determined at 120 h are the following: 0.5 mg/ml IVIG led to  $9.2 \pm 8.5$ ,  $-2.9 \pm 6.2$ , and  $26.4 \pm 7.1\%$  reductions in IgG concentration for the 7E3, AP-3, and 1B7.11 cells, respectively; 5 mg/ml IVIG led to  $34.2 \pm 2.1$ ,  $42.3 \pm 5.1$ , and  $64.6 \pm 1.8\%$  reductions in IgG concentration for the 7E3, AP-3, and 1B7.11 cells, respectively; and 50 mg/ml led to  $69.5 \pm 1.7$ ,  $97.4 \pm 0.2$ , and  $90.4 \pm 0.8\%$  reductions in IgG concentrations for the 7E3, AP-3, and 1B7.11 cells, respectively. Statistically significant differences from control were observed in each cell line ( $p < 0.01$ ) for both cell numbers and antibody concentrations.

Mathematical modeling was used to characterize the time course of the effect of IVIG on cell proliferation, and to estimate the sensitivity of each of these cell lines to IVIG. The best-fit lines from these analyses are shown in figures 1A, 2A, and 3A for the 7E3, AP-3,

and 1B7.11 cell lines, respectively. Table 1 shows the parameter values resulting from the modeling. The IC50 values reveal no significant difference in cell sensitivity to IVIG, suggesting that IVIG effects are not specific for the anti-platelet antibody producing cell lines.

Figures 1B, 2B, and 3B show the time course of IVIG effects on antibody production. Modeling the data revealed that IVIG effects on antibody production could be entirely attributed to the effects of IVIG on the apparent cell growth rate. Addition of IVIG inhibition parameters to the antibody production portion of the model did not improve the fits. Parameters for antibody production obtained from the non-linear least squares regression analysis are shown in table 2.

Neither the cell count nor the IgG concentration data for the 50 mg/ml IVIG samples were used in the modeling analysis, due to concern of potential confounding factors (see discussion). However, the 50 mg/ml IVIG data are shown in figures 1-3, to illustrate that this concentration of IVIG led to almost complete suppression of both cell growth and antibody production.

## **Discussion**

Soon after Imbach et al. reported efficacy of IVIG in ITP, researchers began investigating the mechanism of these effects. The earliest report that IVIG may inhibit autoantibody production in ITP patients came from Tsubakio et al. in 1983, in a study that found decreased titres of various auto-antibodies, in vivo, following IVIG infusion in a small number of patients.<sup>4</sup> Additionally, this study reported suppression of pokeweed mitogen-induced immunoglobulin synthesis, in vitro, from peripheral blood mononuclear cells isolated from the patients that received IVIG. The decreased in vivo autoantibody levels in this study were attributed solely to decreases in antibody production; however, this conclusion is not completely justified, as it is now understood that IVIG treatment increases the elimination rate of autoantibodies, also leading to decreases in antibody levels.<sup>11, 12</sup> Because of the possible dual effects of IVIG on antibody production and antibody elimination, in vivo analyses of IVIG effects on autoantibody production have been difficult.

Other researchers have also studied IVIG effects on antibody production, in vitro, and have concluded that IVIG treatment may lead to decreased antibody production.<sup>5-8</sup> Although it is accepted that IVIG treatment may decrease antibody production in certain experimental systems, IVIG effects on specific anti-platelet antibody production have not been as well studied. We hypothesized that IVIG may have effects on anti-platelet antibody production, in addition to its effects on general antibody production. These specific effects may occur as a result specific binding of anti-platelet antibodies to anti-idiotypic antibodies present in IVIG. There is some evidence to suggest that anti-

idiotypic antibodies may play a role in IVIG therapy of ITP.<sup>13, 14</sup> One pathway by which anti-idiotypic antibodies may lead to decreased antibody synthesis is by co-ligation of the B-cell antigen receptor and the inhibitory Fc $\gamma$ RIIb receptor, leading to apoptosis of the B-cell.<sup>15</sup> In the present work, a model system using hybridoma cells was used to test whether IVIG had specific effects on anti-platelet antibody production. No evidence was found to suggest that the effects of IVIG on anti-platelet antibody producing cells were any greater (or less) than the effects on a control cell line. No significant differences in sensitivity to IVIG effects between the 3 cell lines were found by ANOVA on the IC50 values.

In developing models to characterize the data, it was necessary to incorporate both time and concentration dependencies into the growth rate constants. This was done in an empiric fashion; however, it is reasonable that the growth rates should depend on time and concentration. For example, there is an apparent lag phase before exponential growth begins for hybridoma cells, when a new cell culture is initiated.<sup>16</sup> Additionally, it is apparent that a static culture will have a maximum number of cells that can be supported. Therefore, we feel the empiric function for the growth rate constant is justified.

Modeling of the data also revealed that after accounting for the effects of IVIG on apparent cell growth rate, no further inhibition of antibody production rate was necessary to characterize the antibody data. Thus it appears that the major effect of IVIG in this

system was to regulate either cell growth or death, rather than to decrease the rate of antibody production.

The inhibitory effects of IVIG on cell growth and antibody production occurred at physiologically relevant concentrations of IVIG, suggesting that inhibition of antibody production may occur in vivo. Furthermore, the supra-physiological concentration of IVIG (50 mg/ml) almost completely inhibited the growth of the hybridoma cells (see figure 4). However, the 50 mg/ml data were not used in the modeling analysis, because of potential confounding influences due to high osmolarity. The osmolarity of the 50 mg/ml samples was ~850 mOsm, whereas the 0.5 and 5 mg/ml samples had osmolarities of ~310 and ~360 mOsm, respectively. However, even without using the 50 mg/ml data to characterize IVIG effects, simulations performed using the models predict almost complete suppression of cell growth and significant suppression of antibody production, for cells incubated in the presence of 50 mg/ml IVIG (data not shown). Thus, the complete lack of cell growth and antibody production may result in large part from the influence of IVIG, rather than the high osmolarity. In fact, other researchers have studied IVIG effects on lymphocyte proliferation using both a dialysed and a clinical preparation of IVIG, and have shown that both the clinical (hypertonic) and the dialysed (isotonic) IVIG preparations led to significant decreases in cell viability.<sup>17</sup> Moreover, the decreases in cell viability between cells incubated with the two preparations were very similar up to 40 mg/ml IVIG. However, at 50 mg/ml IVIG, the hypertonic clinical preparation led to greater decreases in cell viability than did the dialysed IgG preparation,

supporting our suspicions that high osmolarity may be a confounding influence with the clinical preparation at 50 mg/ml.

We point out that the current experimental design does not easily lend itself to a mechanistic interpretation concerning how IVIG is decreasing the apparent growth rate of the hybridoma cells. The effect may be due to a decrease in the cell growth rate, an increase in the cell death rate, or both of these effects. Because only total cell numbers were measured (rather than living/dead cells), one cannot easily distinguish between the two types of effects; however, some evidence exists in the literature to suggest that IVIG directly induces cellular apoptosis.<sup>17</sup> The purpose of the present study was to determine if anti-platelet antibody producing cells were more sensitive to IVIG effects than a control cell line. No differences were seen between IVIG effects on the anti-platelet antibody producing cells and on the control cell line; consequently, no further efforts were made to study the mechanism of the general effects of IVIG on antibody production, at this time.

In summary, IVIG treatment decreased the apparent rates of cell growth of 3 hybridoma cell lines, *in vitro*. The decreases in cell growth led to decreases in the apparent rates of antibody production from the cells. No difference was detected between IVIG effects on the anti-platelet antibody producing cell lines and the control cell line. Thus, we conclude that IVIG did not have specific effects on anti-platelet antibody production, in this experimental system. However, because of the general effect of IVIG on antibody production, further studies into the importance of this potential effect of IVIG in ITP are

warranted. Our laboratory is currently developing animal models of ITP with which to gain more insight into possible effects of IVIG on anti-platelet (and general) antibody production, in vivo.

## References

1. Imbach P, Barandun S, d'Apuzzo V, et al. High-dose intravenous gammaglobulin for idiopathic thrombocytopenic purpura in childhood. *Lancet*. 1981;1:1228-31.
2. George JN, Woolf SH, Raskob GE, et al. Idiopathic thrombocytopenic purpura: a practice guideline developed by explicit methods for the American Society of Hematology. *Blood*. 1996;88:3-40.
3. Knapp MJ, Colburn PA. Clinical uses of intravenous immune globulin. *Clin Pharm*. 1990;9:509-29.
4. Tsubakio T, Kurata Y, Katagiri S, et al. Alteration of T cell subsets and immunoglobulin synthesis in vitro during high dose gamma-globulin therapy in patients with idiopathic thrombocytopenic purpura. *Clin Exp Immunol*. 1983;53:697-702.
5. Dammacco F, Iodice G, Campobasso N. Treatment of adult patients with idiopathic thrombocytopenic purpura with intravenous immunoglobulin: effects on circulating T cell subsets and PWM-induced antibody synthesis in vitro. *Br J Haematol*. 1986;62:125-35.
6. Bordet JC, Follea G, Carosella E, Dechavanne M. Intravenous high-dose IgG therapy induced alterations of spleen lymphocyte IgM secretion and T cell subsets

- in patients with idiopathic thrombocytopenic purpura. *Thromb Res.* 1987;47:165-74.
7. Newland AC, Macey MG, Veys PA. Cellular changes during the infusion of high dose intravenous immunoglobulin. *Blut.* 1989;59:82-7.
  8. Bussel JB. Modulation of Fc receptor clearance and antiplatelet antibodies as a consequence of intravenous immune globulin infusion in patients with immune thrombocytopenic purpura. *J Allergy Clin Immunol.* 1989;84:566-77; discussion 577-8.
  9. Hansen RJ, Balthasar JP. An ELISA for quantification of murine IgG in rat plasma: application to the pharmacokinetic characterization of AP-3, a murine anti-glycoprotein IIIa monoclonal antibody, in the rat. *J Pharm Biomed Anal.* 1999;21:1011-6.
  10. Hansen RJ, Balthasar JP. Pharmacokinetics, pharmacodynamics, and platelet binding of an anti-glycoprotein IIb/IIIa monoclonal antibody (7E3) in the rat: a quantitative rat model of immune thrombocytopenic purpura. *J Pharmacol Exp*

11. Hansen RJ, Balthasar JP. Intravenous immunoglobulin effects on platelet count and anti-platelet antibody disposition in a rat model of immune thrombocytopenia. *Blood*. 2002;In review.
12. Bleeker WK, Teeling JL, Hack CE. Accelerated autoantibody clearance by intravenous immunoglobulin therapy: studies in experimental models to determine the magnitude and time course of the effect. *Blood*. 2001;98:3136-42.
13. Berchtold P, Dale GL, Tani P, McMillan R. Inhibition of autoantibody binding to platelet glycoprotein IIb/IIIa by anti-idiotypic antibodies in intravenous gammaglobulin. *Blood*. 1989;74:2414-7.
14. Mehta YS, Badakere SS. In-vitro inhibition of antiplatelet autoantibodies by intravenous immunoglobulins and Rh immunoglobulins. *J Postgrad Med*. 1996;42:46-9.
15. Ballou M. Mechanisms of action of intravenous immune serum globulin in autoimmune and inflammatory diseases. *J Allergy Clin Immunol*. 1997;100:151-7.

16. Abu-Absi NR, Srienc F. Instantaneous evaluation of mammalian cell culture growth rates through analysis of the mitotic index. *J Biotechnol.* 2002;95:63-84.
  
17. Prasad NK, Papoff G, Zeuner A, et al. Therapeutic preparations of normal polyspecific IgG (IVIg) induce apoptosis in human lymphocytes and monocytes: a novel mechanism of action of IVIg involving the Fas apoptotic pathway. *J Immunol.* 1998;161:3781-90.

## Figure Legends

Figure 1. IVIG effects on 7E3-producing hybridoma cells. Panel A. IVIG effects on the apparent growth rate of 7E3-producing cells are shown. Treatment groups are as follows: no IVIG (●), 0.5 mg/ml IVIG (■), 5 mg/ml IVIG (▲), and 50 mg/ml (○). Cells were counted using a Coulter Z1 electronic particle counter. The solid lines represent the best fit of the data, using the mathematical model described in the Methods section, and shown in scheme 1. Parameter values resulting from the modeling are shown in table 2. IVIG decreased the apparent rate of cell growth, with an IC<sub>50</sub> value of 2.9±0.6. Panel B. IVIG effects on the apparent rate of 7E3 production are shown. Treatment groups are designated by the same symbols as for the cell number data in panel A. IgG concentrations were determined via ELISA. Solid lines represent the best fit of the data. IVIG treatment led to decreases in the apparent rate of 7E3 production. The 50 mg/ml data were not used in the modeling analysis, due to potential confounding factors.

Figure 2. IVIG effects on AP-3-producing hybridoma cells. Panel A. IVIG effects on the apparent growth rate of AP-3-producing cells are shown. Treatment groups are as follows: no IVIG (●), 0.5 mg/ml IVIG (■), 5 mg/ml IVIG (▲), and 50 mg/ml IVIG (○). Cells were counted using a Coulter Z1 electronic particle counter. The solid lines represent the best fit of the data, using the mathematical model described in the Methods section, and shown in scheme 1. Parameter values resulting from the modeling are shown in table 2. IVIG decreased the apparent rate of cell growth, with an IC<sub>50</sub> value of 6.4±1.5. Panel B. IVIG effects on the apparent rate of AP-3 production are shown.

Treatment groups are designated by the same symbols as for the cell number data in panel A. IgG concentrations were determined via ELISA. Solid lines represent the best fit of the data. The 50 mg/ml data were not used in the modeling analysis, due to potential confounding factors. IVIG treatment led to decreases in the apparent rate of AP-3 production.

Figure 3. IVIG effects on 1B7.11-producing hybridoma cells. Panel A. IVIG effects on the apparent growth rate of 1B7.11-producing cells are shown. Treatment groups are as follows: no IVIG (●), 0.5 mg/ml IVIG (■), 5 mg/ml IVIG (▲), and 50 mg/ml IVIG (○). Cells were counted using a Coulter Z1 electronic particle counter. The solid lines represent the best fit of the data, using the mathematical model described in the Methods section, and shown in scheme 1. Parameter values resulting from the modeling are shown in table 2. IVIG decreased the apparent rate of cell growth, with an IC50 value of  $4.1 \pm 1.8$ . Panel B. IVIG effects on the apparent rate of 1B7.11 production are shown. Treatment groups are designated by the same symbols as for the cell number data in panel A. IgG concentrations were determined via ELISA. Solid lines represent the best fit of the data. The 50 mg/ml data were not used in the modeling analysis, due to potential confounding factors. IVIG treatment led to decreases in the apparent rate of 1B7.11 production.

Scheme 1. Schematic representation of the mathematical model used to characterize IVIG effects on cell growth and antibody production. Cell and IgG represent cell and IgG concentrations in their respective compartments. Cell growth is determined by a 1<sup>st</sup> -

order rate function,  $K_g(t)$ , that is time- and cell-concentration dependent. It is upon this rate function that IVIG exerts inhibitory effects in this model.  $K_{igg}(t)$  is a zero-order, time- and concentration-dependent rate function governing IgG production.

Table 1. Parameter values obtained from the best fits of the cell concentration data.

Parameter Name	7E3	AP-3	1B7.11
a (hr <sup>-2</sup> )	$2.1 \pm 0.2 \times 10^{-4}$	$9.3 \pm 0.6 \times 10^{-4}$	$3.6 \pm 0.5 \times 10^{-4}$
IC50 (mg/ml)	$2.9 \pm 0.6$	$6.4 \pm 1.5$	$4.1 \pm 1.8$
Cellmax (cells/ml)	$1.5 \pm 1.2 \times 10^6$	$6.9 \pm 0.4 \times 10^5$	$8.2 \pm 0.3 \times 10^5$
Cell0(1) (cells/ml)	$3.2 \pm 0.2 \times 10^4$	$2.4 \pm 0.2 \times 10^4$	$1.8 \pm 0.3 \times 10^4$
Cell0(2) (cells/ml)	$2.7 \pm 0.1 \times 10^4$	$2.5 \pm 0.2 \times 10^4$	$1.8 \pm 0.3 \times 10^4$
Cell0(3) (cells/ml)	$3.3 \pm 0.2 \times 10^4$	$2.8 \pm 0.2 \times 10^4$	$1.7 \pm 0.3 \times 10^4$

Table 2. Parameter values obtained from the best fits of the antibody concentration data.

	7E3	AP-3	1B7.11
b (ng/hr <sup>2</sup> /cell)	$1.4 \pm 0.5 \times 10^{-6}$	$7.7 \pm 0.7 \times 10^{-6}$	$6.7 \pm 0.8 \times 10^{-6}$
IgGmax (ng/ml)	$4 \pm 40 \times 10^4$	$1.2 \pm 0.1 \times 10^4$	$1.3 \pm 0.3 \times 10^4$
IgG0(1) (ng/ml)	$550 \pm 70$	$310 \pm 40$	$620 \pm 70$
IgG0(2) (ng/ml)	$530 \pm 60$	$310 \pm 40$	$540 \pm 60$
IgG0(3) (ng/ml)	$430 \pm 60$	$320 \pm 40$	$500 \pm 60$

Figure 1A.

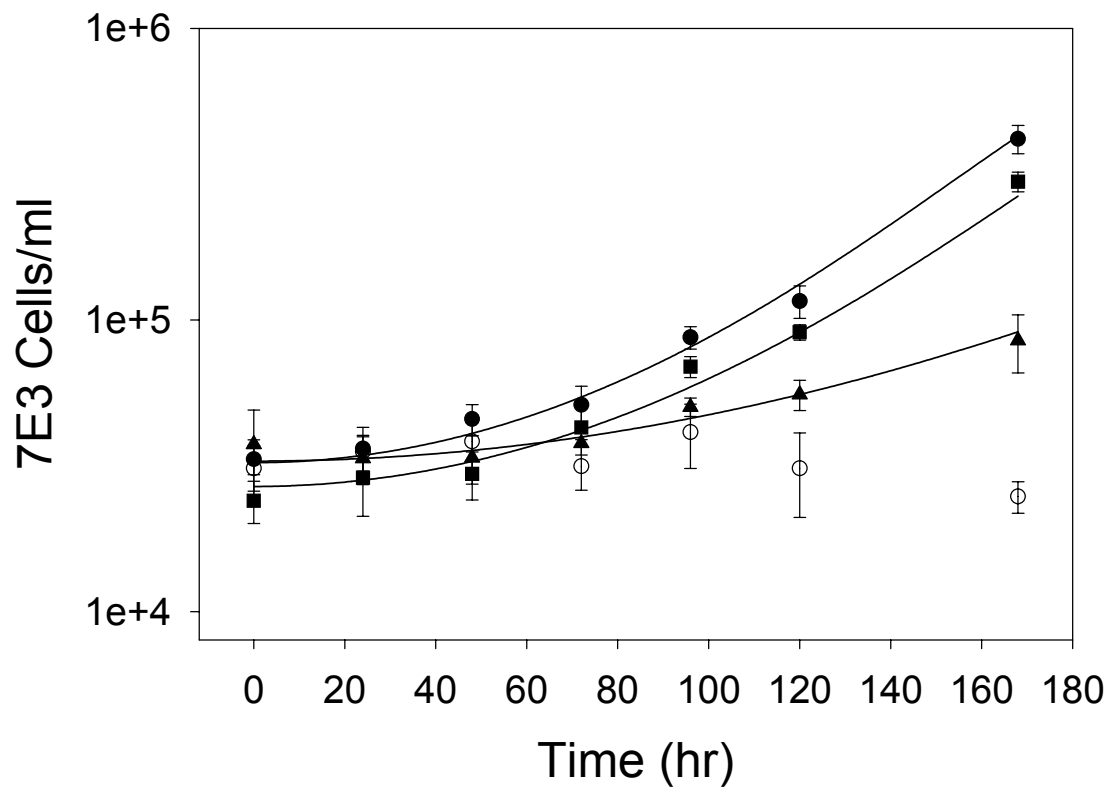


Figure 1B.

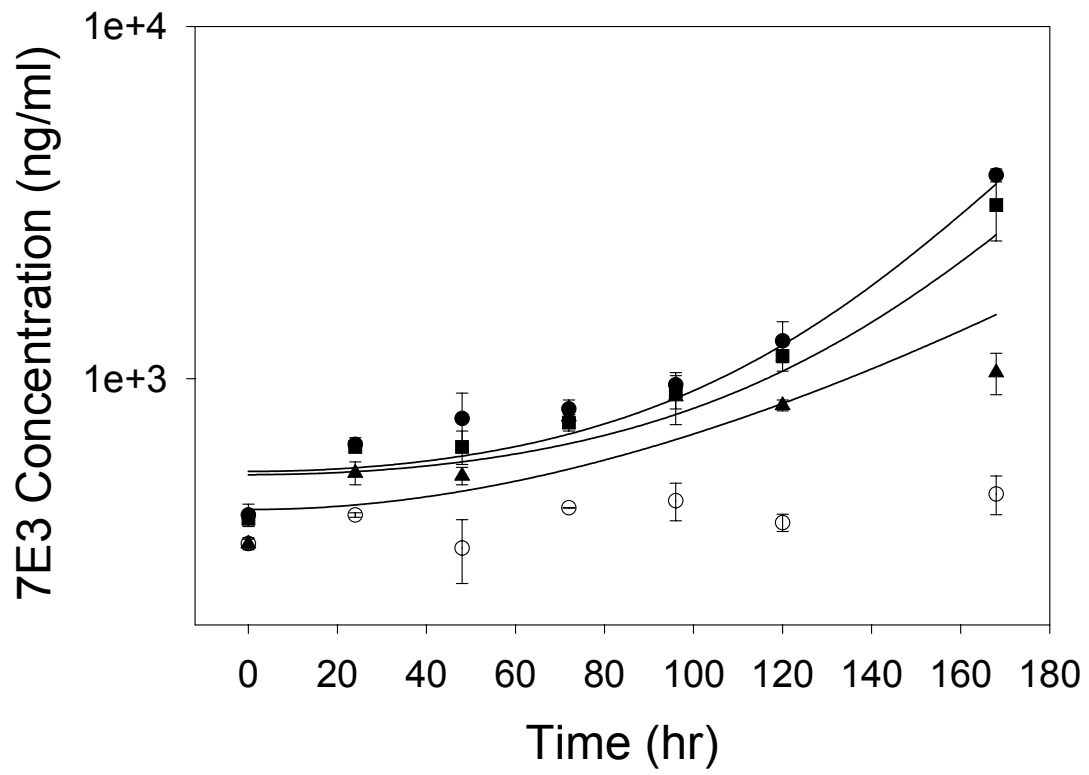


Figure 2A.

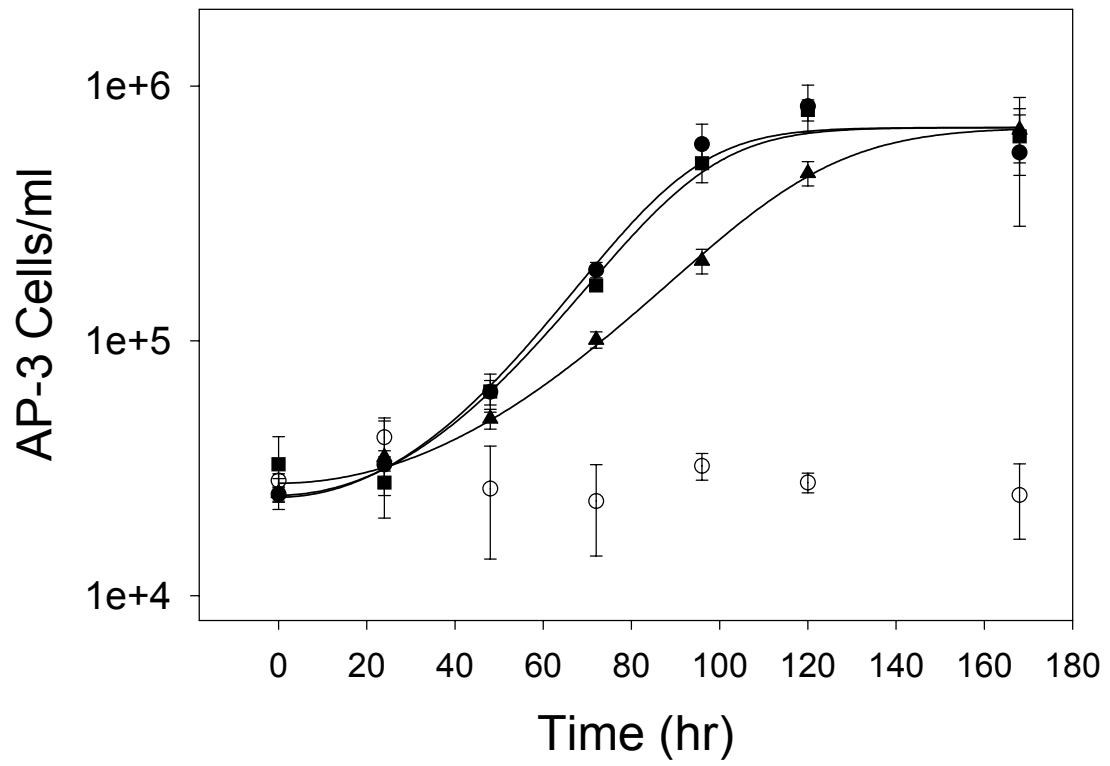


Figure 2B.

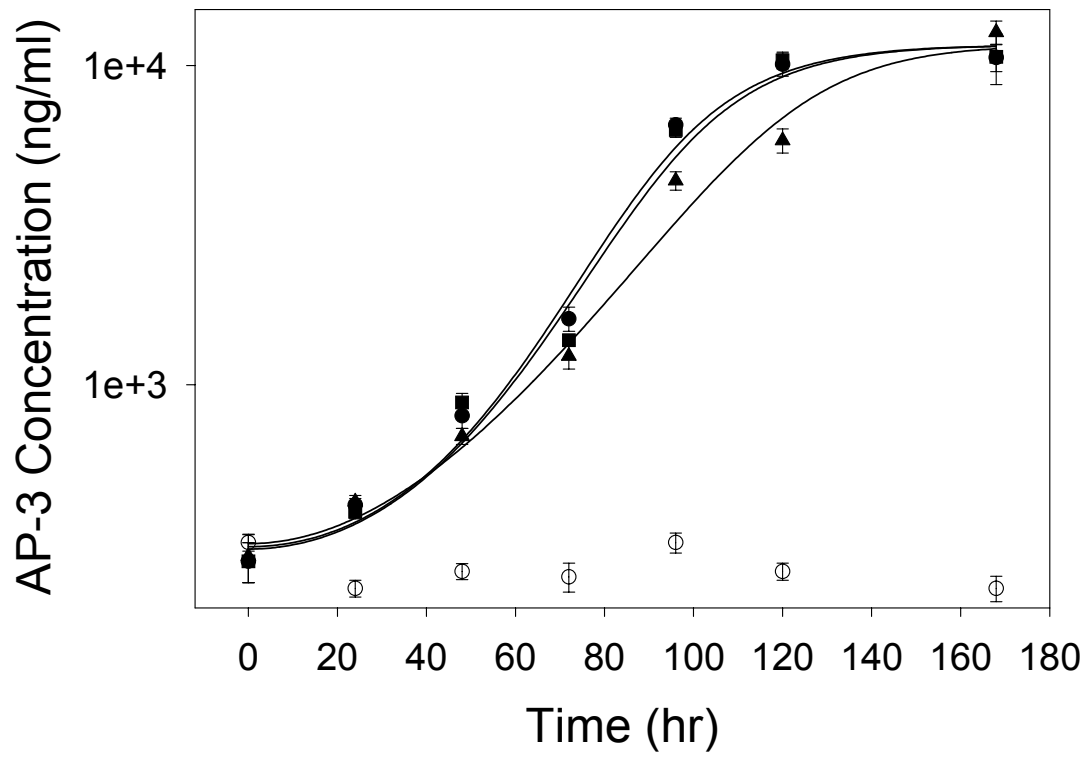


Figure 3A.

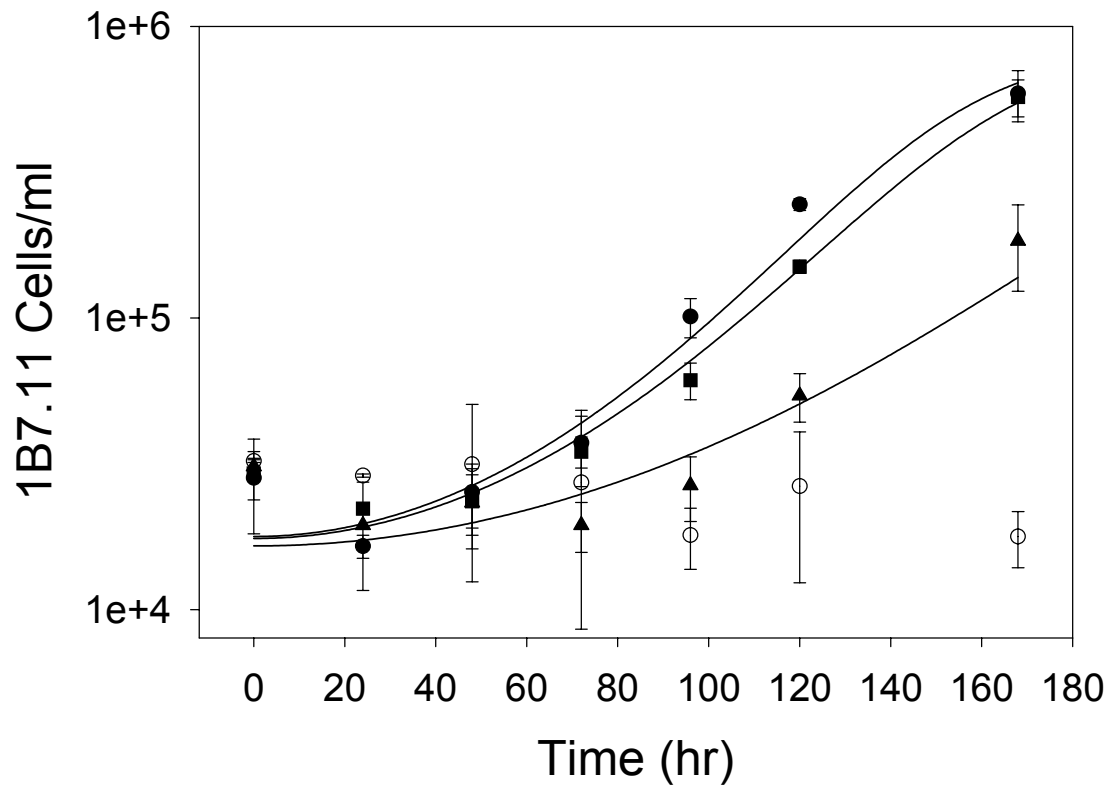
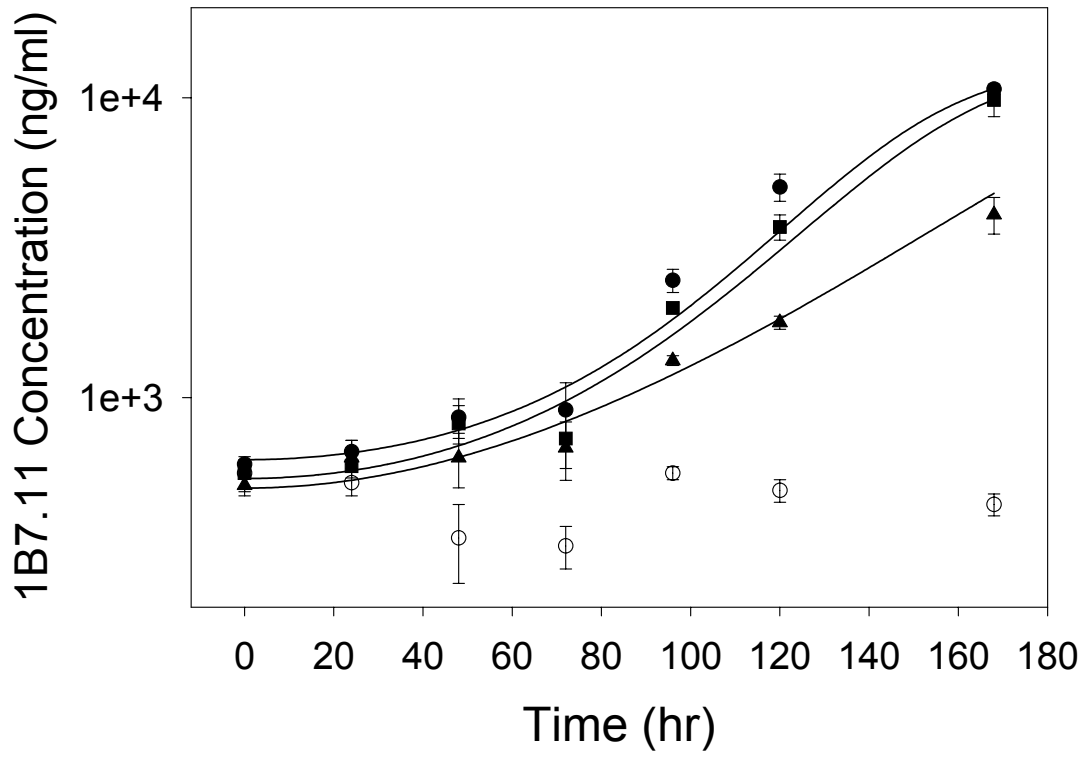
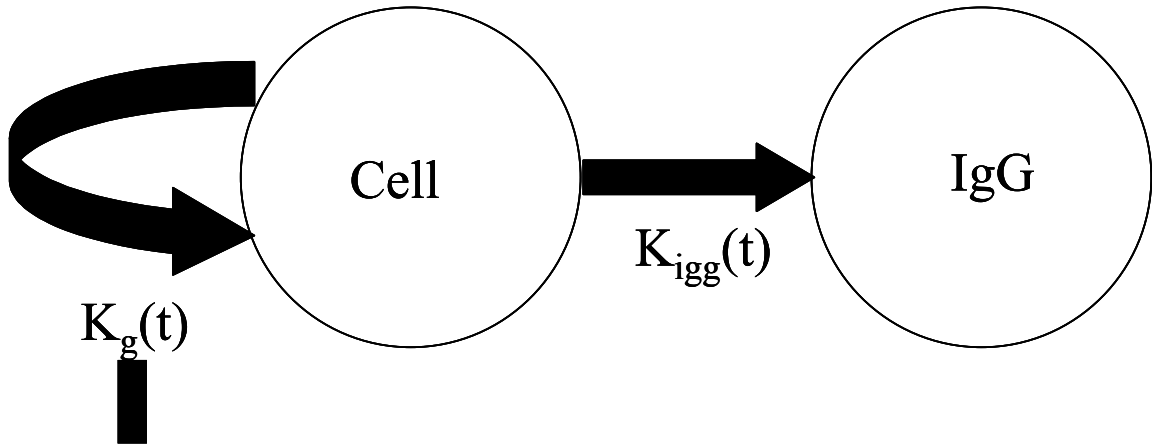


Figure 3B.



Scheme 1.



— Inhibition of  $K_g(t)$  by IVIG

# CHAPTER SEVEN

---

PHARMACOKINETIC AND PHARMACODYNAMIC MODELING OF  
THE EFFECTS OF INTRAVENOUS IMMUNOGLOBULIN ON ANTI-  
PLATELET ANTIBODY DISPOSITION IN A RAT MODEL OF  
IMMUNE THROMBOCYTOPENIA

---

## **Abstract**

Recently, our laboratory reported that intravenous immunoglobulin (IVIG) treatment increased anti-platelet antibody (7E3) clearance in a rat model of immune thrombocytopenic purpura (ITP). However, because of the multi-faceted nature of IVIG therapy, the importance of this increase in anti-platelet antibody clearance to the total therapeutic effect of IVIG was unclear. The purposes of the present study were 1) to develop a new, mechanistic model of IgG pharmacokinetics; 2) develop a pharmacokinetic/pharmacodynamic (PK/PD) model relating 7E3 concentrations to the platelet count time course observed following 7E3 treatment; and 3) use these mathematical models to gain insight into the importance of increased 7E3 clearance relative to the total effect of IVIG in this model of ITP. A mechanism-based pharmacokinetic model was developed that adequately characterized IVIG effects on 7E3 pharmacokinetics. The structure of this model is based on competition between IgG molecules for occupancy of the protective FcRn receptor. The model accurately captured anti-platelet antibody concentration vs. time data in the rat and in the mouse, in the presence and absence of IVIG, and in mice lacking expression of the FcRn receptor. An indirect response PK/PD model was also developed, which accurately characterized 7E3 effects on platelet counts. Using these models, it was estimated that  $50 \pm 11\%$  of the total protective effect of IVIG in this acute model of ITP can be accounted for by this increase in 7E3 clearance. This work demonstrates the potential utility of PK/PD modeling in gaining a better understanding of the relative importance of specific mechanisms of drug action in complicated therapeutic situations.

## **Introduction**

Immune thrombocytopenia (ITP) is an autoimmune disease characterized by decreased platelet counts and increased platelet destruction (Fujisawa et al., 1991; Newland and Macey, 1994). This increased platelet destruction is believed to be due to the interaction of anti-platelet antibodies with proteins on the surface of the platelet, eventually leading to the destruction of the platelet (Berchtold and Wenger, 1993; Fujisawa et al., 1991). Imbach et al. (Imbach et al., 1981) first showed in 1981 that administration of high-doses of pooled immunoglobulin, intravenously, leads to increases in platelet counts in many patients with ITP. However, despite much research over the past 20 years, the mechanism of action of intravenous immunoglobulin (IVIG) treatment in ITP is still unclear.

Various laboratories have reported at least 6 general ways that IVIG may be achieving beneficial effects in ITP. According to studies in humans, and in several different experimental systems, IVIG may increase platelet counts by blocking Fc-mediated platelet destruction (Fehr et al., 1982), interfering with complement mediated platelet destruction (Basta et al., 1989), modulating the idiotype-anti-idiotype network (Berchtold et al., 1989; Mehta and Badakere, 1996), increasing platelet production (Grossi et al., 1986), decreasing anti-platelet antibody production (Tsubakio et al., 1983), and increasing the expression of inhibitory receptors that block platelet phagocytosis (Samuelsson et al., 2001). Unfortunately, it has been very difficult to determine which of these effects, if any, are important for the increase in platelet counts seen following IVIG therapy of ITP in the clinical situation. We feel that determination of the pathways by

which IVIG achieves beneficial effects may lead to the development of new, cost-effective therapies of ITP.

The investigation of mechanisms of IVIG action in humans is complicated by a number of factors. Perhaps most importantly, there are no reliable assays for determination of anti-platelet antibodies (Raife et al., 1997). Without assays for pathogenic antibodies, it is impossible to quantitatively relate the antibody concentrations to the effects produced on the platelet counts. Other complicating factors include the widely fluctuating nature of the disease, and the large inter-patient variability in platelet counts.

We have proposed that the use of animal models of ITP may eliminate some of the difficulties encountered in the human condition, while still providing relevant information to the development of new therapies of ITP. Recently, we reported a quantitative rat model of ITP (Hansen and Balthasar, 2001). This model of ITP was produced by intravenous administration of a monoclonal anti-platelet antibody, 7E3, to rats. Subsequent studies showed that IVIG administration protected the rats from 7E3-mediated thrombocytopenia, in a dose-dependent fashion. In studying IVIG effects in this model, we found that IVIG treatment increased the clearance of 7E3. However, at that time, it was difficult to determine whether this effect of IVIG on anti-platelet antibody disposition was related to the therapeutic effect on platelet counts (Hansen and Balthasar, 2002a).

Because IVIG-mediated increases in anti-platelet antibody clearance had not previously been reported, studies were undertaken to better understand the mechanism of this effect. It was hypothesized that IVIG elicits this effect by saturation of the Brambell receptor (also known as FcRp) (Brambell et al., 1964), which protects IgG from catabolism. The presence of a protective receptor for IgG had been postulated as early as 1964 (Brambell et al., 1964), but was not identified until 1996, when several researchers showed that the FcRp receptor was the same receptor responsible for transporting IgG across the neonatal intestine (FcRn) (Ghetie et al., 1996; Junghans and Anderson, 1996). Mice lacking FcRn demonstrate accelerated rates of IgG elimination and exhibit low levels of endogenous IgG. Studies in control mice and in ‘knockout’ mice lacking expression of the FcRn receptor have revealed that IVIG increases 7E3 clearance in control animals (consistent with our observations in rats), but does not increase 7E3 clearance in knockout animals. This finding is consistent with the hypothesis that IVIG increases anti-platelet antibody elimination by saturation of FcRn (Hansen and Balthasar, 2002b). It is hypothesized that this increase in antibody clearance may be an important contributor to IVIG effects in immune thrombocytopenia, both in the rat model of ITP and in humans.

In this study, we report a general model of IgG pharmacokinetics that characterizes IVIG effects on 7E3 elimination. This model is a mechanistic model, based on competition between IgG molecules for the FcRn receptor. Additionally, we present a pharmacokinetic/ pharmacodynamic (PK/PD) model of 7E3 effects on platelet counts, and use modeling to estimate the importance of the effect of IVIG on 7E3 clearance, relative to the total effects that IVIG has in the model. This work illustrates the concept

of using PK/PD models of disease and therapy to quantitatively determine the importance of one specific pathway in a complex therapeutic situation.

## Methods

*IgG pharmacokinetic model.* To develop a quantitative model of ITP, anti-platelet antibody (7E3) pharmacokinetics (0.8-8 mg/kg) were studied in the presence or absence of IVIG (0-2 g/kg), in jugular vein-cannulated Sprague-Dawley rats. Additional 7E3 (8 mg/kg) pharmacokinetic studies were then performed in mice lacking FcRn receptor expression, and in control mice, again in the presence or absence of IVIG (1 g/kg), to gain a better understanding of the role of FcRn in the observed effects of IVIG on 7E3 elimination. The methodology for obtaining these data is reported elsewhere (Hansen and Balthasar, 2001; Hansen and Balthasar, 2002a; Hansen and Balthasar, 2002b). A simple, mechanism-based pharmacokinetic model was developed to characterize all of the 7E3 concentration vs. time data.

A schematic representation of the pharmacokinetic model is shown in scheme 1. Differential equations describing the model are shown below.

$$\begin{aligned}\frac{dC_1}{dt} &= -k_{up} \times C_1 + k_{ret} \times C_E \times (1 - f_u) \\ \frac{dC_E}{dt} &= k_{up} \times C_1 - k_{ret} \times C_E \times (1 - f_u) - k_{deg} \times C_E \times f_u \\ f_u &= 1 - \frac{K_d + R_t + C_{1,T} - \sqrt{(K_d + R_t + C_{1,T})^2 - 4 \times C_{1,T} \times R_t}}{2 \times C_{1,T}}\end{aligned}$$

In these equations,  $C_1$  and  $C_E$  represent IgG concentrations (nM) in the central and endosomal compartments, respectively.  $k_{up}$  ( $\text{hr}^{-1}$ ) and  $k_{ret}$  ( $\text{hr}^{-1}$ ) are rate constants characterizing the transfer of IgG from the central to the endosomal compartment and vice versa, and  $k_{deg}$  ( $\text{hr}^{-1}$ ) is a rate constant for the elimination of IgG.  $k_{deg}$  acts only on the unprotected IgG, while  $k_{ret}$  acts only on FcRn-bound IgG.  $f_u$  is the fraction of IgG not

bound to FcRn in the endosome,  $C_{1,T}$  is the total IgG concentration (i.e., rat IgG + 7E3 + IVIG) in the central compartment, and  $K_d$  (nM) and  $R_t$  (nM) represent the apparent affinity and capacity of the FcRn-IgG interaction in the endosome. The relationship for  $f_u$  was derived based on the following equilibria model:



In this model, the brackets represent molar concentrations, and the subscripts denote unbound concentrations. Mass balance equations were used for IgG and FcRn to obtain the final relationship for  $f_u$ . The same sets of equations were used to characterize 7E3 pharmacokinetics in both the rat and the mouse, with parameter values estimated separately for the two species.

The 7E3 concentration-time data from the FcRn-deficient and the control mice were fitted simultaneously. Because mice lacking expression of FcRn will have no return of IgG to the central compartment (i.e.,  $1 - f_u = 0$ ), the only parameters necessary to describe 7E3 disposition in these mice were  $k_{up}$  and the volume of the central compartment.  $K_d$  was fixed at a value of 4.8 nM, a value that has been reported for the interaction of mouse IgG with mouse FcRn (Popov et al., 1996).  $k_{ret}$  was set equal to  $k_{up}$ . The steady-state mouse IgG concentration was set to be  $1.47 \times 10^4$  nM (2.2 mg/ml) (Junghans and Anderson, 1996). All other parameters ( $k_{deg}$ ,  $k_{up}$ ,  $V_1$ , and  $R_t$ ) were estimated from a simultaneous fitting of the data.

All six 7E3 rat pharmacokinetic data sets were fit simultaneously. The rat steady-state IgG concentration was  $1.03 \times 10^5$  nM (15.5 mg/ml) (al-Bander et al., 1992).  $K_d$  was fixed

at a value of 500 nM, a value reported for the rat IgG-rat FcRn interaction (Sanchez et al., 1999). Again, in fitting 7E3 data in the rat,  $k_{ret}$  was set equal to  $k_{up}$ , and the remaining parameters were estimated. Initial conditions for the 7E3 equations were determined by back-extrapolation of the 7E3 concentration vs. time plots. Initial conditions for the IVIG concentrations were determined by dividing the dose of IVIG by the average volume of the central compartment, as determined from the 7E3 initial conditions. All data sets were weighted by  $1/y^2$ , and fits were performed using MicroMath Scientist. IVIG, mouse, and rat IgG concentrations were not available for fitting, and were simulated, using the same parameter values as 7E3.

*PK/PD model of 7E3 effects on platelet count.* An indirect response model was used to characterize 7E3 effects on platelet counts. This model is a slight variation of the traditional indirect response model describing drug-mediated stimulation of the elimination of a response (Dayneka et al., 1993). A semi-empirical function, incorporating physiologically relevant parameters describing platelet production and elimination, was used to characterize 7E3 effects on platelet count. The semi-empirical nature of the model was required because of the non-stationary platelet count in control rats. A schematic representation of the model is shown in scheme 2. Plasma 7E3 concentrations were determined using the equations shown above, and the pharmacodynamic parameters were fit separately, according to the equations shown below.

$$\frac{dR}{dt} = K_0(t) - K_{out} \times (1 + S \times C_{7E3}) \times R - K_{stress} \times R$$

$$K_0(t) = K_0^s \times (K_0 + m \times t)$$

In the above equations,  $K_0(t)$  ( $\% \text{ hr}^{-1}$ ) is a platelet input function that is time dependent, and is comprised of  $K_0$  ( $\% \text{ hr}^{-1}$ ), a physiologically relevant parameter describing platelet production, and two empiric parameters,  $K_0^s$  and  $m$  ( $\% \text{ hr}^{-2}$ ), necessary to characterize the baseline platelet count time-course in control rats. Elimination of response is determined by  $K_{\text{out}}$  ( $\text{hr}^{-1}$ ), a physiologically relevant parameter for platelet elimination in control rats, and by  $K_{\text{stress}}$  ( $\text{hr}^{-1}$ ), an empiric parameter also required to characterize the platelet count time-course in control animals.  $K_0$  and  $K_{\text{out}}$  were fixed at 3%/hr and 0.03  $\text{hr}^{-1}$ , respectively, and are considered to be physiologically reasonable values for platelet production and platelet elimination rate constants in cannulated rats (see Meuleman et al. (Meuleman et al., 1980) for platelet kinetics in cannulated rats).  $S$  ( $\text{nM}^{-1}$ ) is a stimulation parameter that allows 7E3 to stimulate the elimination rate of platelets.

*Estimation of the importance of IVIG effects on 7E3 clearance.* The PK model in shown in scheme 1, and the PK/PD model shown in scheme 2 were used to estimate the importance of the increase of 7E3 clearance following IVIG administration, relative to the other effects IVIG may have on platelet count. For each dose of IVIG, the predicted platelet count profiles were generated using the PK/PD model, based on the 7E3 kinetics seen following that dose of IVIG. The effect areas (i.e., area between the effect curve and the baseline) were calculated using WinNonlin software. These effect areas were then compared to the actual effect areas observed following IVIG treatment. The ratio of the predicted decrease in effect area to the actual decrease in the effect area was determined to be the percentage of the total effect of IVIG due to the change in 7E3 pharmacokinetics.

## Results

Best-fit lines characterizing the effect of IVIG on 7E3 pharmacokinetics in control mice, and in mice lacking FcRn expression, are shown in figure 1. As can be seen from figure 1, 7E3 concentrations decline mono-exponentially in mice lacking expression of FcRn. However, mice expressing FcRn show the more characteristic poly-exponential decline of 7E3 concentrations with time. Table 1 lists the parameter values obtained from the fit.

Characterization of 7E3 pharmacokinetics in the rat, in the absence or presence of IVIG, is shown in figures 3 and 4, respectively. At the highest dose of IVIG, 7E3 clearance (determined using non-compartmental analysis) was increased from  $0.78 \pm 0.09$  to  $1.85 \pm 0.19$  ml hr<sup>-1</sup> kg<sup>-1</sup> (Hansen and Balthasar, 2002a). All the rat 7E3 data were fit simultaneously; however, the 7E3-alone and 7E3+IVIG data are plotted separately for added clarity. As can be seen from the figures, this new, relatively simple model of IgG pharmacokinetics was able to characterize 7E3 pharmacokinetics alone, and in the presence of IVIG (i.e, a 2500-fold range of IgG doses), while accounting for endogenous IgG levels. Furthermore, the model was able to adequately characterize 7E3 pharmacokinetics in both the rat and the mouse. The parameter values resultant from the best fits of the 7E3 data in the rat, are also shown in table 1.

The models predict that ~83 and ~79% of the IgG in the endosomal compartment will be bound to FcRn, in the absence of IVIG treatment for mice and rats, respectively. Following IVIG treatment, the model predicts that the fraction of mouse IgG bound to FcRn will reach ~11% at the low point, and the fraction of rat IgG bound will reach

~21% at the low point, following 1 and 2 g/kg doses of IVIG, respectively. Simulations of the expected change in endogenous rat IgG concentrations following IVIG treatment are shown in figure 4, and illustrate the relative magnitude of changes in IgG concentrations that might be predicted for any given endogenous autoantibody concentration following IVIG therapy, in this model.

Effects of 7E3 on rat platelet counts are shown in figure 5, with the lines representing the best-fit of the data using the PK/PD model shown in scheme 2. Resulting parameter values are shown in table 2. The model adequately characterized the time course of 7E3-mediated decreases in platelet counts. The PK/PD model of 7E3 effects on platelet counts, together with the PK model characterizing IVIG effects on 7E3 clearance were used to determine the relative importance of the effect of IVIG on 7E3 clearance to the total effect that IVIG had on preventing 7E3-induced thrombocytopenia in this model. Figure 6, panel A, depicts model predicted platelet counts following 7E3 and IVIG administration. This modeling assumes that the only effect of IVIG on platelet counts is the increased clearance of 7E3 (i.e., the pharmacodynamic relationship between 7E3 concentrations and effects on platelet count remain unchanged). Figure 6, panel B, shows the actual platelet count time-course following IVIG administration, as originally reported in a previous study (Hansen and Balthasar, 2002a). A comparison of panels A and B of figure 6 show that IVIG effects on 7E3 clearance cannot account for the total effect of IVIG on platelet counts in this model. To determine the relative importance of the pharmacokinetic effect of IVIG, effect areas were calculated, and the predicted change in effect area was compared to the actual change in effect area, for each dose of

IVIG (see table 3). The increase in 7E3 clearance can account for  $50\pm 11\%$  of the total effect of IVIG.

## Discussion

For the last 2 decades, researchers have been trying to understand the mechanisms by which IVIG increases platelet counts in patients with ITP. Although many different possible effects of IVIG have been identified, the relative importance of any one effect has been difficult to determine. This study reports the mathematical characterization of a disease model of ITP, in an attempt to determine the relative importance of a new mechanism of IVIG action in ITP, recently reported by our laboratory. In so doing, we have developed a new, general model for IgG pharmacokinetics. This model is especially useful for characterization and prediction of antibody disposition following high doses of antibody. The strengths of the model include its simplicity, its mechanistic basis, and its ability to easily adapt to many different situations.

This new model of IgG pharmacokinetics characterized well the effects of IVIG on 7E3 pharmacokinetics, in both the mouse and the rat. Although the structure of the model readily allowed for characterization of the 7E3 pharmacokinetic data, unfortunately, at this time, not enough data was available to allow for accurate estimation of all of the parameters. For this reason, several assumptions were made to simplify the model, and allow for more reliable estimation of parameter values. For example, the model was simplified by forcing  $k_{ret}$  to equal  $k_{up}$ . Additionally,  $K_d$  values were fixed to reasonable values obtained from the literature. However, these values may also not be relevant, as these  $K_d$  values were determined from in vitro systems, and may not reflect the true affinity for the interaction between IgG and FcRn in the endosome. Furthermore, the  $K_d$  values for endogenous rat (or mouse) IgG, human IgG and 7E3 were assumed to be

identical in this model. This assumption is almost certainly incorrect. Future studies, in which endogenous mouse or rat IgG concentrations and IVIG concentrations are measured, may allow for more accurate estimation of some of the model parameters. However, because the  $K_d$  values obtained from the literature are well below the endogenous IgG levels, accurate estimation of this parameter may prove to be very difficult. Combination of in vitro binding analyses with extensive in vivo data will likely allow for more extensive model development, and more predictive power.

Interestingly, the modeling of IVIG effects on 7E3 kinetics led to predictions that the FcRn receptor, the receptor responsible for protecting IgG from catabolism (Ghetie et al, 1996; Junghans and Anderson, 1996), is almost completely saturated at physiological concentrations of IgG. This prediction is in line with the prediction of Brambell's original empiric model for IgG pharmacokinetics (Brambell et al, 1964). Because of this saturation, modest increases in plasma IgG levels will immediately lead to increases in IgG clearance, as little more IgG can bind to FcRn. This immediate increase in clearance is perhaps most readily observed in the plots of endogenous mouse and rat IgG concentrations following IVIG treatment. The model predicts that mouse and rat IgG concentrations immediately begin to decrease, and then slowly return toward the steady-state values as the total plasma IgG concentrations return toward normal. The accuracy of these predictions will be improved in the future by accumulation of additional data (e.g., endogenous IgG levels and IVIG levels following IVIG administration).

To allow for determination of the importance of the effect of increased 7E3 clearance, relative to the total effect that IVIG has in this rat model of ITP, a PK/PD model was developed. To our knowledge, this is the first model of ITP that is quantitative with respect to anti-platelet antibody concentrations, as well as the first attempt to develop a PK/PD model relating plasma antibody concentrations to the platelet count time course. We feel this type of approach can be invaluable for gaining insight into specific processes, when a complicated situation such as IVIG treatment of ITP is under consideration.

To characterize 7E3 effects on platelet counts, a semi-empiric approach was used. From inspection of the baseline platelet count data in control rats, it was apparent that unknown, 'stress-related' factors were acting to increase the apparent rates of input and elimination of platelets, in control animals. This was likely due to the presence of the cannula, the use of a small amount of heparin to keep the cannula patent, and the sampling strategy (e.g., blood flowing through the cannula may cause platelet activation, leading to changes in the apparent rates of platelet production and elimination). Because of the magnitude of the change in platelet counts from baseline in control animals, it was necessary to account for this change in order to understand 7E3 effects on platelet counts. For this reason, the empiric portion of the model was developed to characterize the changes in platelet counts in the control animals. By separating the input and output rate determinants into empiric, or 'stress-related' portions (defined by  $K_0^s$ ,  $m$ , and  $K_{\text{stress}}$ ), and physiologically relevant portions (defined by  $K_0$  and  $K_{\text{out}}$ ) it was possible to allow 7E3 to act only on the physiologically relevant pathway of platelet elimination.

Because these mathematical models accurately described 7E3 effects on platelet count, as well as IVIG effects on 7E3 concentrations, it was possible to use the models to estimate the importance of IVIG effects on 7E3 concentrations, relative to the total effect of IVIG. The cumulative effect of 7E3 was defined as the area between the baseline and the platelet count time course. Simulations were used to produce predicted platelet count time curves based on 7E3 concentrations following IVIG treatment. These effect areas were then compared to the actual effect areas observed following IVIG treatment (see figure 6 and table 3). Interestingly, the effect of IVIG on 7E3 clearance could account for approximately half of the total effect of IVIG, and is likely a major component of IVIG effects, even in this acute model of thrombocytopenia. This conclusion would be nearly impossible to reach without having mathematical models that characterize the system.

Although the effect of IVIG on anti-platelet antibody clearance were observed in mouse and rat models of ITP, it is reasonable to suggest that IVIG would have similar effects on anti-platelet autoantibody clearance in humans. Though the mechanisms defining IgG catabolism have only recently been well appreciated, it has been known since the 1960's IgG clearance is dose-dependent in humans (Brambell et al, 1964), suggesting that this pathway of IVIG effects would also be relevant in the clinical situation. Better data and mathematical models will be necessary to fully understand the importance of this potential mechanism of action of IVIG in humans. However, based on the simulated endogenous mouse and rat IgG profiles (figure 4), we suggest that this pathway may at least be a minor contributor to IVIG effects in humans, and may be a major contributor. For example, if human autoantibody concentrations follow a similar time-course, as did

the predicted endogenous mouse IgG concentrations (see figure 4), then, depending on the initial autoantibody concentration, one might expect to see a dramatic and prolonged effect on platelet counts due to this mechanism of action alone.

The modeling presented in this work demonstrates the use of PK/PD models to understand the importance of a single mechanism of action of a potentially complex drug therapy. However, both the disease model and the mathematical models have potential for improvement. Future studies will attempt to further incorporate into the disease model, any pathways found to be important to IVIG effects (e.g., IVIG effects on complement- or Fc-mediated platelet destruction). Additionally, new animal models will be developed to overcome the difficulties associated with the non-stationary baseline platelet counts in control animals, and to allow for studies to be performed regarding IVIG effects on anti-platelet antibody production. The relative importance of other mechanisms of IVIG action will be determined, using similar methodology as was used in these studies.

In summary, IVIG effects in ITP patients are potentially multiple and complex. Our group recently reported that IVIG acts to increase the clearance of anti-platelet antibodies, and that this effect is mediated through the FcRn receptor. This work was performed to characterize the effects of IVIG on anti-platelet antibody pharmacokinetics, and to gain greater insight into the importance of that effect relative to the total therapeutic effect that IVIG. It is estimated that increased 7E3 clearance can account for approximately half of the total effect of IVIG in this acute model of ITP. We hypothesize

that this effect would be even more beneficial in the clinical situation, in which anti-platelet antibodies are slowly synthesized, rather than rapidly ‘dumped’ into the system. We propose that this general modeling approach may be useful in gaining further insight into the relevant mechanisms of IVIG action in ITP, and will point to the most effective targets for new therapies of ITP.

## References

al-Bander HA, Martin VI and Kaysen GA (1992) Plasma IgG pool is not defended from urinary loss in nephrotic syndrome. *Am J Physiol* **262**:F333-337.

Basta M, Langlois PF, Marques M, Frank MM and Fries LF (1989) High-dose intravenous immunoglobulin modifies complement-mediated in vivo clearance. *Blood* **74**:326-333.

Berchtold P, Dale GL, Tani P and McMillan R (1989) Inhibition of autoantibody binding to platelet glycoprotein IIb/IIIa by anti-idiotypic antibodies in intravenous gammaglobulin. *Blood* **74**:2414-2417.

Berchtold P and Wenger M (1993) Autoantibodies against platelet glycoproteins in autoimmune thrombocytopenic purpura: Their clinical significance and response to treatment. *Blood* **81**:1246-1250.

Brambell F, Hemmings W and Morris I (1964) A theoretical model of gamma-globulin catabolism. *Nature* **203**:1352-1355.

Dayneka NL, Garg V and Jusko WJ (1993) Comparison of Four Basic Models of Indirect Pharmacodynamic Responses. *J Pharmacokin Biopharm* **21**:457-478.

Fehr J, Hofmann V and Kappeler U (1982) Transient reversal of thrombocytopenia in idiopathic thrombocytopenic purpura by high-dose intravenous gamma globulin. *N Engl J Med* **306**:1254-1258.

Fujisawa K, TE OT, Tani P, Loftus JC, Plow EF, Ginsberg MH and McMillan R (1991) Autoantibodies to the presumptive cytoplasmic domain of platelet glycoprotein IIIa in patients with chronic immune thrombocytopenic purpura. *Blood* **77**:2207-2213.

Ghetie V, Hubbard JG, Kim JK, Tsen MF, Lee Y and Ward ES (1996) Abnormally short serum half-lives of IgG in beta 2-microglobulin-deficient mice. *Eur J Immunol* **26**:690-696.

Grossi A, Vannucchi AM, Casprini P, Morfini M and Ferrini PR (1986) Effects of high-dose intravenous gammaglobulin on kinetic parameters of <sup>51</sup>Cr-labelled platelets in chronic ITP. *Haematologica* **71**:123-127.

Hansen RJ and Balthasar JP (2001) Pharmacokinetics, pharmacodynamics, and platelet binding of an anti-glycoprotein IIb/IIIa monoclonal antibody (7E3) in the rat: A quantitative rat model of immune thrombocytopenic purpura. *J Pharm Exp Ther* **298**:1-7.

Hansen RJ and Balthasar JP (2002a) Intravenous immunoglobulin effects on platelet count and anti-platelet antibody disposition in a rat model of immune thrombocytopenia.

*Blood. Submitted.*

Hansen RJ and Balthasar JP (2002b) Intravenous immunoglobulin mediates effects on anti-platelet antibody clearance via the FcRn receptor. *Blood. Submitted.*

Imbach P, Barandun S, d'Apuzzo V, Baumgartner C, Hirt A, Morell A, Rossi E, Schoni M, Vest M and Wagner HP (1981) High-dose intravenous gammaglobulin for idiopathic thrombocytopenic purpura in childhood. *Lancet* **1**:1228-1231.

Junghans RP and Anderson CL (1996) The protection receptor for IgG catabolism is the beta2-microglobulin-containing neonatal intestinal transport receptor. *Proc Natl Acad Sci USA* **93**:5512-5516.

Mehta YS and Badakere SS (1996) In-vitro inhibition of antiplatelet autoantibodies by intravenous immunoglobulins and Rh immunoglobulins. *J Postgrad Med* **42**:46-49.

Meuleman DG, Vogel GMT and van Delft AML (1980) Effects of intra-arterial cannulation on blood platelet consumption in rats. *Thrombosis Research* **20**:44-55.

Newland AC and Macey MG (1994) Immune thrombocytopenia and Fc receptor-mediated phagocyte function. *Ann Hematol* **69**:61-67.

Popov S, Hubbard JG, Kim J-K, Ober B, Ghetie V and Ward ES (1996) The stoichiometry and affinity of the interaction of murine Fc fragments with the MHC class I-related receptor, FcRn. *Molec. Immun.* **33**:521-530.

Raife TJ, Olson JD and Lentz SR (1997) Platelet antibody testing in idiopathic thrombocytopenic purpura [letter]. *Blood* **89**:1112-1114.

Samuelsson A, Towers TL and Ravetch JV (2001) Anti-inflammatory activity of IVIG mediated through the inhibitory Fc receptor. *Science* **291**:484-486.

Sanchez LM, Penny DM and Bjorkman PJ (1999) Stoichiometry of the interaction between the major histocompatibility complex-related Fc receptor and its Fc ligand. *Biochemistry* **38**:9471-9476.

Tsubakio T, Kurata Y, Katagiri S, Kanakura T, Tamaki T, Kuyama J, Kanayama Y, Yonezawa T and Tarui S (1983) Alteration of T cell subsets and immunoglobulin synthesis in vitro during high dose gamma-globulin therapy in patients with idiopathic thrombocytopenic purpura. *Clin Exp Immunol* **53**:697-702.

## Figure Legends

Figure 1. 7E3 pharmacokinetics in mice. Mice were dosed with IVIG (1 g/kg), or saline, followed by 7E3 (8 mg/kg). Treatment groups are designated as follows: 7E3+saline in control mice (●); 7E3+IVIG in control mice (■); 7E3+saline in FcRn-deficient mice (○); and 7E3+IVIG in FcRn-deficient mice (□). IVIG increased 7E3 clearance in control mice, but not in knockout mice, demonstrating the importance of this receptor in mediating the effect of IVIG on 7E3 clearance. Data were fit, simultaneously, to the model shown in scheme 1; resulting parameter values are shown in table 1.

Figure 2. 7E3 pharmacokinetics in rats. Rats were dosed intravenously with 0.8 (●), 4 (■), or 8 mg/kg (▲) 7E3. 7E3 concentrations were determined using an ELISA. Data were fit (together with the data shown in figure 3) to the model shown in scheme 1. Parameter values obtained from the fit are listed in table 1.

Figure 3. Characterization of IVIG effects on 7E3 pharmacokinetics in the rat. Rats were dosed intravenously with 0.4 (●), 1 (■), or 2 g/kg (▲) IVIG, followed by 7E3 (8 mg/kg). 7E3 concentrations were determined using an ELISA. Data were fit (together with the data shown in figure 2) to the model shown in scheme 1. Parameter values obtained from the fit are listed in table 1.

Figure 4. IVIG effects on endogenous mouse and rat plasma IgG concentrations. Simulations were performed, using the parameter values listed in table 1, and the model shown in scheme 1, to predict the effect of IVIG on endogenous mouse (panel A) and rat

(panel B) IgG concentrations. Panel A. The upper line is the predicted endogenous mouse IgG concentrations following 7E3 dosing alone. The lower line is the predicted endogenous mouse IgG concentrations following IVIG (1 g/kg). Panel B. The lines represent predicted endogenous rat IgG concentrations following 7E3 alone (top line), 0.4 g/kg IVIG (2<sup>nd</sup> line), 1 g/kg IVIG (3<sup>rd</sup> line) or 2 g/kg IVIG (bottom line).

Figure 5. Characterization of 7E3-mediated thrombocytopenia. An indirect response PK/PD model (scheme 2) was developed to characterize 7E3 effects on platelet count. These rats received saline (○), 0.8 (◇), 4(□), or 8(Δ) mg/kg 7E3, dosed intravenously. Platelet counts were determined using electronic particle counters. Best-fit lines are shown; parameter values obtained from the fit are listed in table 2.

Figure 6. Importance of increased 7E3 clearance to total effect of IVIG. Simulations to determine the relative importance of the effect of IVIG on 7E3 clearance were performed. The models shown in schemes 1 and 2, and the parameters shown in tables 1 and 2, were used to simulate the expected platelet count time course following IVIG treatment, assuming there were no effects of IVIG other than the increase in clearance of 7E3 (panel A). Actual platelet count time courses following IVIG and 7E3 treatment are shown in panel B. IVIG treatment groups are designated as follows: saline (●), 0.4 g/kg (■), 1 g/kg (▲), and 2 g/kg (◆). All animals received 8 mg/kg 7E3. IVIG effects on 7E3 clearance can account for 50±11% of the total effect of IVIG in this model (see table 3).

Scheme 1. Schematic representation of a new model for IgG pharmacokinetics. This model for IgG pharmacokinetics is based upon protection of IgG catabolism by the FcRn receptor. IgG moves from the central compartment to the endosome, where it can bind to the FcRn receptor. Bound IgG returns to the central compartment, and unbound IgG is eliminated. Differential equations describing the change in IgG concentrations with time for each compartment are shown in the text. Notation is also defined in the text.

Scheme 2. Schematic representation of an indirect response PK/PD model for 7E3-induced thrombocytopenia. Thrombocytopenia is induced in the rat by administration of an anti-platelet antibody (7E3). 7E3 concentrations are described by the model in shown in scheme 1. 7E3 concentrations in the central compartment then drive the pharmacodynamic response, by causing an increase in the elimination rate of platelets. The symbols are described in the text.

Table 1. Pharmacokinetic parameters for 7E3.

Parameter	Mouse	Rat
$k_{up}$ (d <sup>-1</sup> )	1.03±0.09	2.5±0.6
$k_{deg}$ (d <sup>-1</sup> )	0.43±0.34	3.0±4.3
$K_d$ (nM)	4.8 <sup>a</sup>	500 <sup>a</sup>
$R_t$ (nM)	1.22±0.30×10 <sup>4</sup>	8.3±3.0×10 <sup>4</sup>
$V_1$ (ml kg <sup>-1</sup> )	66.9±2.0	39.9±6.0

<sup>a</sup>Parameter value fixed

**Table 2. Pharmacodynamic parameters for 7E3.**

Parameter	Value
S (nM <sup>-1</sup> )	0.070±0.019
K <sub>stress</sub> (hr <sup>-1</sup> )	0.71±0.21
K <sub>0</sub> <sup>stress</sup>	16.6±5.3
m (% hr <sup>-2</sup> )	0.16±0.03
K <sub>0</sub> (% hr <sup>-1</sup> )	3 <sup>a</sup>
K <sub>out</sub> (hr <sup>-1</sup> )	0.03 <sup>a</sup>

<sup>a</sup>Parameter values were fixed

Table 3. Importance of PK effect of IVIG relative to the total effect

Dose of IVIG (g kg <sup>-1</sup> )	Pred. AUCE (% hr)	Actual AUCE (% hr)	% Total Effect
0	1713	1718±379	-
0.4	1552	1308±650	39.3
1	1462	1309±473	61.4
2	1347	978±504	49.6

Figure 1.

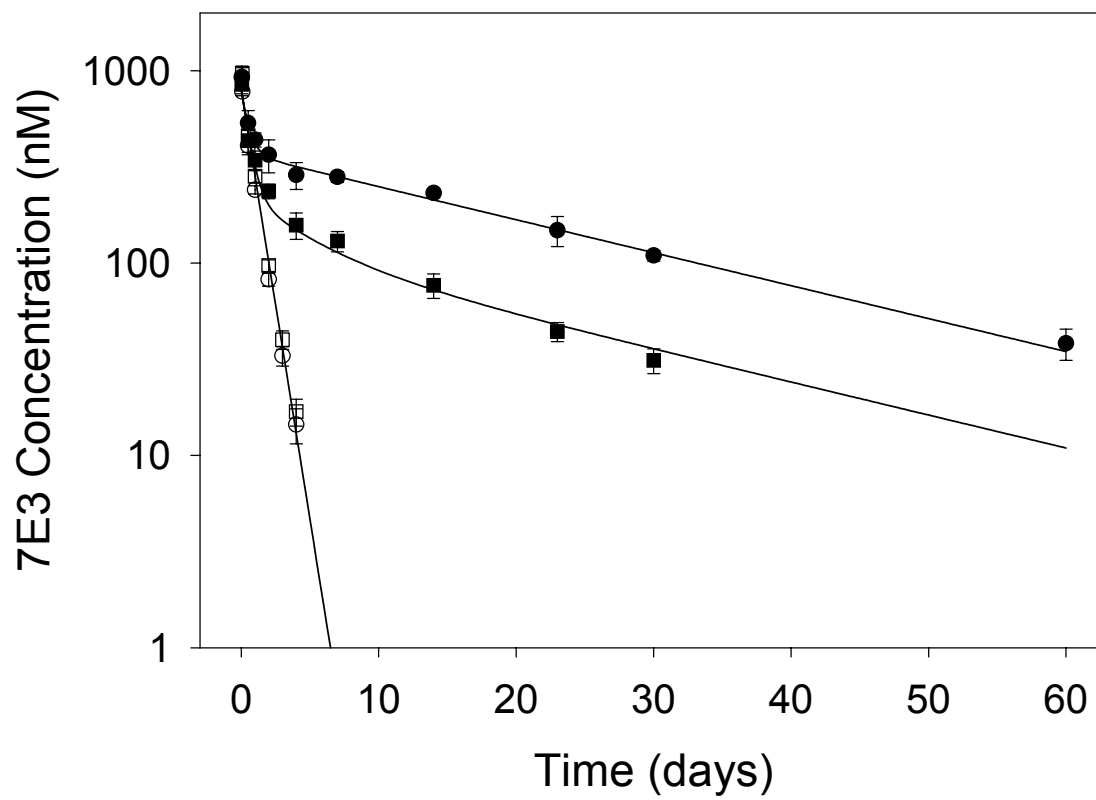


Figure 2.

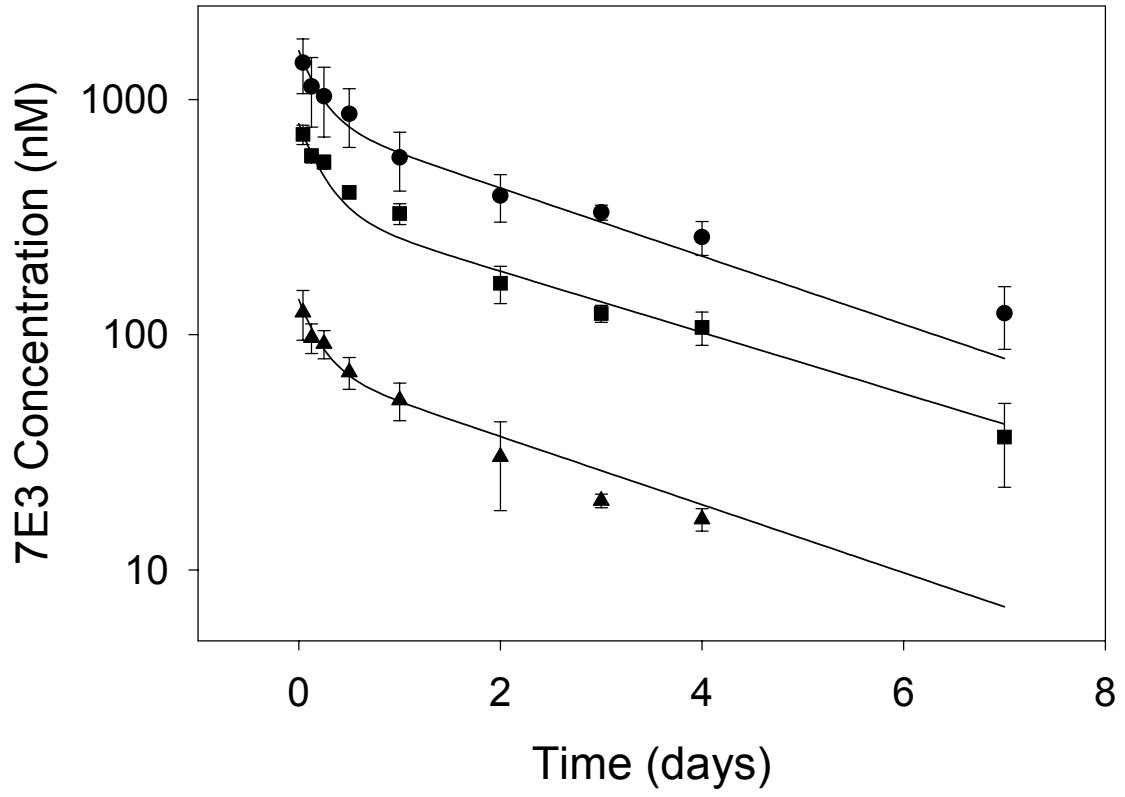


Figure 3.

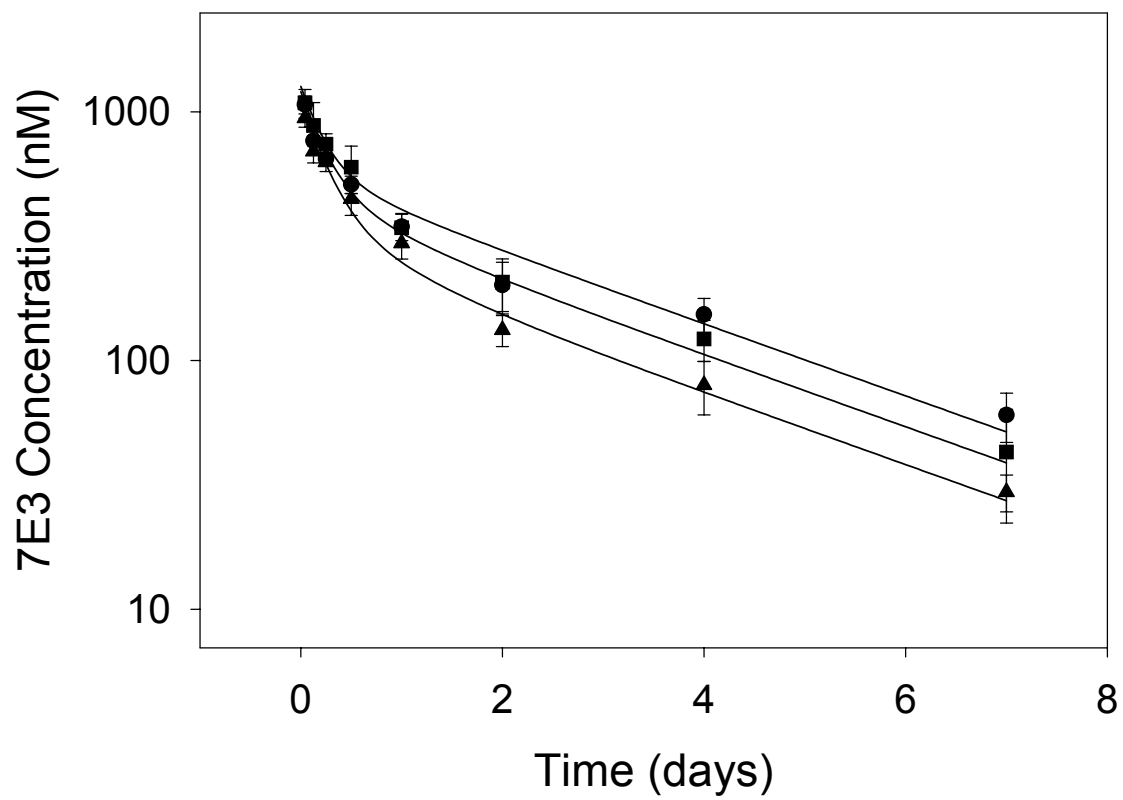


Figure 4A.

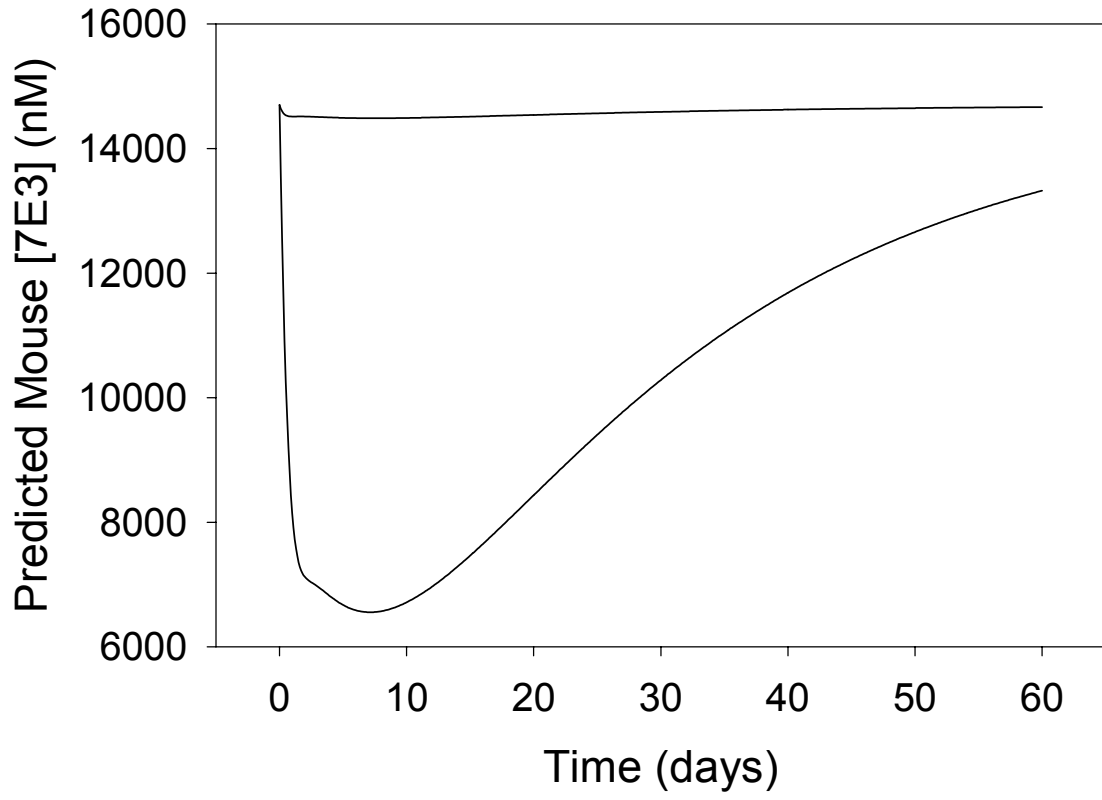


Figure 4B.

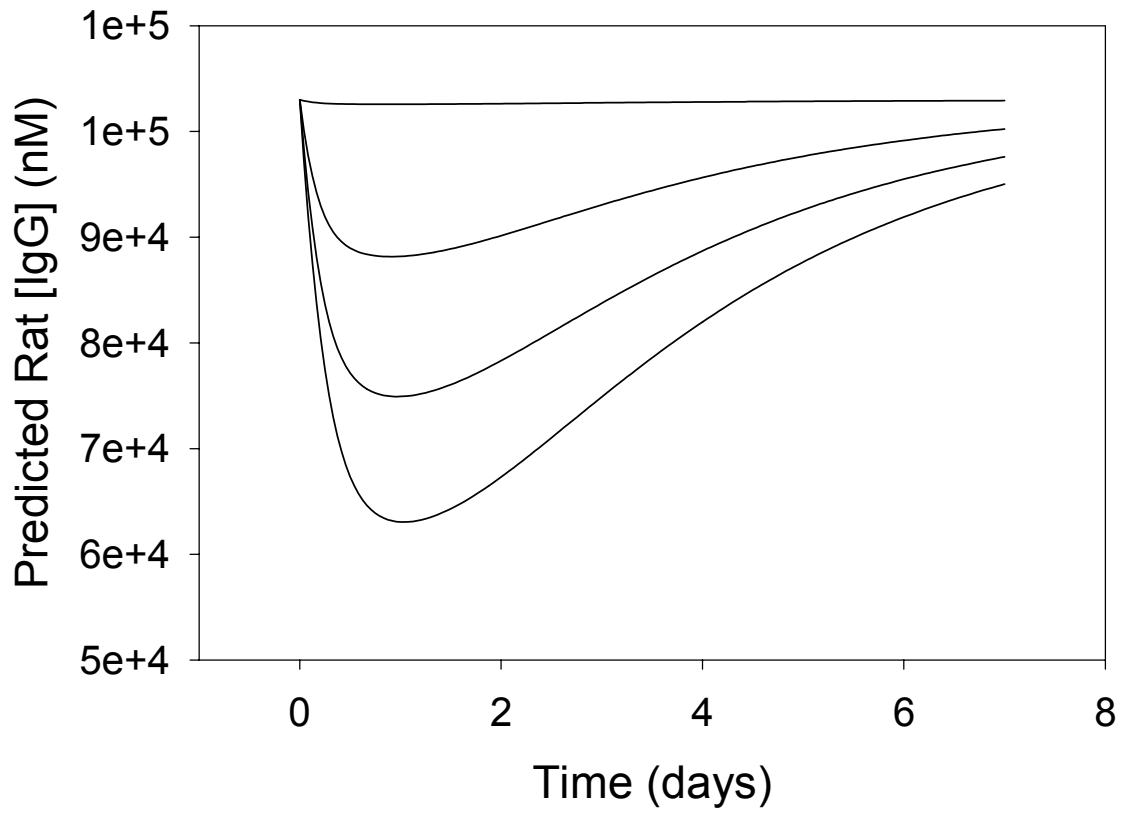


Figure 5.

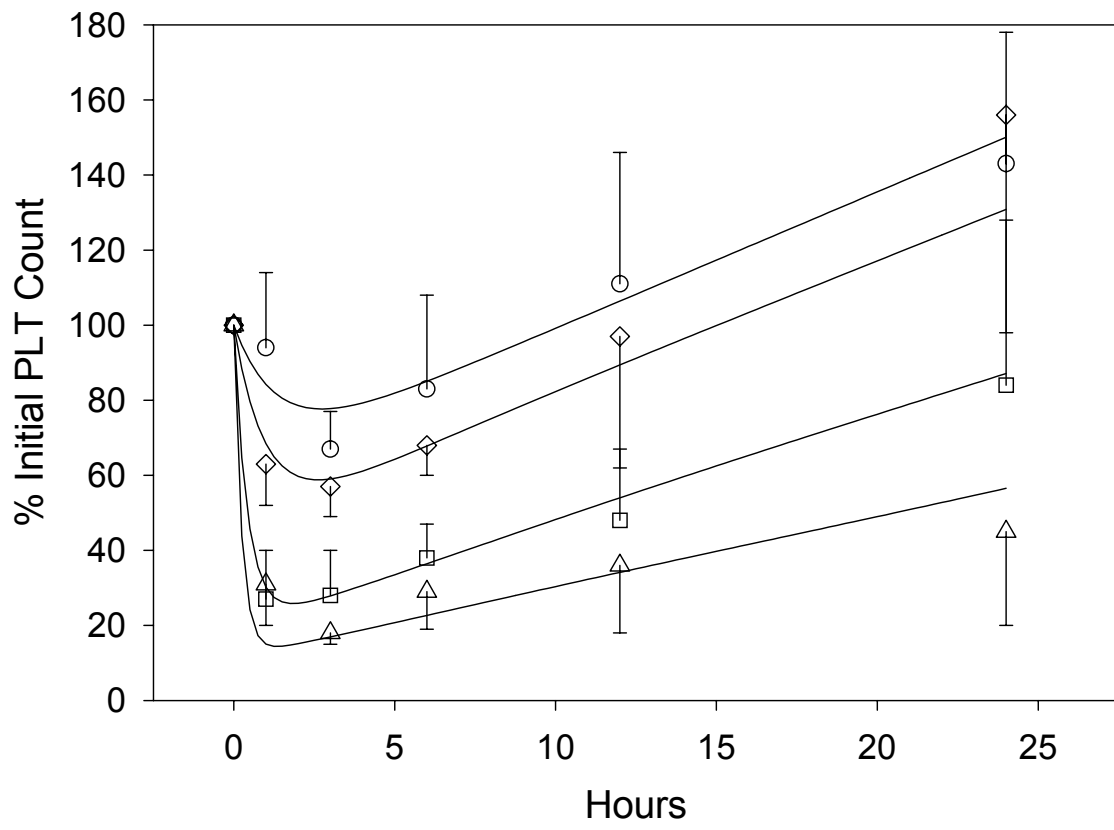


Figure 6A.

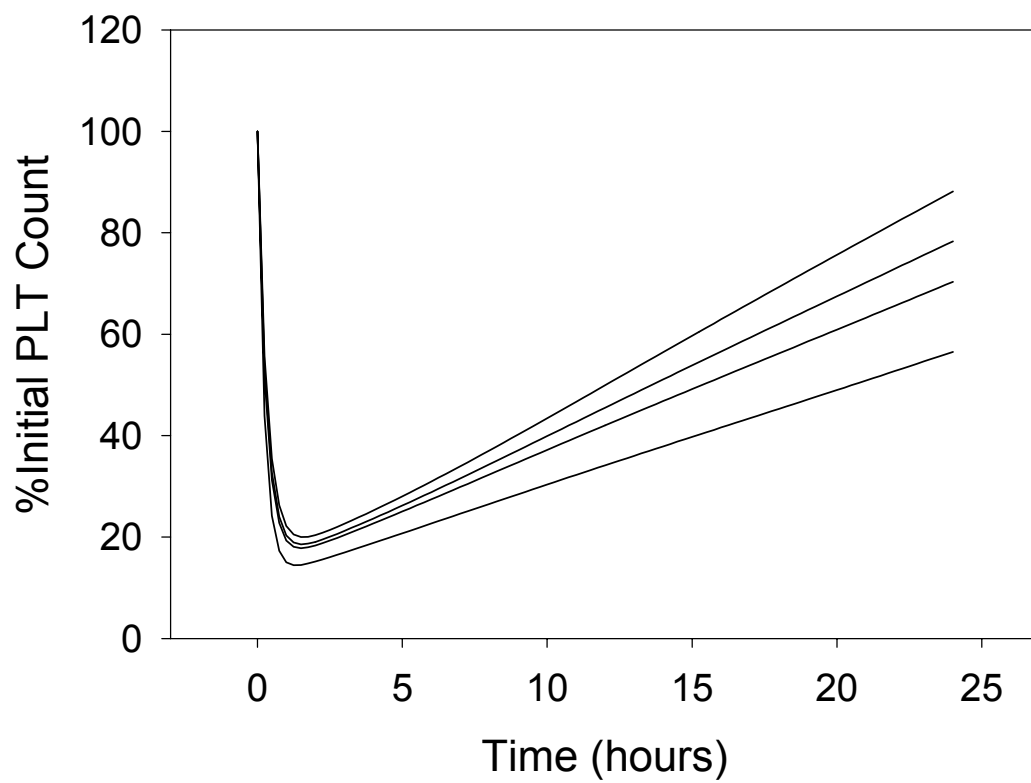
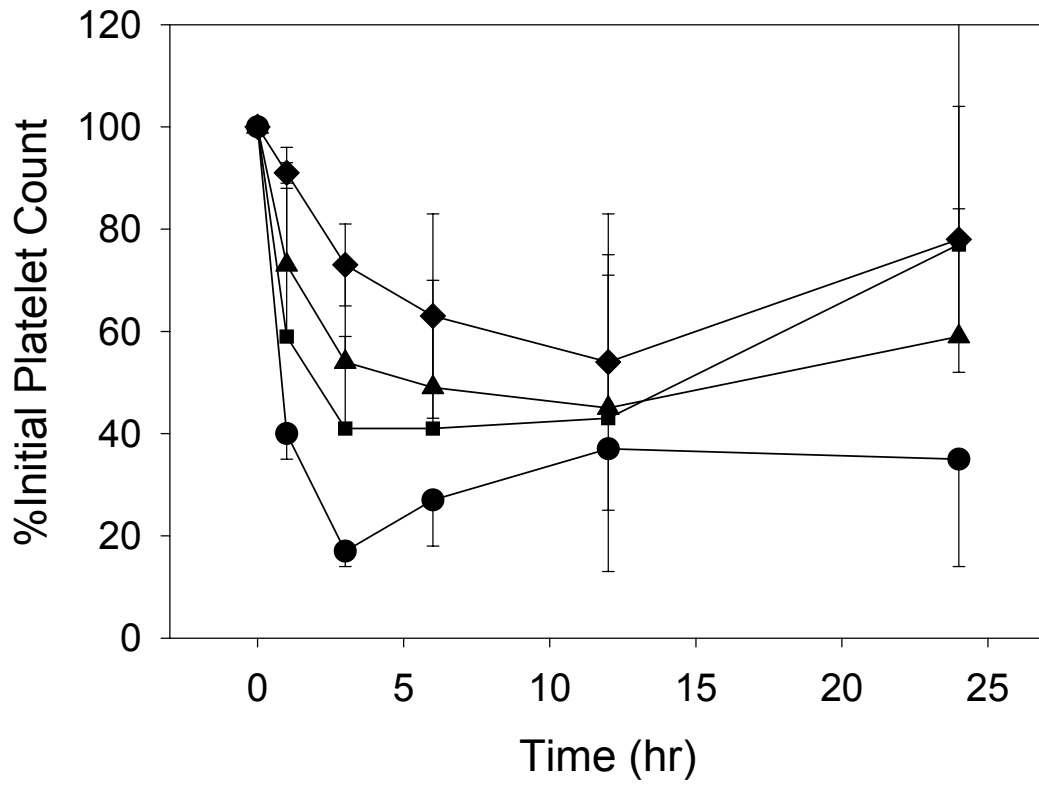
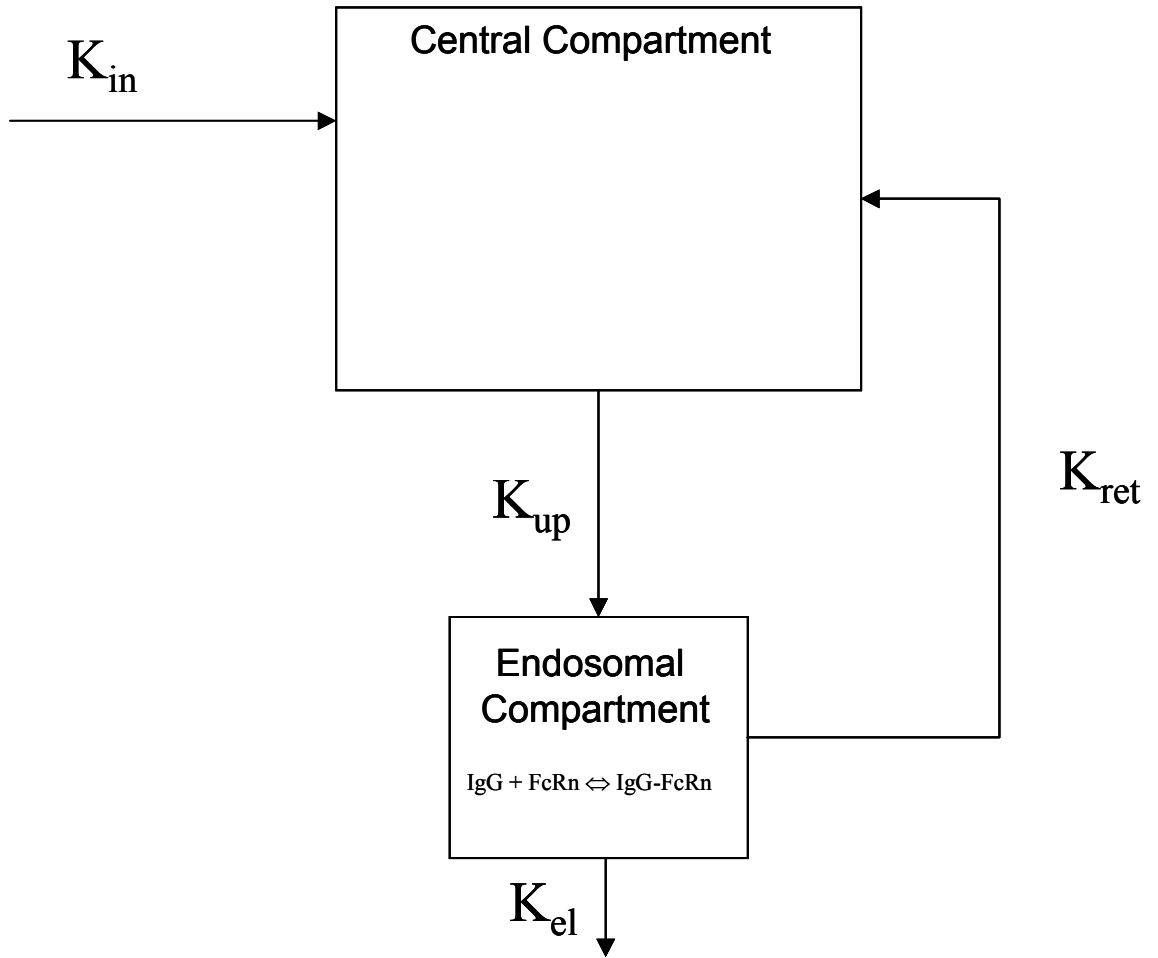


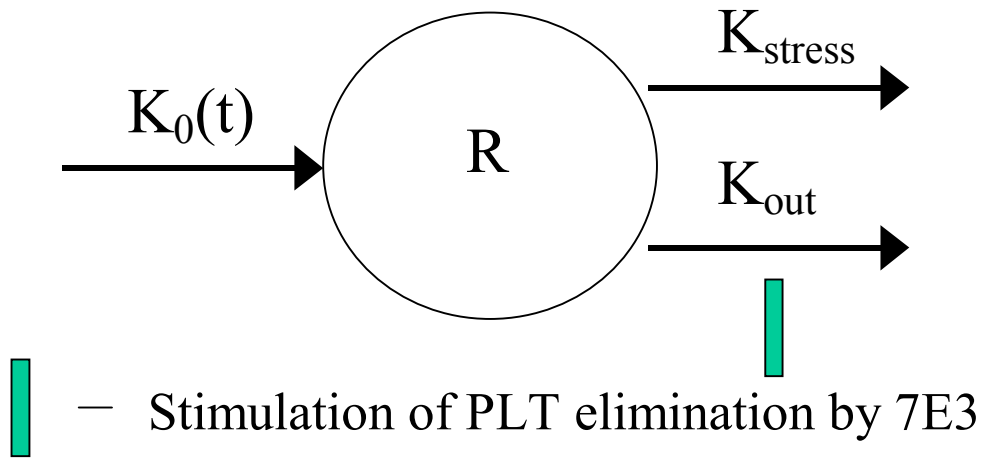
Figure 6B.



Scheme 1.



Scheme 2.



# CHAPTER EIGHT

---

## CONCLUSIONS

---

Although intravenous immunoglobulin (IVIG) therapy has been used to treat patients with immune thrombocytopenia (ITP) for more than 20 years, the mechanism(s) by which beneficial effects are achieved is still unclear. Many effects of IVIG have been identified, either in humans or in various experimental models of ITP, but the relative importance of any one effect is unknown. The focus of this dissertation was the development and use of experimental models of ITP, with which to better understand IVIG mechanism of action.

A major focus of this dissertation was to present the general concept of using pharmacokinetic/pharmacodynamic (PK/PD) modeling, together with quantitative animal models of disease, to understand the relative importance of any one mechanism of drug action, in a complex therapeutic situation. This general approach has been applied in an attempt to gain a better understanding of IVIG treatment of ITP. Chapters 2-5 presented experiments performed to lay the foundation of this general approach, and chapter 7 demonstrated its application.

In other studies, an *in vitro* model system was used to determine the effects of IVIG on anti-platelet antibody production (chapter 6), a potential mechanism of IVIG action that could not be studied in the rat model presented in this dissertation. This work suggested that IVIG treatment may lead to decreased anti-platelet antibody production, but that these effects may not be specific to anti-platelet antibody producing cells.

To facilitate the development of a passive model of ITP, we have produced, purified and characterized large quantities of murine anti-platelet antibodies (see chapters 2 and 3). Cells producing the anti-platelet antibodies were obtained from commercial sources, and then either injected into mice, or grown in culture, to produce the desired quantities of antibody. Antibodies were purified using Protein G affinity chromatography, and were then characterized using SDS-PAGE and a specific activity assay developed in our laboratory. Anti-platelet antibody preparations obtained using these techniques were determined to be >90% pure.

Once purified anti-platelet antibodies were obtained and characterized, an enzyme-linked immunosorbent assay (ELISA) was developed for application to the pharmacokinetic characterization of anti-platelet antibody disposition in the rat (see chapter 2). This sandwich ELISA was validated with respect to intra- and inter-assay variability, using anti-platelet antibody-containing quality control samples. Intra-assay and inter-assay recoveries of anti-platelet antibodies were within 10 and 20% of 100%, respectively. The assay had no appreciable cross reactivity with pooled rat IgG, making this an ideal assay to determine plasma pharmacokinetics of mouse antibodies in the rat.

To characterize a quantitative model of ITP, a range of anti-platelet antibody doses were studied, in the rat. The anti-platelet antibody selected for model development, 7E3, was administered to the rat through a jugular vein cannula (0.8-8 mg/kg). The ELISA developed in chapter 2 was applied to the determination 7E3 concentrations in plasma, platelet counts were determined using electronic particle counters, and bleeding tendency

was assessed following a standardized tail incision. Administration of 7E3 caused rapid, severe, antibody-mediated thrombocytopenia, and increased bleeding tendency, the two characteristics most identified with ITP in the clinical condition (see chapter 3). Thus, an animal model, quantitative with respect to both anti-platelet antibody concentrations and platelet counts, was in place with which to study IVIG effects.

Studies of IVIG effects in the rat model of ITP showed that IVIG protected animals from severe 7E3-mediated thrombocytopenia, in a dose-dependent fashion (see chapter 4). Interestingly, the dose-dependency of IVIG effects has not been well studied. Our results suggest that studies investigating optimal dosing strategies of IVIG in ITP may be beneficial. Because of the quantitative nature of the rat model of ITP, with respect to anti-platelet antibody concentrations, this model allowed for characterization of IVIG effects on anti-platelet antibody disposition, a study which had never before been possible. Perhaps the most significant finding presented in this dissertation, IVIG treatment increased the clearance of the anti-platelet antibody, in a dose-dependent fashion. This increase in anti-platelet antibody clearance was shown to be a general effect in this model (i.e., not facilitated by specific interactions between IVIG and 7E3), and may contribute to the beneficial effects seen following IVIG treatment in this model and in humans.

Further studies were performed to investigate the mechanism by which IVIG increased anti-platelet antibody clearance. It was hypothesized that IVIG acted by competition with 7E3 for occupancy of the recently identified FcRn receptor, responsible for

protecting IgG from catabolism. Studies performed in mice lacking expression of the FcRn receptor supported this hypothesis, by demonstrating the importance of the presence of the FcRn receptor in mediating this effect of IVIG on 7E3 clearance (see chapter 5).

Having obtained experimental support for a new mechanism of IVIG action in ITP, together with a quantitative animal model of the disease, the general approach of using disease and PK/PD models to quantitatively estimate the relative importance of a single mechanism of action was then demonstrated (chapter 7). A mechanism-based model for IgG pharmacokinetics was presented, that accurately characterized 7E3 kinetics under diverse circumstances (e.g., in the presence or absence of IVIG, in the mouse and the rat, and in mice lacking expression of the FcRn receptor). Additionally, an indirect response PK/PD model was developed that accurately characterized 7E3-mediated thrombocytopenia. Application of these models suggested that ~50% of the total effect of IVIG, in this acute, passive model of ITP, could be accounted for by this increase in clearance of 7E3 by IVIG. Simulations using these models predicted that this effect might be even more pronounced in the human condition.

In summary, a new quantitative model of ITP has been developed in the rat. Efficacy of IVIG in this model of ITP was demonstrated, and experimental evidence for a new mechanism of IVIG action of ITP was presented. This work showed that IVIG may affect anti-platelet antibody production, and that these effects were not specific for anti-platelet antibodies, in a model system. A new approach to the study of IVIG mechanism

of action in ITP was demonstrated through the use of quantitative disease models and PK/PD modeling analyses. This type of analysis has led to, and is expected to continue to lead to, a better understanding of IVIG mechanism of action in ITP. It is hoped that these studies will lead to the development of new, improved therapies of ITP and other autoimmune conditions.